May 2006

Examining the role of the central melanocortin system in the regulation of adaptive thermogenesis of brown adipose tissu

Adriana Voss-Andreae

EXAMINING THE ROLE OF THE CENTRAL MELANOCORTIN SYSTEM IN THE REGULATION OF ADAPTIVE THERMOGENESIS OF BROWN ADIPOSE TISSUE

by Adriana Voss-Andreae

A DISSERTATION

Presented to the Neuroscience Graduate Program

and the Oregon Health & Science University

School of Medicine

in partial fulfillment of

the requirements for the degree of

Doctor of Philosophy

May 2006

School of Medicine
Oregon Health & Science University

CERTIFICATE OF APPROVAL

This is to certify that the Ph.D. dissertation of
Adriana Voss-Andreae
has been approved

[redacted]

Advisor

[redacted]

Member

[redacted]

Member

[redacted]

Member

[redacted]

Member

TABLE OF CONTENTS

LIST OF TABLES AND FIGURES

Introduction:

ACKNOWLEDGMENTS

I am indebted to Roger Cone for his mentorship, guidance and incredible patience throughout my graduate studies. I also owe a very special thank you to Wei Fan for his invaluable guidance and help with the subject matter at the heart of this dissertation.

I am grateful to the members of my thesis committee for their time and for their insightful comments and suggestions along the way.

My appreciation goes to all the members of the Cone lab, particularly to Jon Murphy, whose technical assistance was truly appreciated and to Kate Ellacott for all of her intellectual, technical and editorial help with this dissertation and most importantly for her friendship. She has made my graduate experience both more stimulating and far more enjoyable.

Thanks to my dear friends Michaela and David McMahon, who are always there for me.

My deepest gratitude to Sibylle and Hans-Peter Voss-Andreae, my parents in-law, for all of their love and support from afar.

This thesis is dedicated to my parents, Mina Weissmann and George Weissmann, as well as Michael May, to whom I owe everything, and to my beloved husband, Julian Voss-Andreae, who is a consummate source of support, encouragement and inspiration. I could not have done this without him.

ABSTRACT

Previous work from our laboratory has shown that the melanocortin system is required for the acute homeostatic responses to increased dietary fat (Butler et al., 2001). In this study we examine the mechanism underlying the energy expenditure defect observed in melanocortin-4 receptor null (MC4R-/-) mice. Using specific polysynaptic retrograde tracing from interscapular brown adipose tissue (IBAT) coupled with dual labeling immunohistochemistry, we show co-expression of MC4R-green fluorescent protein-immunoreactivity (MC4R-GFP-IR) and the attenuated pseudorabies virus (PRV)-IR in many hypothalamic and brain stem regions known to play an important role in non-shivering thermogenesis, demonstrating an anatomical link between the central melanocortin system and the sympathetically-mediated regulation of IBAT thermogenic function. Additionally, using both genetic and pharmacological antagonism, we show that intact MC4R signaling is required to appropriately up-regulate UCP1 in response to physiological stimuli, such as a high-fat diet and short-term cold exposure. Our results that MC4R-/- and agouti related peptide (AGRP)-treated mice on a high-fat diet have a similar increase in their total serum 3,5,3'-triiodothyronine (T_3) levels to wild-type controls also suggests that the MC4R-mediated up-regulation of UCP1 in response to a high-fat diet is independent of the central hypothalamic-pituitary-thyroid (HPT) axis. Our data showing that UCP1 is up-regulated normally in MC4R-/- mice after longer periods of cold exposure suggests that melanocortin system-mediated non-shivering thermogenesis may be differentially regulated by diet and cold or alternatively that compensatory mechanisms may develop in these animals after long-term cold exposure.

This study provides a neuroanatomic and physiological basis for the regulation of non-shivering thermogenesis by the melanocortin system and furthers our insight into a potential mechanism by which the melanocortin system regulates energy expenditure in response to an increase in dietary fat and cold exposure. In a separate double *in situ* hybridization study, we find a high degree of glutamic acid decarboxylase (GAD) and MC4R mRNA co-expression in neurons of sexually dimorphic nuclei, suggesting a mechanism by which melanocortin signaling may mediate sexually divergent effects on energy homeostasis.

INTRODUCTION

The obesity epidemic

Obesity and obesity-related diseases are a leading cause of morbidity and mortality in western countries. Obesity is defined as a body mass index (BMI) > 30.0 and overweight as a BMI > 25.0 (where BMI= weight (kg)/height $(m)^2$). Over 60% of the U.S. population is overweight and over 25% are considered obese, with an alarming increase in the number of pediatric cases (at preschool age, 16-22% are overweight, and about 10% are obese) (Center for Disease Control and Prevention, 2004; Hedley et al., 2004; Rocchini, 2002). Obesity and obesity-related diseases, such as non-insulin-dependent diabetes mellitus (type II diabetes), some forms of cancer (including breast and colon), osteoarthritis, sleep apnea, hypertension and cardiovascular disease, are the leading causes of morbidity and mortality in the U.S. (Must et al., 1999; Visscher and Seidell, 2001; Zimmet et al., 2001). Even amongst pediatric cases, 58% of overweight children have at least one risk factor for heart disease, such as high cholesterol or high blood pressure (Freedman et al., 1999), and pediatric type II diabetes, almost non-existent two decades ago, is increasingly observed (Young et al., 2000). Obesity has recently developed into a global epidemic (Friedrich, 2002; James et al., 2001) with diabetes being projected to double in half of the world's developing regions over the next two decades (Narayan et al., 2006). Today's unhealthy lifestyle, with its decrease in physical activity and increase in caloric intake, as well as the societal factors that promote it, are the largest contributors to the rapidly increasing prevalence of obesity over the recent decades.

The genetics of obesity

Heredity plays a very important role in determining a person's predisposition to becoming overweight or obese (Froguel and Boutin, 2001). Studies with twins and adopted children have suggested the influence of heritability of obesity to be somewhere between 30-80% (Bouchard and Perusse, 1993; Stunkard et al., 1986; Stunkard et al., 1990). From an evolutionary perspective, it is advantageous to develop mutations that increase the body's energy efficiency in times of limited access to food (sometimes referred to as the "thrifty genotype"). But lifestyle changes in the last century have turned these evolutionary advantages into a potential disadvantaged predisposition to becoming morbidly obese.

Short-term dietary changes have had very little impact in helping patients achieve weight loss over longer periods of time (Grodstein et al., 1996; Kramer et al., 1989). In fact, both humans and rodents seem to be quite resistant to maintenance of weight loss and when overfed or underfed return to what appears to be a given "set weight". This and other observations have led to the present model of body weight regulation which, based on the original proposal of an adipostat or lipostat, is described as a negative feedback system in which the CNS is able to maintain a constant body weight by detecting the amount of energy or fat stores the body has and regulate feeding behavior and energy expenditure to homeostatically maintain the level of adipose stores (Kaiyala et al., 1995; Kennedy, 1953). The first notion of distinct "feeding" and "satiety" centers in the CNS came from lesioning experiments in which lesions to certain hypothalamic regions caused rats to have a disturbed metabolism and rendered them either severely hyperphagic (with lesions of the ventromedial nucleus or disrupting connections to the paraventricular nucleus)(Hetherington and Ranson, 1940; Saper et al., 1976; Swanson and Sawchenko, 1980) or hypophagic (with lesions of the lateral hypothalamus)(Anand and Brobeck, 1951a; Anand and Brobeck, 1951b). More evidence for the homeostatic regulation of body weight came from early cross-circulation, or parabiosis, experiments between rats caused to be obese by lesions in the ventromedial hypothalamus (VMH) and control rats, leading to the starvation, and ultimately death, of the control rats (Hervey, 1959). These experiments led to the suggestion that a factor existed that circulates in the bloodstream and acts on a receptor in the hypothalamus in order to regulate feeding behavior. This hypothesis was further strengthened by observations from parabiosis experiments in two obese mutant mouse strains, the *obese* (Lep^{ob}/Lep^{ob}) and *diabetes* (Lep^{db}/Lep^{db}) mice (Coleman, 1973; Coleman and Hummel, 1969; Hausberger, 1959). Parabiosis between Lep^{ob}/Lep^{ob} and lean control mice suppressed weight gain in Lep^{ob}/Lep^{ob} mice, wheras parabiosis between Lep^{db}/Lep^{db} mice and lean controls led to a profound hypophagia in the control mice. These results led to the suggestion that Lep^{ob}/Lep^{ob} mice were lacking a humoral satiety factor while Lep^{db}/Lep^{db} mice were lacking its receptor. Twenty years later the gene encoding this factor, *leptin*, was identified by positional cloning (Zhang et al., 1994), followed by the cloning of its receptor (Tartaglia et al., 1995), leading to an explosion in the field.

The *obese* gene (*ob*) encodes a 146-amino acid, 16 kDa, peptide hormone termed leptin (from the Greek word *leptos*, meaning thin). Leptin is primarily synthesized by adipocytes (Green et al., 1995; Lonnqvist et al., 1995; Maffei et al., 1995), with minor contributions from placenta (Hoggard et al., 1997; Masuzaki et al., 1997), stomach (Bado et al., 1998; Mix et al., 1999), rat skeletal muscle (Solberg et al., 2005), heart (Green et al., 1995), and secreted into the blood stream. *Lep*^{ob}/*Lep*^{ob} mice, which are leptin deficient, develop hyperphagia and an early onset diabetes accompanied by hyperinsulinemia, hyperglycemia, hypercorticosteronemia, dyslipidemia, low thyroid levels and decreased thermogenesis. This obesity syndrome can be reversed if *Lep*^{ob}/*Lep*^{ob} mice are treated with exogenous leptin. A very similar obesity syndrome can be observed in *Lep*^{db}/*Lep*^{db} mice, which have a mutation in the *diabetes (db)* gene, and thus cannot make functioning leptin receptors (Chen et al., 1996; Lee et al., 1996). A better understanding of a number of genetically obese rodent models, including *obesity* and *diabetes*, as well as *agouti, fatty* and *tubby*, have shed considerable light on some of the important genes and pathways involved in energy regulation. The agouti obesity syndrome, found in mice carrying the autosomal dominant *agouti* alleles *lethal yellow* (A^{y}) and *viable yellow* (A^{vy}), exhibits a unique phenotype of hyperphagia, a maturity-onset moderate obesity with an increase in hepatic lipogenesis rates, adipocyte hypertrophy and depressed basal lipolytic rates, increased linear growth, moderate hyperinsulinemia and yellow hair pigmentation (Bultman et al., 1992; Miltenberger et al., 1997). Early parabiosis experiments with A^{y} mice indicated that agouti was not a circulating factor or hormone like leptin (Wolff, 1963). Instead, previous skin transplantation experiments suggested that agouti was produced in hair follicles and acted in a more local fashion (Silvers and Russell, 1955).

The *agouti* gene encodes a 131-amino acid secreted peptide normally found in the hair follicles of mice, where it blocks the action of melanocortin-stimulating hormone (α-MSH) on melanocortin-1 receptors (MC1R) (Lu et al., 1994), thereby switching the synthesis of the black-brown pigment eumelanin to the yellow pigment pheomelanin

(Miltenberger et al., 1997). Five melanocortin receptors have been cloned to date (Chhajlani and Wikberg, 1992; Fathi et al., 1995; Gantz et al., 1993a; Gantz et al., 1993b; Gantz et al., 1994) which are all members of the G-protein-coupled receptor family that activate the cAMP-dependent signaling pathway. The yellow mouse obesity syndrome occurs when, because of a gene rearrangement, the *agouti* gene is placed under the control of another transcriptional promoters and becomes ectopically overexpressed throughout the entire body (Argeson et al., 1996; Bultman et al., 1992; Duhl et al., 1994a; Duhl et al., 1994b; Michaud et al., 1994a; Michaud et al., 1994b). For instance in the A^y mouse, the deletion upstream of the *agouti* gene of all but the promoter and first noncoding exon of a ubiquitously expressed gene called *Raly*, causes *agouti* to be under the transcriptional control of the *Raly* promoter, resulting in the ubiquitous expression of the agouti protein (Bultman et al., 1992; Michaud et al., 1994a). In the brain agouti can block the action of α-MSH on the central melanocortin receptors, with a particularly high specific affinity for the MC4R (Lu et al., 1994). An endogenous brain homologue was subsequently discovered termed agouti related protein (AGRP), which in the CNS is expressed almost entirely in the hypothalamic arcuate nucleus (ARC) (Bultman et al., 1992; Ollmann et al., 1997; Shutter et al., 1997).

The melanocortin system and obesity

Two key sets of experiments demonstrated the importance of central melanocortins in regulating energy homeostasis. In the first set of experiments normal wild-type C57BL/6J mice, injected intracerebroventricularly (ICV) with a synthetic antagonist of the MC3R and MC4R, SHU9119, became markedly hyperphagic (Fan et al., 1997). Conversely, when these same normal mice were treated ICV with the agonist MTII, they became hypophagic. In the second set of experiments, a targeted deletion of the MC4R gene (MC4R-/-)(Huszar et al., 1997), or overexpression of the endogenous antagonist at the MC4R, AGRP (Graham et al., 1997; Ollmann et al., 1997), resulted in mice with an obesity syndrome that once again mimicked that of the yellow agouti mouse (with the exception of the yellow coat color, which results from MC1R blockade). Interestingly, MC4R-/- mice are more obese than heterozygous mice that have one functioning MC4R gene, which are in turn more obese than mice with two functioning genes (Huszar et al., 1997). The MC4R genes have a unique gene dosage effect in which heterozygous loss of the gene leads to intermediate phenotypes, leading to the suggestion that the melanocortin system has the ability to act like a rheostat on energy stores (Cone, 2005).

A similar dominantly inherited obesity syndrome was discovered in humans who had a null mutation in the gene encoding pro-opiomelanocortin (POMC), the precursor of α-MSH. Subsequently, MC4R mutations were found in a number of obese human subjects and MC4R haploinsufficiency was discovered in about 4-6% of individuals with severe pediatric-onset obesity, making it the most common form of monogenic obesity in humans to date (Farooqi et al., 2000; Lubrano-Berthelier et al., 2003; Vaisse et al., 1998; Yeo et al., 1998). This high frequency might exist because even partial loss-of-function mutations in heterozygous individuals result in a phenotype, and because MC4R haploinsufficient humans retain normal reproductive function. Carriers of functionally relevant MC4R mutations have a 4.5-fold increased risk of becoming obese in comparison with non-carriers (Hinney et al., 2003). As in MC4R-/- mice, MC4R deficiency in humans is associated with increased BMI, appetite, height, lean mass, bone mineral density and hyperinsulinemia, and homozygotes are more severely affected than heterozygotes (Farooqi et al., 2003). These finding demonstrate that the melanocortin system probably plays a very similar function in humans and rodents in regulating energy homeostasis. Leptin defieciency has also been found in humans, but is far less common than MC4R deficiency. Similar to the rodent *Lep*$^{ob/}$/*Lep*^{ob} syndrome, leptin deficient humans are characterized by severe, early-onset obesity and hyperphagia, hyperinsulinemia, advanced bone-age, although some phenotypes observed in rodents, such as growth retardation and reduced energy expenditure, have not yet been clearly observed in humans (Montague et al., 1997; Strobel et al., 1998). In both rodents and humans, the agouti and MC4R-/- obesity syndromes have milder phenotypes than the *Lep*$^{ob/}$/*Lep*^{ob} syndrome, with less severe obesity, hyperphagia and hyperinsulinemia, an apparently intact reproductive system and adrenal system, and a relatively intact satiety mechanism.

Another important finding that supports the melanocortin system's central role in regulating energy homeostasis is the location of its receptors. In particular the MC4R, although widely expressed in the CNS, is highly expressed in areas known to be important in feeding behavior and energy regulation, including the PVH, the ARC, the lateral hypothalamic area (LH) and the dorsomedial hypothalamus (DMH) (Mountjoy et al., 1994).

POMC is precursor to the β-endorphins, ACTH and the melanocortin stimulating hormones (α-, β- and γ-MSH) and is expressed peripherally in the pituitary, skin and hair follicles, and centrally in the ARC and commissural nucleus of the solitary tract (cNTS)

(Jacobowitz and O'Donohue, 1978; Palkovits et al., 1987; Watson et al., 1978). Melanocortin peptides mediate their effects on a family of related G protein-coupled receptors, MC1R-MC5R. MC1R, MC2R and MC5R act in the periphery to regulate the production of skin and hair pigment (Suzuki et al., 1996), adrenal glucocorticoid production (Penhoat et al., 2002; Xia and Wikberg, 1996), and exocrine gland secretion (Chen et al., 1997) respectively. The MC3R and MC4R are widely expressed in the CNS (Kishi et al., 2003; Lindblom et al., 1998; Mountjoy et al., 1994). AGRP is expressed solely in the ARC, and both POMC and AGRP neurons send out projections to various sites throughout the brain including key hypothalamic and brainstem areas that express the MC3R and MC4R and are known to be critical to energy homeostasis (Bagnol et al., 1999; Haskell-Luevano et al., 1999).

A number of studies further demonstrate that the melanocortin system plays an important role in energy expenditure. For instance, female MC4R-/- mice that are food restricted to the amount consumed by age-matched wild-types, i.e. pair-fed, become heavier than wild-types (Ste Marie et al., 2000), indicating that at least part of their obesity is caused by defects in energy expenditure in addition to hyperphagia. In addition, ICV treatment with an MC3R and MC4R agonist, such as melanotan II (MTII) increases energy expenditure (measured as oxygen consumption)(Chen et al., 2000b; Cowley et al., 1999; Hwa et al., 2001; Jonsson et al., 2001; Pierroz et al., 2002), while treatment with the endogenous MC3R and MC4R antagonist AGRP decreases energy expenditure (Goto et al., 2003; Small et al., 2003). The effect of intraperitoneal injection of MTII on oxygen consumption is not observed in MC4R-/-, suggesting a role for the MC4R in the regulation of energy expenditure (Chen et al., 2000b). MC3R-/- mice, on the other hand, have a decrease in lean mass and increase in fat mass, but do not exhibit a decrease in oxygen consumption, even on a high-fat diet, suggesting they do not have the same defect in energy expenditure (with the exception of reduced physical activity)(Butler et al., 2000; Chen et al., 2000a). Both MC3R-/- and MC4R-/- have decreased physical activity and an increase in the respiratory exchange ratio (RER), indicating they have a defect in fatty acid oxidation (Butler, 2006). However wild-type or MC3R-/- fed a moderate- or high-fat diet have a 10-20% increase in oxygen consumption, indicating a normal diet-induced thermogenesis (DIT), whereas MC4R-/- do not exhibit an increase in oxygen consumption with an increase in dietary fat, suggesting they have a defect in DIT (Butler et al., 2000; Butler et al., 2001).

Energy expenditure and adaptive thermogenesis

Gaining weight is the result of an imbalance in energy homeostasis over time, when energy intake (calories consumed) is greater than energy expenditure. Total energy expenditure represents conversion of oxygen and food (or energy stores) into carbon dioxide, water, heat (from exothermic reactions) and work on the environment. Energy expenditure can be divided into three categories: Resting energy expenditure (or obligatory thermogenesis), adaptive energy expenditure (or facultative thermogenesis), and work performed on the environment (also known as the thermic effect of exercise or physical activity) (Sims and Danforth, 1987). Resting energy expenditure is defined as the amount of energy, measured in calories, that an organism uses in order to perform the metabolic functions required to keep it alive, including maintaining a homeothermic temperature at rest and basic cellular and organ maintentance and function. Resting energy expenditure typically comprises 60-75% of the total energy expenditure. Adaptive energy expenditure is an additional regulated resting energy expenditure in response to environmental changes, such as cold exposure or food intake. The term thermogenesis stems from the resting energy expenditure that can be measured directly as heat produced (direct calorimetry), or indirectly as the amount of oxygen consumed (indirect calorimetry).

Energy expenditure can be increased by either increasing ATP utilization (for example, by increasing physical acitivity or growth) or "uncoupling" fuel oxidation from work (i.e. ATP consumption without work). The term adaptive thermogenesis is used when an animal produces heat in response to a change in environment independently of obligatory demands and provides no net synthesis or mechanical work. This can be achieved through the synthesis and degradation of proteins, the esterification and lipolysis of fatty acids/triglycerides, or the pumping and leakage of ions across membranes. Examples of adaptive thermogenesis include the ability to maintain body warmth in cold ambient temperatures (cold-induced non-shivering thermogenesis), the ability to regulate energy balance after a change in diet (or diet-induced thermogenesis (DIT); either from amount or composition of the diet) and response to various pathological stumuli (such as inflammation, infection or injury). Adaptive thermogenesis is regulated by hypothalamic centers that integrate environmental and visceral cues and alter the efferent sympathetic output to target tissues.

Most animal models of obesity have been found to have a decrease in energy expenditure, but the literature remains controversial for human obesity, with some studies reporting an association between decreased energy expenditure and subsequent weight gain or obesity (Griffiths and Payne, 1976; Griffiths et al., 1990; Matsumoto et al., 2001; Ravussin et al., 1988; Roberts et al., 1988), and others reporting no such association (Davies et al., 1991; DeLany et al., 1995; Goran et al., 1998; Stensel et al., 2001; Stunkard et al., 2004; Stunkard et al., 1999; Weinsier et al., 2003). A number of factors may account for the conflicting findings in these studies. Measuring energy intake and expenditure is relatively inaccurate, particularly in humans, due to any combination of factors including technological limitations, methodological errors, sample size and compliance/inaccurate reporting issues with subjects. These factors make measurements of small imbalances very challenging. In addition, resting energy expenditure measurements in obese subjects need to be normalized for their increased lean and adipose masses, factors which in themselves increase resting energy expenditure. These calculations are often based on certain assumptions, such as the amount of energy expended by a given quantity of lean mass or adipose tissue, which are prone to some variation. A number of other factors may also make it difficult to accurately measure the excess weight gain due to the imbalance between energy intake and expenditure, including strong environmental influences, the likely possibility that excess weight gain occurs in spurts during particular windows of time (due to genetic and environmenatal influences) and genetic influences (polymorphisms in genes that influence individual susceptibility to obesity; for instance in a study of heterogenous populations some individuals may have genetic variations that lead to excess food intake, while others may have variations that reduce energy expenditure, but analysis of the overall group would see no influence of either)(Roberts and Leibel, 1998). Twin studies in humans suggest that differences in weight gain in response to long-term overfeeding (of a fixed amount of added kcal/day) are influenced by genetic makeup (Bouchard et al., 1990). Even a very small imbalance between energy intake and energy expenditure can lead to obesity given sufficient time, therefore even small inaccuracies in measurement or methodology can lead to completely different outcomes. Therefore, although the majority of studies report no differences in energy expenditure between lean and obese subjects, it ultimately remains to be seen whether defects in energy expenditure contribute to obesity in humans.

Diet is a powerful regulator of adaptive thermogenesis. Resting metabolic rate can dramatically decrease upon starvation or underfeeding (Dulloo and Jacquet, 2001; Leibel et al., 1995; Shibata and Bukowiecki, 1987; Wadden et al., 1990), leading to an increase in metabolic efficiency and contributing to the reduced effectiveness of short-term calorie restrictive diets. Conversely, feeding or overfeeding dramatically increases metabolic rates and decreases metabolic efficiency in humans and rodents (Leibel et al., 1995; Shibata and Bukowiecki, 1987). Increased fat mass in obese subjects also appears to be associated with a small, but significant, reduction in the thermic effect of food (the post-prandial increase in energy expenditure associated with digestion, absorption, and increased sympathetic activity)(Segal et al., 1990; Segal et al., 1989). There is some evidence that diet-induced thermogenesis exists in humans and that energy expenditure does play a role in human obesity, from studies such as the Pima Indian study and twin studies (Bouchard et al., 1990; Leibel et al., 1995; Maffeis et al., 2001; Ravussin et al., 1988; Tataranni et al., 2003).

Organs that contribute most to adaptive thermogenesis are skeletal muscle, liver and BAT. Human newborns and small mammals use BAT for thermoregulatory heat production. In rodents at ambient temperatures, nearly one half of energy metabolism may be related to BAT (Foster and Frydman, 1979), which is arguably also the most important site of adaptive thermogenesis in these animals (Cannon and Nedergaard, 2004).

BAT and uncoupling protein 1

BAT was first recognized as a thermogenic organ in 1960s (Ball and Jungas, 1961; Smith and Hock, 1963). Brown adipocytes are multilocular lipid storage cells and are characterized by their high content of large mitochondria packed densly with cristae. BAT is a highly vascularized unique organ existing in all mammals. UCP1, a protein found predominantly in BAT, is the most critical feature differentiating BAT from white adipose tissue (WAT) and is considered to be the most physiologically relevant measure of BAT recruitment (Cannon and Nedergaard, 2004). The thermogenic function of BAT is primarily attributable to the 32kDa protein UCP1 (formerly known as 'thermogenin'), which is expressed in its mitochondria and acts as a proton carrier activated by free fatty acids. UCP1 disassociates or 'uncouples' the respiratory chain from ATP production, thus leading to heat production and a profound decrease in metabolic efficiency (Figure 1). UCP1's 'uncoupling' properties arise from its ability to serve as a proton leakage across the mitochondrial matrix, dissipating the proton gradient generated by the oxidation of fuel as a result of the electron transport chain. UCP1 is critical for rodents to maintain their body temperature during cold exposure (Enerback et al., 1997). UCP1 knockout mice do not become obese, even on a high-fat diet, suggesting that UCP1 is not necessary for body weight regulation (Enerback et al., 1997). However, UCP-DTA transgenic mice, with toxigene-mediated ablation of BAT, appear to have a defect in DIT and become obese when fed a high-fat diet (Hamann et al., 1996; Hamann et al., 1998). In parallel with metabolic efficiency, fasting leads to decreased UCP1 levels (Rothwell and Stock, 1982) whereas a calorie-dense"cafeteria" diet or high-fat diet leads to increases in UCP1 levels (Archer et al., 2005; Li et al., 2004; Margareto et al., 2001; Nedergaard et al., 1984; Portillo et al., 1998; Rippe et al., 2000; Rippe et al., 2003; Surwit et al., 1998). Furthermore, increased body weight and total body lipid content are significantly greater in UCP-DTA mice on a high-fat diet than the additive individual effects of a high-fat diet (in control mice) and decreased BAT (in chow-fed mice), suggesting a synergistic interaction between diet and decreased BAT. The discrepancies between the UCP1 knockout and the BAT-ablated models remain largely unexplained, but the evidence points toward an important, yet perhaps not critical, role for UCP1 in DIT and weight regulation.

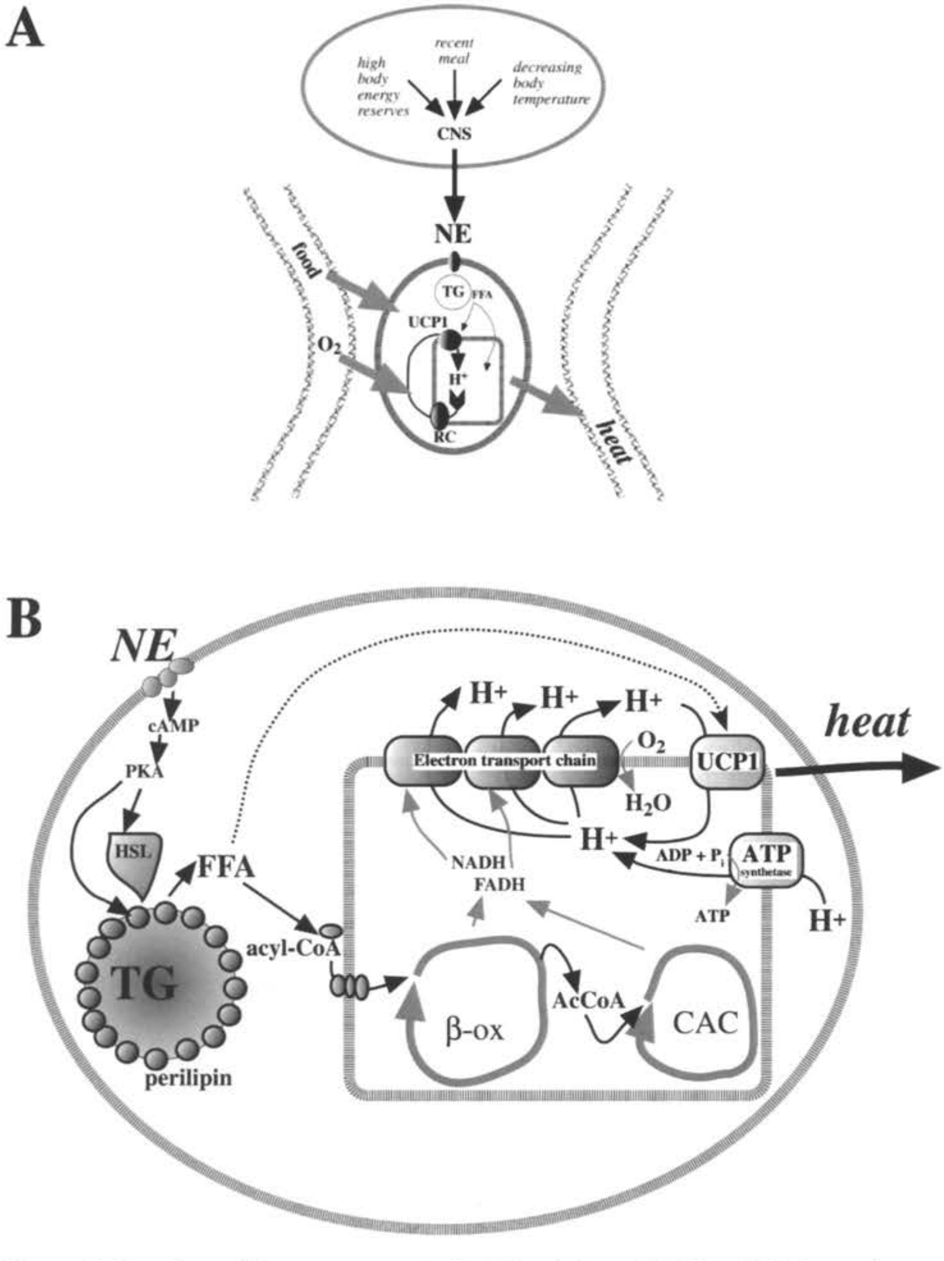

Figure 1: Overview of the acute control of BAT activity and UCP1. (**A**) Information on body temperature, feeding status, and body energy reserves is coordinated in the CNS. When there is reason to decrease metabolic efficiency or increase the rate of heat production, a signal is transmitted via the sympathetic nervous system to individual brown adipocytes. The released NE initiates triglyceride breakdown in brown adipocytes, primarily via β_3-adrenergic receptors. The intracellular signal is transmitted via cAMP and PKA (**B**), leading to the release from triglycerides (TG) of free fatty acids (FFA) that are both the acute substrate for thermogenesis and the regulators of UCP1 activity. FFA are activated to acyl CoAs which, through combustion via β•oxidation (β-ox) and the citric acid cycle (CAC), leads to the formation of the reduced electron carriers FADH and NADH, which are then oxidized by the electron transport chain, ultimately through oxygen consumption. This results in the pumping out of protons from the mitochondria and the formation of a proton-motive force that drives the protons back into the mitochondrial matrix through UCP1, thus uncoupling mitochondrial combustion from ATP production. The energy stored in the proton-motive force is released as heat. The outcome is that NE-induced stimulation of thermogenesis leads to an increased up-take of food and oxygen from the blood by BAT, which increases heat production. RC, respiratory chain; HSL, hormone sensitive lipase. Figure and text modified from (Cannon B, 2004).

Sympathetic control of BAT thermogenesis

In rodents, BAT is dispersed throughout the body as distinct pads, although they may be found within white adipose tissue depots to a varying degree in different animals or strains (Cannon and Nedergaard, 2004). Although they all have the same basic function, the interscapular BAT pads (IBAT) are the largest and most accessible of the BAT pads, and are therefore also the most studied. Each IBAT pad receives most of its innervation from sympathetic postgangionic neurons. Information about an animal's ambient temperature is sent, through peripheral thermal sensors, to specific hypothalamic and hindbrain areas. A series of neural circuits in other brain regions, such as the raphe pallidus (RPa), are then activated and stimulate preganglionic sympathetic nerves in the spinal cord (Morrison, 1999; Morrison, 2004). Preganglionic sympathetic nerves, located primarily in the intermediolateral cell column (IML) of the thoracic spinal cord, synapse onto postganglionic neurons located in in the stellate ganglion and thoracic paravertebral ganglia projecting through five posterior branches of the intercostal bundle to each IBAT pad. These postganglionic nerves innervate brown adipocytes to activate heat production.

The sympathetic nervous system (SNS) influences a range of functions, from body temperature to blood pressure regulation, via release of the neurotransmitters norepinephrine (NE) and epinephrine, which act on their receptors, the α- and β-adrenergic receptors. The SNS is thought to be one of the efferent pathways by which the brain regulates adaptive thermogenesis (Landsberg et al., 1984; Lowell and Bachman, 2003; Thomas and Palmiter, 1997) (Figure 2). BAT thermogenesis is entirely dependent on sympathetic stimulation. Surgical sympathetic denervation of BAT completely prevents the BAT thermogenic response to physiological stimuli such as cold exposure or increased caloric consumption (Rothwell and Stock, 1984). The SNS also regulates blood flow to BAT (and thus input as metabolic substrates for thermogenesis and output as heat delivery to the body), as well as BAT proliferation and differentiation, mitochondriogenesis, and expression of UCP1 (by phosphorylation of the transcription factor cAMP response element-binding protein (CREB)). The β-adrenergic receptors (βARs) control the ability of NE to stimulate adipocyte lipolysis and thermogenesis. The βARs are members of a large family of G protein-coupled receptors. Stimulation of the βARs by NE leads to increased lipolysis in white adipocytes and non-shivering thermogenesis in BAT. When NE binds to the β-adrenergic Gs-coupled receptors on the surface of BAT adipocytes, a cAMP-PKA-mediated pathway activates hormone-sensitive lipase (HSL), which in turn stimulates the release of free fatty acids from triglyceride. The intracellular free fatty acids activate UCP1 (overcoming the strong inhibition by purine nucleotides) and are used as the substrates of thermogenesis as they enter the β-oxidation cycle in the mitochondria. The NE-activated cAMP-PKA-mediated pathway also increases UCP1 transcription via the cAMP response element binding protein (CREB) and the cAMP response element (CRE). The binding of peroxisome proliferator-activated receptor-γ (PPAR-γ), a nuclear receptor expressed in white and brown fat, and PPAR-γ co-activator (PGC-1) are critical for the UCP1 enhancer function.

The three βAR subtypes are all expressed in white and brown adipocytes, but unlike

β_1AR and β_2AR, which are widely expressed, the β_3AR, first discovered in 1989 (Emorine et al., 1989), is found predominantly in brown adipocytes. Oxygen consumption is elevated in wild-type mice after treatment with a β_3-adrenergic agonist, but not in UCP1-knockout mice, suggesting that UCP1 is entirely responsible for the β_3-adrenergic agonist induced increase in oxygen consumption (Inokuma et al., 2005). Acute or chronic selective β_3AR agonist treatment, which is associated with increased density of BAT UCP1 within typically WAT depots (Champigny et al., 1991; Collins et al., 1997; Fisher et al., 1998; Himms-Hagen et al., 1994; Sasaki et al., 1998), is able to prevent or reverse obesity and hyperglycemia and stimulate thermogenesis, without affecting food intake (Arch et al., 1984; Collins et al., 1997; Collins and Surwit, 1996; Himms-Hagen et al., 1994; Inokuma et al., 2005; Sasaki et al., 1998). Mice that lack all three βAR subtypes (β-less mice) do develop a mild obesity (mostly from increased body fat), increased leptin levels, decreased oxygen consumption, decreased UCP1 protein levels and a failure to increase UCP1 levels with cold exposure, without affecting food intake, thyroid levels or physical activity (Bachman et al., 2002). Unlike mice deficient in norepinephrine (NE) and epinephrine (affecting both α- and β-adrenergic receptor activation), which do not have a propensity to become obese on a high-fat diet (Ste Marie et al., 2005), β-less mice have a defect in diet-induced thermogenesis and when fed a high-fat diet gain twice as much as predicted from the combined effects of diet and genotype (Bachman et al., 2002) (Figure 3).

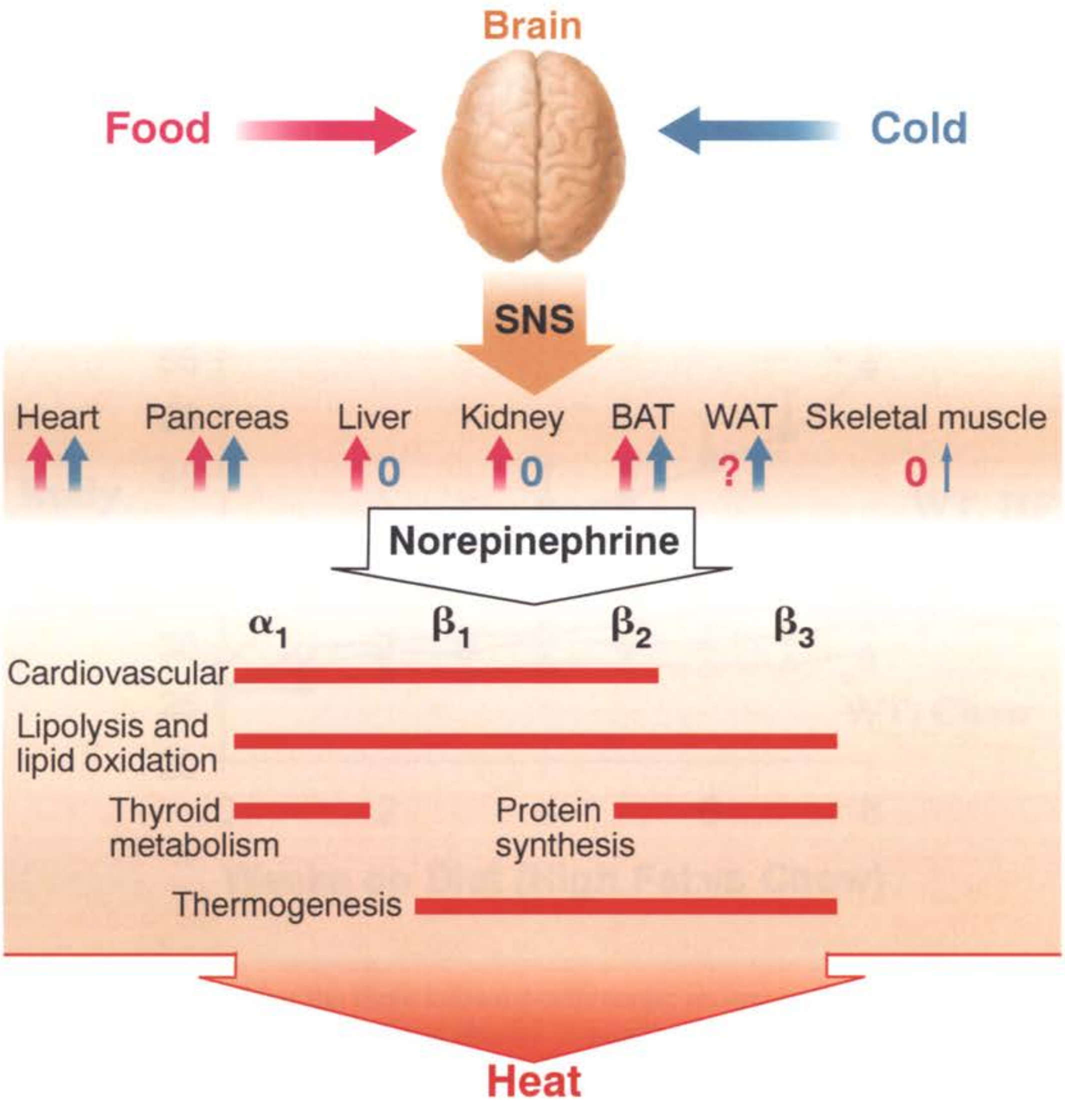

Figure 2: Activation of thermogenesis by the sympathetic nervous system (SNS). In response to food (pink) or to cold (blue), SNS activity increases in a variety of tissues and organs. The thick and thin arrows depict marked and mild increases in SNS activity, respectively. SNS activity has been assessed with techniques that measure the 24-hour turnover of the SNS neurotransmitter norepinephrine (NE) in rat heart, pancreas, liver, kidney, brown adipose tissue (BAT), white adipose tissue (WAT), and skeletal muscle. No change or an unknown change in SNS activity is indicated by the by the symbols "0" and "?", respectively. Through release of NE, which acts on some or all of the four adrenergic receptors (α, β_1, β_2, β_3) present in these tissues, the activated SNS coordinates cardiovascular and metabolic events. These events cooperate to increase heat production: both cold-induced (nonshivering) thermogenesis and diet-induced thermogenesis (DIT). From (Dulloo and Jacquet, 2001)

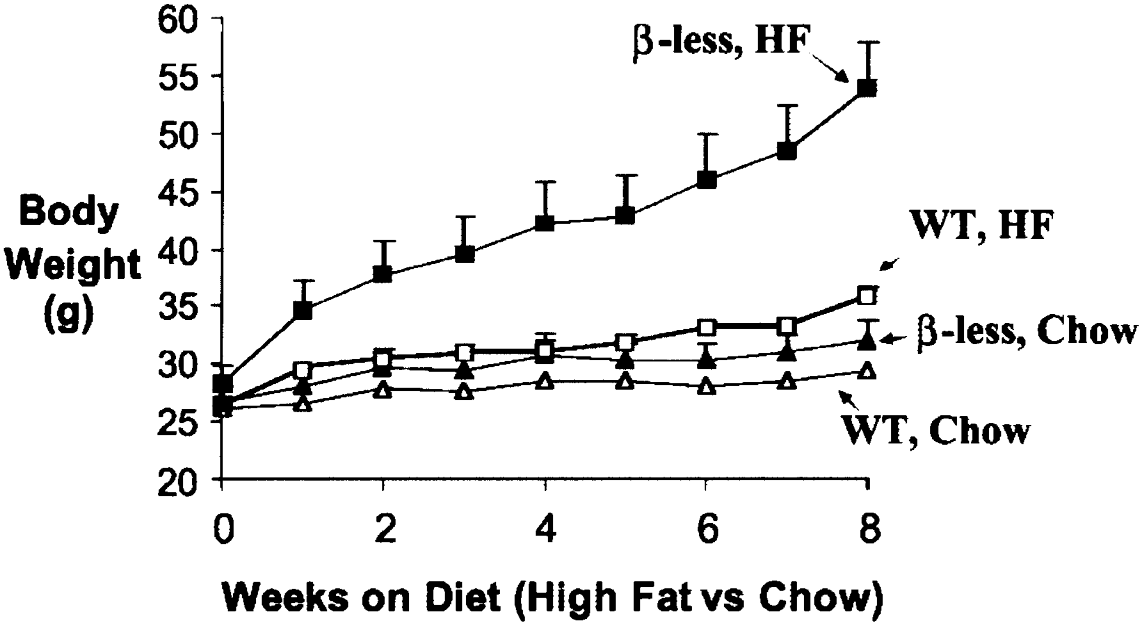

Figure 3: Mice lacking the three known β-adrenergic receptors (β-less) mice are extremely sensitive to diet-induced obesity. 3-month-old male wild-type (WT) control and β-less mice were fed a normal chow (12%kcal from fat) or a high-fat (HF) (58% kcal from fat) diet (n=8 in each group) for 8 weeks. The β-less mice, but not the WT mice, developed massive obesity (final body weight= 53.84±3.9 versus 35.7±0.9g; P values are <0.05 at all time points compared to WT mice). All data are the mean ±SEM. From (Bachman et al., 2002)

Energy expenediture and the hypothalamic-pituitiary-thyroid axis

Thyroid hormones are also important in the regulation of energy expenditure and act synergistically with the SNS to control obligatory and adaptive thermogenesis (Lowell and Spiegelman, 2000; Rehnmark et al., 1990). Thyroid hormones have metabolic effects in various organs, such as increased lipolysis in adipose tissue and increased cardiac contractility, and they generally increase the activity of membrane-bound Na^+-K^+ATPase, thereby increasing heat production and stimulating oxygen consumption (Brent, 1994). Thyroid hormone secretion is stimulated by pituitary thyroid-stimulating hormone (TSH). TSH secretion (and its increased biological activity) is in turn stimulated by the hypothalamic peptide thyrotropin-releasing hormone (TRH). The thyroid gland synthesizes the hormones 3,5,3'-triiodothyronine (T_3) and 3,5,3',5'-tetraiodothyronine (thyroxine, or T_4). Free T_4 and T_3 are in equilibrium with the protein-bound hormones in plasma and tissue and circulate in much smaller concentrations. It is the free (unbound) T_4 and T_3 in plasma which are physiologically active and which inhibit TSH secretion by the pituitary by regulating the biosynthesis of TRH in the hypothalamus. The thyroid gland secretes about 20 times more T_4 than T_3, and 87% of circulating T_3 is derived from peripheral conversion of T_4 to T_3. T_3 is more potent than T_4. Almost all, 99.98%, of the circulating T_4 is bound to thyroxine-binding globulin and other plasma proteins, so that the biological half-life of free T_4 is much longer (6-7 days) than that of T_3 (30 hours), which is 99.8% protein-bound. The effects of T_4 and T_3 and those of the catecholamines epinephrine and NE are closely connected. They both increase the metabolic rate and stimulate the nervous system and heart. The transcriptional effects of T_3 can also lead to increased density and responsiveness of β-ARs (Bahouth, 1991; el Hadri et al., 1996; Kanasaki et al., 1994; Wahrenberg et al., 1986; Wahrenberg et al., 1994).

Although T_3 has been reported to be able to vigorously stimulate UCP1 expression with only minimal SNS involvement (Branco et al., 1999), UCP1 transcriptional regulation is generally thought to rely on the synergism between T_3 and NE (Bianco et al., 1988; Lanni et al., 2003), which relies on functional T_3-response elements (TREs) and CREB in the UCP1 gene promoter (Cassard-Doulcier et al., 1994; Rabelo et al., 1995; Rim and Kozak, 2002). BAT was relatively recently recognized as a major target for T_3 (Bianco et al., 1992; Bianco et al., 1988; Carvalho et al., 1991). The physiological effects of T_3 within cells often occur at the transcriptional level upon binding to thyroid hormone receptors (TRα and TRβ) belonging to the superfamily of nuclear hormone receptors. TRα1 and TRβ, which are expressed in BAT, are essential for normal adrenergic responsiveness to cold exposure and for mediating T_3 induced UCP1 expression respectively (Ribeiro et al., 2001). BAT expresses thyroid hormone receptor and type II T_4 5'-deiodinase (DII), which catalyzes the conversion of T_4 to the more biologically active T_3. DII is also activated by the SNS and inhibited by its substrate, T_4. In rats, T_3 produced in BAT accounts for about half of the total systemic conversion of T_4 to T_3 (Silva and Larsen, 1985).

Hypothalamic TRH plays a critical role in the regulation of the HPT axis. In the parvocellular PVH, TRH is synthesized from prothyrotropin releasing hormone (proTRH) by prohormone convertase (PC) 1/3 and PC2 (Nillni et al., 1995; Nillni and

Sevarino, 1999; Schaner et al., 1997). TRH neurons in the PVH project to the median eminence where they release TRH into the hypohysial-portal system and stimulate the production and secretion of thyroid stimulating hormone (TSH) in the pituitary. TSH, in turn, stimulates thyroid hormone synthesis and release from the thyroid gland. TRH is also regulated by nutritional states. To conserve energy during food deprivation, TRH expression in the PVH, and the subsequent large reduction in thyroid hormone levels in rodents, decreases their metabolic rate (Blake et al., 1991). The decrease in proTRH by fasting is reversed with leptin administration (Ahima et al., 1996), which upregulates TRH gene expression in the PVH (Legradi et al., 1997). Leptin can directly stimulate proTRH gene expression by activating transcription at the signal transducer and activator of transcription 3 (STAT3) response element on the TRH promoter (Guo et al., 2004). Fasting-induced suppression of proTRH expression can also be completely reversed to normal fed levels with ICV administered α-MSH (Fekete et al., 2000). In addition to leptin receptors, TRH neurons in the PVH express MC4R and are densely innervated by α-MSH-containing and AGRP-containing axon terminals in both rats and humans, which are also leptin-responsive (Fekete et al., 2000; Harris et al., 2001; Legradi and Lechan, 1999; Mihaly et al., 2000). Additionally, NPY and AGRP, produced in the ARC and induced during fasting, are potent negative regulators of TRH gene expression in the PVH (Fekete et al., 2001; Fekete et al., 2002a). G-protein coupled MC4R signaling increases preproTRH expression through CREB phosphorylation (Harris et al., 2001) which then binds a cAMP response element (CRE) and activates transcription at the TRH promoter. Leptin-stimulated TRH release in neuronal cultures is partially inhibited by the MC4R antagonist SHU9119 (Nillni et al., 2000). These data suggest that in addition to direct regulation of TRH expression, leptin can also indirectly regulate TRH expression via the melanocortin system (Figure 4). The melanocortin system's ability to regulate the hypothalamic-pituitary-thyroid (HPT) axis will be discussed in further detail in chapter two.

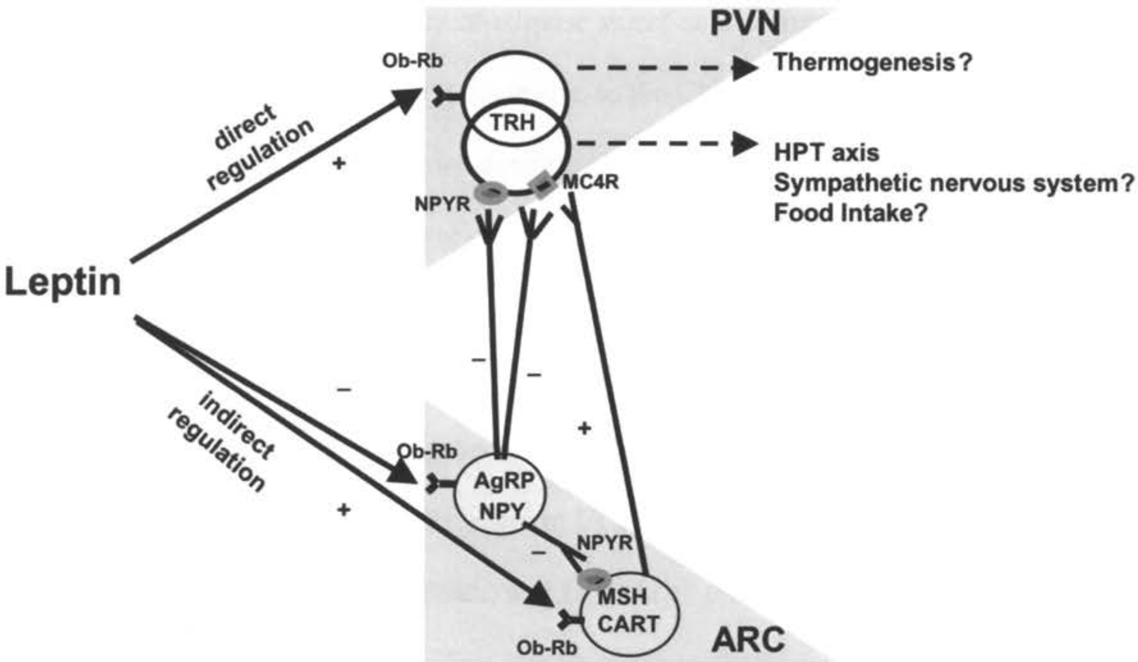

Figure 4: Proposed model of leptin action on prothyrotropin releasing hormone (proTRH) neurons located in the paraventricular hypothalamic nucleus (PVN). AgRP, Agouti-related protein; NPY, Neuropeptide Y; MSH, α-melanocyte-stimulating hormone; CART, cocaine and amphetamine regulated transcript; ARC, hypothalamic arcuate nucleus. From (Perello M, 2006)

Leptin, MC4R and BAT

Serum leptin levels are decreased with fasting and increased with obesity and play a critical role in signaling the amount of adipose stores and/or signaling the process of fat accumulation in adipocytes and adipocyte size to the CNS (Mantzoros and Moschos, 1998). *Lep^{ob}/Lep^{ob}* and MC4R-/- mice develop obesity even when pair-fed to wild-type controls, suggesting that both rodent obesity models have a defect in balancing energy expenditure with intake (Coleman, 1978; Ste Marie et al., 2000). Leptin's role in activating BAT thermogenesis is well documented. *Lep^{ob}/Lep^{ob}* mice completely lose the ability to thermoregulate when exposed to cold temperatures (Trayhurn et al., 1977). *Lep^{ob}/Lep^{ob}* mice have a profound decrease in UCP1 levels and BAT-mediated thermogenesis (Commins et al., 1999b) and *Lep^{ob}/Lep^{ob}* mice treated with leptin acutely acitvate BAT thermogenesis, including increased sympathetic nerve activity, increased NE turnover and increased UCP1 (Collins et al., 1996; Commins et al., 1999a; Haque et al., 1999; Minokoshi et al., 1999; Rouru et al., 1999; Scarpace and Matheny, 1998; Scarpace et al., 1997; Wang et al., 1997), which is absent when treating UCP1-ablated mice with leptin (Commins et al., 2001). Therefore UCP1 is necessary for leptin-induced thermogenesis in rodents. Leptin is thought to stimulate BAT thermogenesis and metabolic rate through its ability to activate the sympathetic nervous system, leading to activation of pregangionic neurons in the spinal cord (Haynes et al., 1997). Several hypothalamic regions innervate the sympathetic preganglionic neurons in the thoracic spinal cord, including the PVH and the LH (Cechetto and Saper, 1988; Saper et al., 1976;

Strack et al., 1989).

Leptin is also known to mediate some of the central melanocortin system's effects on regulation of energy homeostasis (Fan et al., 1997; Seeley et al., 1997). Leptin receptor is expressed in POMC neurons (Cheung et al., 1997) and NPY/AGRP neurons (Hakansson et al., 1998; Mercer et al., 1996) in the ARC nucleus. Leptin activates POMC/CART neurons in the ARC (Mizuno et al., 1998; Schwartz et al., 1997; Thornton et al., 1997) that project to the PVH, the LH, the retrochiasmatic area (RCA) and spinal sympathetic pre-ganglionic neurons (SPNs) (Elias CF, 1998; Elmquist, 2001; Seeley et al., 1997). When PRV is injected into IBAT, retrogradely labeled PRV-infected cells in the RCA and lateral ARC were found to co-localize extensively with POMC cells (37%), leptin receptor (69%) and cocaine and amphetamine-related transcript (CART) (79%) (Oldfield et al., 2002). Increasing evidence suggests that the MC4R mediates at least some of leptin's activation of BAT, particularly through stimulation of UCP1 (Satoh et al., 1998; Li et al, 2003)(Ste Marie et al., 2000; Zhang et al., 2005). The MC3R, on the other hand, does not appear to mediate leptin's ability to increase UCP1 expression (Zhang et al., 2005). Overall, these results indicate that MC4R expressing neurons, including those in the PVH, might be mediating at least part of leptin's stimulatory effect on BAT thermogenesis, although, in one study, 3rd ventricle ICV administration of the MC3R and MC4R antagonist, SHU9119, did not inhibit leptin-induced BAT sympathoexcitation (Haynes et al., 1999). Unlike MC4R-/- mice, however, Lep^{ob}/Lep^{ob} mice exhibit a normal increase in oxygen consumption when switched from a low-fat to a high-fat diet and do not exhibit the same increase in weight gains, suggesting that leptin is not involved in acute DIT (Butler et al., 2001).

Neuroanatomy of the melanocortin system

As previously mentioned, there are two sites of POMC expression in the brain: the hypothalamic ARC, which contains most of the POMC neurons, and the brain stem NTS. ARC POMC neurons, many of which co-express CART, send fibers to most of the other hypothalamic nuclei, with particularly dense fibers seen in the periventricular nucleus, the PVH and the perifornical regions (reviewed in (Cone, 2005; Ellacott and Cone, 2004)) (Figure 5). ARC POMC neurons also send large fiber bundles to nuclei in the septal region, including the bed nucleus of the stria terminalis (BST) and the lateral septal nucleus. More caudally, POMC fibers project to the periventricular nucleus of the thalamus and through the medial amygdyla (MeA). POMC fibers project to the brainstem via two descending bundles: Through the periaquaductal gray (PAG) and dorsomedial tegmentum, which innervate the rostral NTS and lateral reticular nucleus (A5-C1 regions), and the ventral tegmental area, which innervate the rostral NTS, the ventrolateral medulla (A1 region), the nucleus ambiguous and the IML of the spinal cord (Broberger and Hokfelt, 2001; Cechetto and Saper, 1988; Swanson and Kuypers, 1980). Dual innervation from the ARC and brainstem POMC neurons are found at the locus coeruleus, the parabrachial nucleus, the paragigantocellular nucleus, the rostral NTS, the dorsal motor nucleus of the vagus and the lateral reticular nucleus (Joseph and Michaël, 1988; Palkovits and Eskay, 1987). The MC4R is expressed throughout the brain, including all the areas known to receive POMC projections (Kishi et al., 2003; Mountjoy et al., 1994). NPY/AGRP neurons send fibers to many, but not all, of the same sites as

ARC POMC neurons, including dense projections to the PVH, DMH, BST and lateral septal nucleus (Broberger et al., 1998b; Haskell-Luevano et al., 1999).

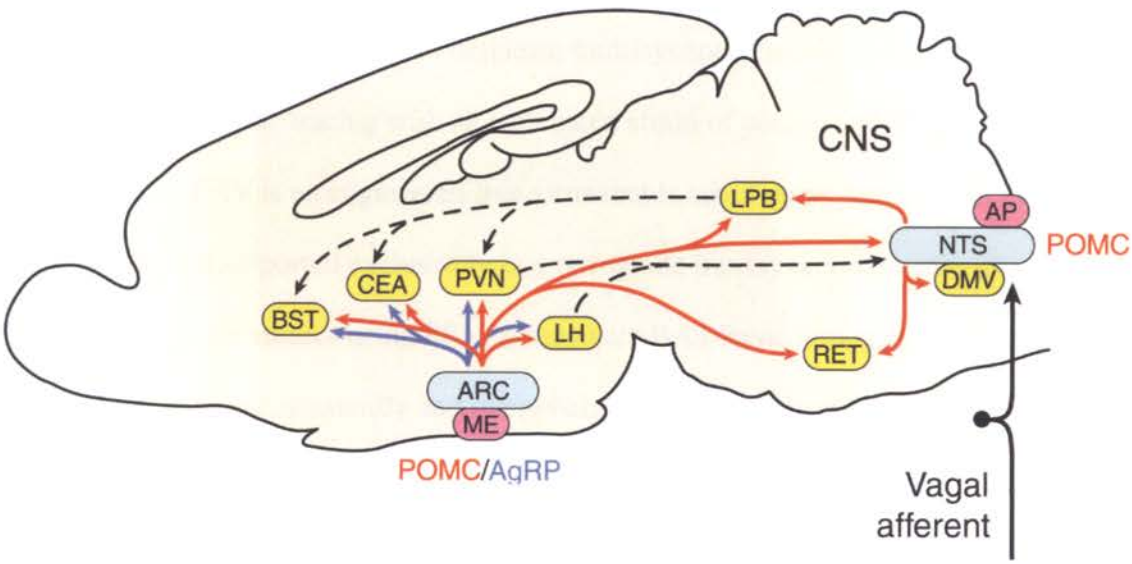

Figure 5. Schematic of the central melanocortin system circuitry. POMC neurons in the hypothalamic arcuate nucleus (ARC) and the nucleus tractus solitarius (NTS) in the brainstem receive and integrate humoral signals. Blue, nuclei containing POMC neurons; magenta, circumventricular organs adjacent to POMC neurons; yellow, a small sample of representative nuclei containing MC4R-positive neurons that may serve to integrate adipostatic and satiety signals; red arrow, representative POMC projections; blue arrows, representative AgRP projections; dashed arrows, secondary projections linking POMC neurons in hypothalamus and brainstem with common effector sites; AP, area postrema; BST, bed nucleus of the stria terminalis; CEA, central nucleus of the amygdala; DMV, dorsal motor nucleus of the vagus; LH, lateral hypothalamic area; LPB, lateral parabrachial nucleus; ME, median emininence; PVN, paraventricular nucleus of the hypothalamus; RET, reticular nucleus. Figure modified from (Cone, 2005)

Pseudorabies virus as a tool for the discovery of polysynaptic circuits

The central circuitry regulating BAT thermogenesis has been extensively studied. One of the most powerful methods used to delineate multisynaptic circuits in the brain has been the use of transynaptic tracing with an attenuated strain of pseudorabies virus (PRV). The attenuated PRV is an engineered live virus that is taken up by terminals at the site of injection and is transported exclusively in a retrograde transsynaptic manner (Strack et al., 1989). Previous studies using PRV to inoculate BAT have demonstrated that the stellate ganglion are consistently and overwhelmingly of the phenotype associated with the innervation of adipocytes (containing tyrosine hydroxylase and calbindin, but not NPY) and rarely of the phenotype shown to project to blood vessles (containing tyrosine-hydroxylase and NPY, but no calbindin) (Grkovic and Anderson, 1997; Oldfield et al., 2002). This suggests that although BAT has a rich supply of blood vessels, PRV exhibits a specificity for neurons innervating adipocytes, which comprises 80% of the tissue volume. Transynaptic retrograde tracing using PRV is a time-dependent process (Aston-Jones and Card, 2000; Card et al., 1993). In BAT-injected rats sacrificed after short PRV post-inoculation periods, or early survival times (2-3 days), second order neurons are labeled, intermediate survival times (3-4 days) label third order neurons and late survival times (4-5 days) label fourth order neurons (Cano et al., 2003; Oldfield et al., 2002). Animals are generall not kept at survival times of longer than 6 days in order to prevent the animals from getting too ill. This type of temporal analysis has been carried out in a number of organs and tissues, including BAT, and is an effective tool in establishing the hierarchical order of neurons in a multisynaptic circuitry.

BAT and the melanocortin system

The central control of the sympathetic outflow to BAT in the rat is exerted largely by the hypothalamic nuclei (Amir, 1990a; Amir, 1990b; Amir, 1990c; Amir and De Blasio, 1991; Amir et al., 1989; Perkins et al., 1981; Sakaguchi et al., 1988; Yoshimatsu et al., 1993) (which are critically involved in the regulation of thermogenesis, energy homeostasis and feeding behavior) and by central noradrenergic and serotonergic pathways in the brainstem and pons (Cano et al., 2003; Fyda et al., 1991; Morrison, 1999; Morrison, 2001a; Morrison, 2001b; Sahakian et al., 1983). Retrograde labeling of the neural circuitry after PRV injection into BAT (Cano et al., 2003) contains many areas that overlap with the melanocortin system circuitry, including the PVH, RPa, RVLM, gigantocellular reticular nucleus and A5 region at early survival times; the ARC, LH, DMH, PAG, paragigantocellular nucleus, locus coeruleus, and NTS at intermediate survival times; and the preoptic area, posterior hypothalamus, parabrachial nucleus, BST and area postrema at long survival times. The overlapping circuitry between the central melanocortin and SNS-BAT circuitries, in combination with the melanocortin system's role in the regulation of energy expenditure, the defect in DIT observed in MC4R-/-, and evidence from a series of pharmacological studies looking at the effects of melanocortin agonists and antagonists on the regulation of UCP1 (which will be discussed in the following chapter) together strongly suggest the melanocortin system's involvement in the regulation of BAT thermogenesis (Figure 6).

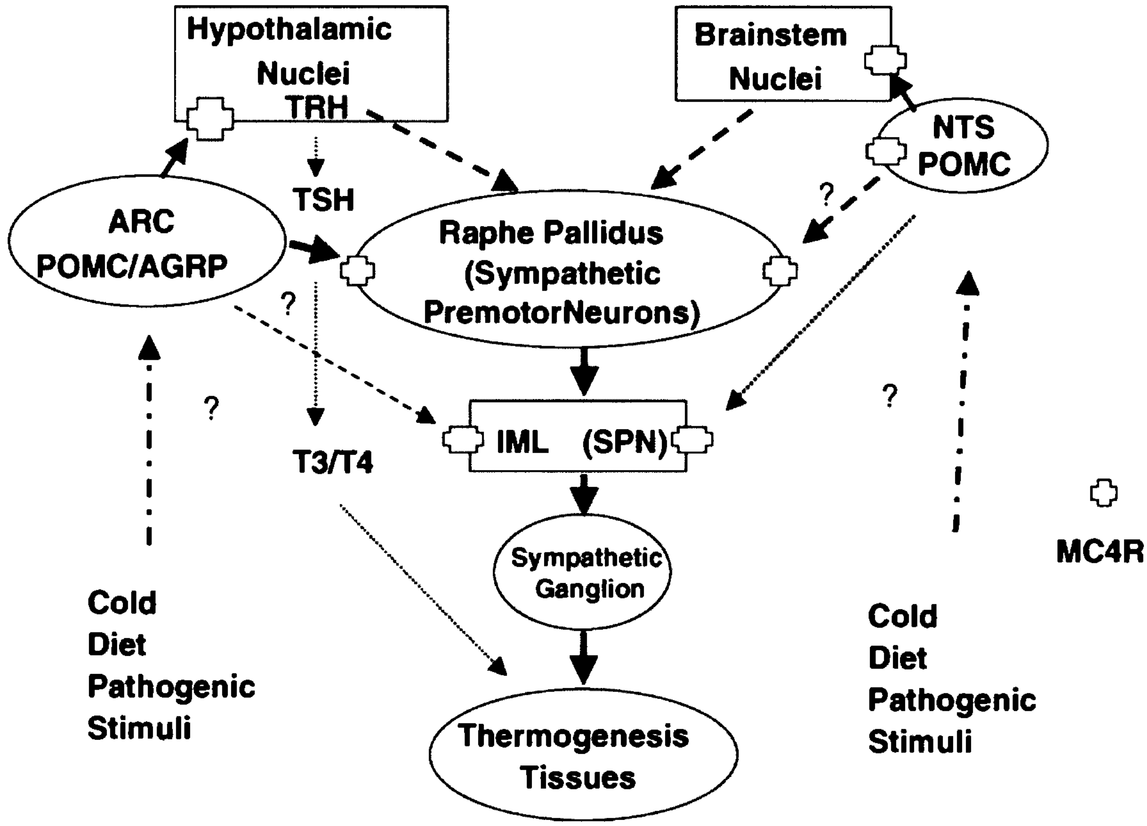

Figure 6: Model for the hypothesized regulation of adaptive thermogenesis by the central melanocortin system. Multiple circuits exist by which the central melanocortin system regulates thermogenesis in effector tissues such as BAT. These include neuroendocrine pathways as well as direct and indirect projections from POMC and/or MC4R-expressing neurons to the sympathetic premotor neurons in the raphe pallidus and/or to the sympathetic preganglionic neurons (SPN) in the intermediolateral nucleus (IML). Changes in dietary content, for example, may recruit multiple neurohumoral signal pathways to activate the central melancortin system, which, in turn, could increase sympathetic outfow to thermogenic target tissues, and/or activate the TRH-TSH-T_3 axis, to dissipate excess ingested energy and thereby maintain energy homeostasis. From (Fan et al., 2005)

SPECIFIC AIMS AND OUTLINE OF THE THESIS

On a moderate fat diet wild-type C57BL/6J mice maintain energy homeostasis while melanocortin-4 receptor null (MC4R-/-) on the same background gain weight at a rapid rate, unable to compensate for increased caloric content (Butler et al., 2001). MC4R-/- mice have a profound defect in acute diet-induced thermogenesis caused by a failure to increase their basal and total oxygen consumption in response to an increase in dietary fat, but it is not understood what the underlying cause(s) of this defect is. In rodents at ambient temperatures, nearly one half of energy metabolism may be related to BAT, which is arguably also the most important site of adaptive thermogenesis in these animals. In wild-type animals, high-fat, or 'cafeteria', diets are known to induce an up-regulation of mitochondrial UCP1 levels in intrascapular brown adipose tissue (IBAT) (Archer et al., 2005; Li et al., 2004; Margareto et al., 2001; Nedergaard et al., 1984; Portillo et al., 1998; Rippe et al., 2000; Rippe et al., 2003; Surwit et al., 1998). At the same time, a variety of pharmacological studies have implicated the central melanocortin system in the regulation of UCP1 (Haynes et al., 1999; Small et al., 2001; Williams et al., 2003; Yasuda et al., 2004). The melanocortin system has also been implicated as a mediator of TRH regulation (Fekete et al., 2000; Fekete et al., 2002a; Harris et al., 2001; Legradi and Lechan, 1999; Mihaly et al., 2000). Thyroid hormones are also important in the regulation of energy expenditure, and UCP1 transcriptional regulation relies on the synergism between T_3 and NE (Lanni et al., 2003). In this study we have combined neuroanatomical, physiological and pharmacologic approaches to delineate the circuitry through which the central melanocortin system may regulate IBAT thermogenesis and reveal the potential physiological roles of the central melanocortin system in the regulation of adaptive thermogenesis of BAT.

The goals of this thesis are to:

1. Define the specific neuronal circuitry between MC4R-expressing neurons in the CNS and IBAT and determine their hierarchical anatomy.
2. Determine the physiological roles of the central melanocortin system in the regulation of UCP1 under physiological conditions that are known to trigger BAT thermogenesis, in particular diet-induced thermogenesis and cold-induced thermogenesis.
3. Assess the putative role of the hypothalamic-pituitiary-thyroid axis in the melanocortin-mediated regulation of UCP1 expression in response to a high-fat diet.
4. Determine in what brain regions the MC4R is co-expressed with glutamic acid decarboxylase (GAD) and whether POMC and NPY/AGRP neurons modulate GABA release by directly contacting MC4R positive GABA interneurons in the PVH.

CHAPTER ONE

Anatomical circuitry between central melanocortin-4 receptor expressing regions and interscapular brown adipose tissue

Adriana Voss-Andreae, Roger D. Cone and Wei Fan

ABSTRACT

The melanocortin system has been shown to play an important role in regulating energy homeostasis in both rodents and humans. There have been a wealth of studies examining the melanocortin system's role in food intake, but little is known about the mechanisms that the melanocortin system uses in its regulation of energy expenditure. Here we use a neuroanatomical approach to demonstrate that specific subsets of MC4R-expressing neurons in various nuclei of the CNS that regulate sympathetic outflow are poly-synaptically associated with interscapular brown adipose tissue (IBAT). The attenuated psuedorabies virus (PRV) trans-synaptic retrograde tracing was performed in MC4-R-green fluorescent protein (MC4R-GFP) transgenic mice, which express GFP under control of the MC4R promoter. PRV was injected into IBAT and, in combination with dual immunohistochemistry (IHC) and fluorescent visualization techniques, the number of MC4-R positive neurons that contain PRV immunoreactivity were determined. First-, second- and third-order neurons were distinguished based on variations in duration of infection. We found extensive co-localization of PRV and MC4R in a number of areas including in the intermediolateral cell column (IML) of the thoracic spinal cord, paraventricular hypothalamic nucleus (PVH), gigantocellular reticular nucleus (Gi), and the raphe pallidus (RPa) at the earliest post-infection stages. Areas of co-localization at intermediate stages post-infection include the nucleus of the solitary tract (NTS), periaqueductal gray (PAG), and lateral hypothalamic area (LH). Areas of co-localization in the late stage post-infection include the dorsomedial hypothalamic nucleus (DMH), the lateral parabrachial nucleus and the locus coeruleus. The results of this study help to define the neuronal circuits and provide the neuroanatomic substrate through which the

melanocortin system regulates an important thermogenic effector site, IBAT.

INTRODUCTION

A number of pharmacological studies provide evidence that the melanocortin system is involved in mediating interscapular brown adipose tissue (IBAT)-induced thermogenesis. For example, chronic and acute central administration of melanocortin agonists and antagonists (including AGRP) cause an increase or decrease, respectively, in uncoupling protein-1 (UCP1) expression levels, oxygen consumption and IBAT sympathetic nerve activity (Baran et al., 2002; Cettour-Rose and Rohner-Jeanrenaud, 2002; Cowley et al., 1999; Haynes et al., 1999; Li et al., 2004; Small et al., 2001; Williams et al., 2003; Yasuda et al., 2004; Zhang et al., 2004). Additionally, mice with post-embryonic ablation of agouti related peptide (AGRP) neurons have increased UCP1 expression in addition to reduced total body fat and plasma insulin (Bewick et al., 2005). The melanocortin-4-receptor (MC4R) appears to also mediate at least part of leptin's activation of IBAT through stimulation of UCP1 (Li et al., 2003; Satoh et al., 1998; Ste Marie et al., 2000). The MC4R is expressed in numerous brain regions including areas known to regulate autonomic activity and thermoregulation, in addition to feeding behavior (Kishi et al., 2003; Liu et al., 2003; Mountjoy et al., 1994). These regions include a number of areas known through viral retrograde tracing studies to provide inputs to IBAT (Bamshad et al., 1999; Cano et al., 2003; Oldfield et al., 2002)(Figure 1). A subset of areas known to express the MC4R (Kishi et al., 2003; Liu et al., 2003) and known to innervate IBAT, are also activated by cold exposure (Cano et al., 2003) (Figure 2). These areas include the paraventricular hypothalamus (PVH), raphe pallidus (RPa), periaqueductal grey (PAG), the dorsomedial hypothalamus (DMH), the preoptic area (POA), the lateral parabrachial nucleus and the medial part of the nucleus tractus solitarius (NTSm).

Although it has been shown that the melanocortin system is key to both short-term and long-term energy regulation at hypothalamic and caudal brainstem nuclei, and that IBAT appears to be a site of action in the melanocortin system's regulation of energy homeostasis, very little is known about the central circuitry used by the melanocortin system in its regulation of IBAT-mediated thermogenesis. The attenuated PRV-Bartha is a powerful tool that has been used extensively for defining multisynaptic circuitry in a number of systems and is transported exclusively in a time-dependent retrograde trans-synaptic fashion (Aston-Jones and Card, 2000). This study uses a neuroanatomical approach to define the circuitry through which the central melanocortin system circuits innervate IBAT. Attenuated pseudorabies (PRV) trans-synaptic retrograde tracing was used to map the polysynaptic pathways between IBAT and MC4R expressing regions in the brain and spinal cord. First-, second- and third-order sympathetic neurons were distinguished based on careful timing of the animal survival times.

MATERIALS AND METHODS

Animals

C57BL/6J mice were maintained in a standard 12-hour light-dark cycle with *ad libitum* access to food (Harlin Teklad's standard laboratory mouse chow H8604) and water.

PRV injections

Work with the active virus was conducted in a Biosafety level 2 containment facility dedicated exclusively to these experiments and the health of the animals was carefully monitored through the post-inoculation period. All procedures conformed to National

Institutes of Health Guide for the Care and Use of Laboratory Animals and were approved by the Institutional Animal Care and Use Committee of OHSU.

Under full anesthesia with ketamine hydrochloride, MC4R-GFP mice (kindly provided by Dr. Jeffrey Friedman, Rockerfeller University, NY, NY) received a series of injections with attenuated PRV (PRV-Bablue, kindly provided by Dr. Lynn Enquist, Princeton University, Princeton, NJ and grown by Dr. Todd Wisner and Dr. David Johnson, OHSU, Portland, OR) into the left and right upper site of the exposed IBAT. $2x10^9$ pfu/ml of PRV was used in a total of 200nl per injection at 6 injection sites per IBAT pad, using a 30-gauge needle connected to a Hamilton syringe, as adapted from previously described methods (Bamshad et al., 1999; Card et al., 1993; Loewy et al., 1994; Oldfield et al., 2002). Injections were made carefully under magnification and the injection site subsequently cleaned with saline-soaked swabs and the skin sewn closed. To confirm the specificity of the circuits traced by the virus, two animals used in negative control experiments underwent a sympathectomy by bilaterally severing the five branches of the sympathetic nerves innervating their IBAT. The time course of infection was empirically determined by carefully observing the pattern of infection at exactly 2, 3, 4 and 5 day survival times. The animals were then sacrificed under deep anesthesia with ketamine hydrochloride and transcardially perfused with 0.9% saline followed by 4% paraformaldehyde-borate fixative (pH 9.5) through the left ventricle of the heart. Brains and spinal cords were removed and post-fixed for two hours in 4% paraformaldehyde-borate and overnight in a 20% sucrose solution at 4°C, before being processed for immunohistochemical (IHC) visualization.

Fluorescence immunohistochemistry

To determine which PRV-IR positive neurons co-express the MC4-R-GFP, distinct fluorochromes were used for PRV and GFP. IHC was performed using standard procedures. Briefly, post-fixed brains and spinal cords were blocked, sliced into 30 μm coronal sections on a freezing-stage sledge microtome and collected into eight serially ordered sets of sections. A 1:8 series of sections were incubated at 4°C overnight in potassium phosphate buffered saline (KPBS; pH 7.4) containing 2% normal donkey serum and 0.4% Triton-X-100 (LKPBS), followed by incubation with guinea-pig polyclonal antibody against PRV (1:5000; NIAID, Bethesda, MD) and a rabbit polyclonal antibody against GFP (1:10,000; Molecular Probes, Eugene, OR) in LKPBS for 72 hours at 4°C. Sections were then rinsed several times in KPBS lasting one hour followed by incubation with Cy3-conjugated donkey anti-guinea pig immunoglobulin G (IgG; 1:2000; red fluorescence; Jackson ImmunoResearch Laboratories, West Grove, PA) and Alexafluor 488 conjugated donkey anti-rabbit IgG (H+L) (1:1000; green fluorescence; Molecular Probes; Eugene, OR) in KPBS containing 0.4% Triton-X-100 for one hour at room temperature. Sections were then rinsed thoroughly in KPBS. All sections were mounted onto gelatin-coated slides, air-dried and coverslipped with mounting media (Biomeda, Foster city, CA). Immunofluorescence was visualized by using a Zeiss Axioplan photomicroscope with a filter set for visualization of Alexafluor 488 (excitation range: 425-525 nm, emission range 500-600 nm) and Cy3 (excitation range: 500-560 nm, emission range: 560-650 nm). PRV-IR is identified as red fluorescence, and MC4R neurons are recognized by green fluorescence. Images were overlayed using Adobe Photoshop and double-labeled neurons are presented as yellow. High magnification analysis was used to determine whether overlapping yellow images were due to colocalization in the same neuron or overlap of independently labeled neurons.

RESULTS

Spinal cord and brain regions co-expressing MC4R-GFP and PRV following inoculation of IBAT

100% of twelve male MC4-RGFP mice injected with PRV became infected. We did not observe as much variability in the extent of infection within each survival interval as reported in other studies (Bamshad et al., 1999; Cano et al., 2003; Oldfield et al., 2002). It is possible that our use of a higher titer of virus in a different species (mice versus Siberian hamsters and rats) could account for at least some of this difference. Distribution patterns of PRV-infected neurons at varying infection times (2, 3, 4, and 5 days) allowed us to determine the order of labeling throughout the spinal cord and CNS and were very similar to those seen in previous studies performed in Sprague-Dawley rats (Cano et al., 2003; Oldfield et al., 2002). Two control mice that underwent a sympathectomy did not show any signs of infection in the brain or spinal cord at 5 days post-injection indicating that the virus was infecting the brain specifically via the sympathetic nerves projecting to IBAT. The number of co-expressing neurons in the spinal cord and brain regions at different post-infection durations are summarized in Table 1.

Although most of the labeled areas throughout the spinal cord and brain were singly labeled for either MC4R or PRV, our analysis focused on areas in which co-localization was observed. For all calculations, consecutive sections from a 1:8 set of sections per animal were analyzed, and the results for three animals for each infection time averaged. The spinal cords of animals sacrificed at 2 (n=3) and 3 (n=3) days post-inoculation were sectioned coronally.

At 2 days post-injection (n=3) PRV infection was predominantly restricted to the spinal cord. Co-localization of MC4R and PRV was seen in the intermediolateral cell column (IML) in the thoracic spinal cord (co-expression in 58% of the PRV-infected neurons and 45% co-expression of MC4R expressing neurons)(Table 1, Day 2) (Figure 2 D, E, F).

At 3 days post-injection (n=3) co-localization of MC4R and PRV was seen in the thoracic spinal cord, and in two regions in the brain (Table 1, Day 3), the RPa (co-expression in 67% of all PRV-infected neurons, and 61% of MC4R expressing neurons in the RPa) and the Gi (co-expression in 41% of the PRV-infected neurons and 26% of MC4R expressing neurons). Additionally, two of the animals began to show co-localization of PRV and MC4R in the PVH dorsal parvicellular (dpv) subdivision and one animal began to show co-localization in the rostroventrolateral medulla (RVLM).

At 4 days post-injection (n=3) co-localization of MC4R and PRV began to become more widespread. Colocalization was still apparent in the RPa, Gi, dpvPVH, RVLM as well as in several new regions (Table 1, Day 4) including the PAG, ventrolateral part (PAGvl) (4 co-localized neurons, making up 15% of all PRV-infected neurons and 26% of all MC4R neurons) and the NTSm (co-expression in 42% of all PRV-infected neurons and 56% of all MC4R expressing neurons) (Figure 2 A, B, C). In the PVH, co-expression in all the animals was first observed at day 4, as well as a large increase in the number of PRV-infected neurons, primarily in the dpv, ventral parvocellular (vpv), and lateral parvicellular (lp) (co-expression in 20% of all PRV-infected neurons and 42% of all MC4R neurons in the PVH) (Figure 3 A, B, C). The number of singly labeled PRV neurons and the number of co-localized neurons increased from day 2 in the RVLM (co-expression in 12% of all PRV-infected neurons and 12% of all MC4R-expressing neurons) and in the RPa (co-expression in 47% of all PRV-infected neurons and 90% of all MC4R-expressing neurons) (Figure 3 D, E, F).

At 5 days post-injection (n=3) co-localization of MC4R and PRV was seen in all the same regions as in day four with small increases in the number of PRV-infected neurons in those areas (Table1, Day5). From day four to five, the most substantial increase seen in the number of PRV-infected and co-localized cells was in the PVH (co-expression in 30% of all PRV-infected neurons and 72% of all MC4R expressing neurons). There were also increases in the Gi (co-expression in 8% of all PRV-infected neurons and 50% of all MC4R neurons) and the RVLM (co-expression in 18% of all PRV-infected neurons and 25% of all MC4R neurons). The first co-localized neurons were detected in the LH at day five and, although small in number, they were observed in all animals (co-expression in 10% of all PRV-infected neurons and 22% of all MC4R expressing neurons). The first co-localized cells were also detected in the caudal part of the pontine reticular nucleus (co-expression in 12% of all PRV-infected neurons and 17% of all MC4R expressing neurons), the laterodorsal tegmental nucleus (co-expression in 73% of all PRV-infected neurons and 40% of all MC4R neurons), the DMH (co-expression in 9% of all PRV-infected neurons and 30% of all MC4R neurons) and the locus coeruleus (co-expression in 18% of all PRV-infected cells and 31% of all MC4R).

DISCUSSION

The retrograde transsynaptic progression of the attenuated PRV-Bablue is time-dependent, thus providing information on the hierarchical order of multi-synaptic circuits. According to previously published results, rats surviving 2-3 days after PRV injection into their IBAT exhibit labeling of second order neurons, 3-4 days post-injection labels third order neurons, and 4-5 days post-injection labels fourth order neurons (Cano et al., 2003; Oldfield et al., 2002). The sites of PRV infection in the brain and spinal cord resulting from IBAT injection and the rate of progression were very similar to those found in previous studies, enabling us to compare our PRV-Bablue labeling results with previous studies done in rats. In addition, we can be confident about the labeling specificity in our study since sympathectomized mice did not exhibit any labeling in the spinal cord or brain and because it has been previously shown in rats that supraspinal labeling is specific for the input to IBAT adipocytes and not blood vessels (Cano et al., 2003; Oldfield et al., 2002).

In this study of IBAT, we focus principally on those PRV-infected areas that also express MC4R. Trans-synaptic tracing by injection of attenuated PRV-Bablue into the IBAT of MC4R-GFP transgenic mice, coupled with dual-labeling immunohistochemical techniques, reveals a specific subset of dual-labeled MC4R-GFP/PRV-IR neurons in multiple nuclei at various levels of the CNS. These nuclei, which contain varying degrees of dual-labeled neurons, are found throughout the CNS, including the IML of the spinal cord, brainstem, midbrain and hypothalamus. These data provide the first evidence for potential action sites of MC4R signaling in the regulation of sympathetic outflow to IBAT, and suggest that a complex network of MC4R-expressing neurons in multiple nuclei at various levels of the CNS may participate in the regulation or modulation of sympathetically-mediated IBAT thermogenesis.

Our data, together with previous studies demonstrating that central administration of melanocortin agonists and antagonists cause an increase or decrease, respectively, in UCP1 expression levels or IBAT sympathetic nerve activity (Baran et al., 2002; Cettour-Rose and Rohner-Jeanrenaud, 2002; Haynes et al., 1999; Li et al., 2004; Small et al., 2001; Williams et al., 2003; Yasuda et al., 2004; Zhang et al., 2004), provide strong evidence in support of the hypothesis that central MC4R signaling plays an important role in the regulation of IBAT thermogenesis. Here we discuss some of the key sites with respect to both central melanocortin signaling and IBAT function.

Each IBAT pad receives most of its sympathetic innervation from postganglionic neurons in the stellate ganglion and thoracic paravertebral ganglia projecting through five posterior branches of the intercostal bundle to each IBAT pad. Sympathetic preganglionic neurons (SPNs) innervating IBAT are found primarily in the IML of spinal cord segments T4-T6 (Cano et al., 2003). MC4R mRNA positive neurons in the IML have been previously shown to co-express choline acetyltransferase mRNA, providing evidence that they are autonomic preganglionic neurons (Kishi et al., 2003). Interestingly, a subset of hypothalamic POMC/CART neurons send direct projections to the spinal cord and α-MSH fibers are detected in the spinal cord (Elias CF, 1998; Kohler et al., 1984). Our results show co-localization of MC4R and PRV in the IML of the thoracic spinal cord at the earliest post-infection times, suggesting that the IML is one of the sites of action in the melanocortin circuitry involved in the regulation of IBAT sympathetic nerve activity. It remains to be determined what role MC4R signaling in the IML plays in the regulation of IBAT thermogenesis.

In this study we also show that the PVH is among the first brain regions to contain neurons co-expressing PRV-IR and MC4R-GFP-IR and contains one of the largest numbers of PRV and MC4R co-localized neurons. The PVH is known to play a critical role in integrating autonomic and neuroendocrine systems and in the regulation of energy homeostasis. The PVH has long been thought to play a role in IBAT activation and is a known site of MC4R expression (Kishi et al., 2003; Liu et al., 2003; Mountjoy et al., 1994). Local injection of glutamate into the PVH causes an increase in the electrical firing rate of sympathetic nerves innervating IBAT (Yoshimatsu et al., 1993) and a concentration-dependent increase in IBAT temperature which is blocked by pretreatment with a sympathetic ganglionic blocker or β-adrenergic receptor antagonist (Amir, 1990c).

The PVH is also involved in integrating information from leptin and the melanocortin system (Cowley et al., 1999; Cowley et al., 2001). Co-expression of MC4R-GFP-IR and PRV-IR in a subset of neurons in the PVH suggests that the PVH is a potential action site for the melanocortin system in the regulation of sympathetic ouflow to IBAT, which is consistent with previous observations that microinjection of the melanocortin agonist MTII into the PVH stimulates oxygen consumption in mice (Cowley et al., 1999). One previous study, which used PRV as a retrograde tracer from IBAT, has shown that PRV-infected cells in the retrochiasmatic area and lateral arcuate nucleus co-localize extensively with POMC (37%), leptin receptor (ObR) (69%) and cocaine-and amphetamine-regulated transcript (CART) expressing neurons (79%) (Oldfield et al., 2002). These POMC/CART neurons in the arcuate nucleus are known to project to the PVH, LH, and spinal SPNs and are activated by leptin (Elmquist, 2001). Therefore, it would be interesting for future study to determine whether the MC4R and PRV co-expressing neurons we found in the PVH might be mediating at least part of leptin's stimulatory effect on IBAT thermogenesis.

Neurons of the PVHpv are also known to have direct projections to SPNs in the IML (Cechetto and Saper, 1988; Luiten et al., 1985) and PVH regions that are activated by cold exposure (Baffi and Palkovits, 2000; Miyata et al., 1995) are also the first hypothalamic or forebrain regions to be infected with PRV after injection into IBAT (Bamshad et al., 1999; Cano et al., 2003; Oldfield et al., 2002), making it likely that the PVH contains neurons regulating sympathetic outflow to IBAT. These data, along with our findings that demonstrate that the PVH contains one of the largest numbers of PRV and MC4R co-localized neurons, suggest that the PVH may be an important site in the melanocortin system's regulation of IBAT.

The raphe nuclei (raphe magnus, pallidus and obscurus) provide the principal descending serotonergic projections to the spinal cord and provide direct projections to spinal sympathetic pregangionic neurons in the IML (Loewy, 1981). The RPa has been proposed to contain sympathetic premotor neurons that mediate thermogenesis and thermoregulation (Morrison, 2004). The RPa receives direct projections from many hypothalamic and brainstem nuclei important to autonomic regulation, including the arcuate, the preoptic area, the PVH, the LH, the DMH, the PAG, the parabrachial nucleus and the Gi (Hermann et al., 1997; Hosoya, 1985; Hosoya et al., 1987; Nogueira et al., 2000; Sim and Joseph, 1991; Thor and Helke, 1987; Zagon, 1993). Additionally, the RPa is one of the earliest infection sites in the brain following injection of PRV-Bartha into IBAT (Cano et al., 2003; Oldfield et al., 2002) and also expresses the MC4R (Kishi et al., 2003; Liu et al., 2003; Mountjoy et al., 1994). Our results demonstrate that about 90% of MC4R-GFP neurons in the RPa co-express PRV-IR at 4 days after PRV injection, suggesting that the RPa is also a potential action site for MC4R signaling-mediated regulation of sympathetic outflow to IBAT. Consistent with this, preliminary experiments also show that the significant increases in oxygen consumption observed after ICV 3rd or 4th ventricle injection of the MC3/4R agonist MTII in C57BL/6J mice are reversed with functional inhibition of RPa neurons by microinjection of glycine or muscimol, and conversely micro-injection of the MC3/4R agonist melanotan II (MTII) into the RPa area significantly increases oxygen consumption in C57BL/6J mice and increases IBAT SNA in anesthetized and artificially ventilated rats (Fan W, unpublished observation).

The DMH receives input from most major hypothalamic nuclei, sends major projections to the PVHpv, and appears to have a functional relationship with the RPa in the activation of IBAT (Cao et al., 2004). Blockade of inhibitory input to neurons in the DMH leads to an increase in IBAT sympathetic nerve activity and IBAT temperature, mediated through the RPa. Furthermore, bilateral injection of the MC3/4R agonist MTII directly into the DMH significantly stimulates IBAT UCP1 mRNA expression in *ad libitum*-fed lactating female rats, indicative of increased sympathetic ouflow to IBAT (Chen et al., 2004). These results suggest that the MC4R is involved in regulating sympathetic outflow from the DMH to IBAT and suggest a functional role for the MC4R in the DMH for the regulation of IBAT activity. Our neuroanatomical results, showing that 30% of the MC4R-GFP-IR expressing neurons in the DMH are co-localized with PRV-IR from IBAT, further strengthen this hypothesis.

The LH is one of the major cold-sensing areas infected at an intermediate stage after PRV injection into IBAT (Cano et al., 2003). As in the PVH, there is also evidence that leptin differentially regulates arcuate neuropeptide Y (NPY) and POMC neurons that project to the LH (Elias et al., 1999). Furthermore, AGRP induces c-Fos expression in the LH (Hagan et al., 2001), and AGRP, NPY and α-MSH-IR axons in the LH, most likely stemming from arcuate projections, intensely innervate both melanin-concentrating hormone (MCH) and orexin neurons (Broberger et al., 1998a; Elias et al., 1998). In addition, up to 55% of virus-infected neurons in the LH, retrogradely labeled from IBAT, contain MCH (Oldfield et al., 2002). MCH has been shown to be important in the integration of energy homeostasis downstream of leptin (Pereira-da-Silva et al., 2003; Segal-Lieberman et al., 2003; Shimada et al., 1998). Moreover, LH lesions cause an increase in oxygen consumption, core body temperature, IBAT sympathetic firing rate and NE turnover, while activation of the LH leads to a decrease in the sympathetic firing rate of IBAT which in turn inhibits IBAT thermogenesis (Arase et al., 1987; Bernardis and Bellinger, 1993; Bray, 1984; Holt and York, 1988; Sakaguchi et al., 1988; Yoshida et al., 1983). Blockade of hypothalamic MCH expression by antisense MCH oligonucleotide results in increased UCP1 expression and increased relative body fat (Pereira-da-Silva et al., 2003), while central administration of MCH infusion decreases expression of UCP1 (Ito et al., 2003), suggesting that MCH may reduce IBAT thermogenic function. Consistent with this, α-MSH appears to be a functional antagonist of MCH as MCH expression is augmented when central melanocortin signaling is reduced in agouti mice or following ICV treatment of AGRP or SHU9119 (Hanada et al., 2000; Ludwig et al., 1998). In addition to its hypothalamic projections, the LH also sends and receives projections to and from brainstem areas, including the NTS, lateral parabrachial nucleus, PAGvl, and the RPa, and sends direct projections to the spinal cord and regions containing sympathetic pre-motor neurons (Cechetto and Saper, 1988; Simerly, 2002). Collectively these results, together with our data showing significantly high levels of MC4R and PRV co-localization in the LH and many of the areas it projects to, suggest that melanocortin and/or NPY/AGRP projections from the hypothalamus or brainstem may innervate MC4R expressing MCH neurons in the LH and play a role in regulating the inhibitory effect of MCH on IBAT thermogenesis. However, at least one study showed no co-localization between MC4R-GFP-IR and MCH mRNA in the LH (Liu et al., 2003).

PRV retrograde labeling from IBAT indicate that Orexin A neurons of the LH also innervate IBAT (Oldfield et al., 2002). These orexin neurons, which have been shown to send projections to NPY and POMC arcuate neurons, also appears to activate IBAT thermogenesis (Funahashi et al., 2003; Monda et al., 2003; Muroya et al., 2004). Furthermore, the activation of the BAT SNA by the LH appears to be dependent on the activation of neurons in the DMH and RPa (Cerri and Morrison, 2005). It would be interesting to further elucidate the interaction of these systems in IBAT thermogenesis.

Our study shows the lateral parabrachial nucleus containing a small number of PRV-IR neurons at late stages of infection after PRV injection into IBAT, some of which co-localize with MC4R expressing neurons. The parabrachial nucleus, considered an important integration site for autonomic regulation, receives projections from the spinal cord and NTS (Hermanson and Blomqvist, 1997; Standaert et al., 1986), and also receives sensory information about temperature from the skin. The lateral parabrachial nucleus is activated by cold exposure (Baffi and Palkovits, 2000; Menendez et al., 1996; Miyata et al., 1995), is involved in the central mechanisms of thermogenesis induced by cold exposure (Kobayashi and Osaka, 2003) and exhibits high levels of c-Fos expression after cold exposure in the same sites as PRV-IR neurons retrogradely labeled from IBAT (Cano et al., 2003). The parabrachial nucleus also receives AGRP/NPY terminals from the arcuate nucleus (Broberger et al., 1998b) and POMC terminals from the arcuate nucleus and NTS (Joseph and Michael, 1988; Moga et al., 1990; Yamazoe et al., 1984) and expresses the leptin receptor (Grill et al., 2002). These studies are interesting in light of our findings since together they potentially propose a new role for the melanocortin system in this brain region.

The locus coeruleus, another site where we saw small amounts of MC4R and PRV co-localization at a late post-injection stage, is one of two principal nuclei in the brain stem containing noradrenergic neurons. The locus coeruleus receives its major inputs from the paragigantocellular nucleus and the nucleus prepostius hypoglossi as well as inputs from the PVH and spinal cord (Aston-Jones et al., 1991), with a functional circuit between the suprachiasmatic nucleus via the DMH to the locus coeruleus (Aston-Jones et al., 2001). The locus coeruleus is thought to have an important role in the noradrenergic regulation of sleep, arousal and attention. In certain animals IBAT activation is known to be essential to arousal from hibernation and involved in arousal from daily torpor, as well as being correlated to an increase in slow wave sleep (Cannon and Nedergaard, 2004; Dewasmes et al., 2003). Cold exposure for 3 or 24 hours induces neuronal activity and c-Fos expression in the locus coeruleus (Miyata et al., 1995). The locus coeruleus expresses both leptin receptors (Grill et al., 2002) and MC4R (Kishi et al., 2003), and in contrast to the RPa, locus coeruleus noradrenergic neuronal firing rate decreases following ICV injection of MTII and increases following ICV injection of AGRP, suggesting a differential regulation of the serotonergic and noradrenergic neuronal systems (Kawashima et al., 2003). It would be interesting, therefore, in light of our finding, to further examine the role that the melanocortins have in regulating IBAT functions that involve this noradrenergic locus. It is very possible that if we had been able to extend our experiment one more day, then we would have seen larger amounts of co-expression in this region as well as other regions such as the POA, an area that contains neurons that are thermosensitive as well as receiving somatosensory input from skin and spinal thermoreceptors.

The NTS is the only other brain region, aside from the hypothalamic arcuate nucleus, which contains POMC neurons. The NTS, which also expresses MC4R (Kishi et al., 2003; Mountjoy et al., 1994), sends direct projections to the spinal cord (Amendt et al., 1979) and is likely to be an important area for the integration of information from areas such as the gastrointestinal system, hypothalamic feeding centers, and other autonomic input centers (Chang and Scott, 1984; Howes et al., 1989; King et al., 1989; Koegler and Ritter, 1998; Van Buskirk and Erickson, 1977). There is some evidence that a lesioning of the NTS reduces the functional capacity of IBAT (Fyda et al., 1991). Cold exposure for 3 or 24 hours induces c-Fos expression in the NTS (Cano et al., 2003; Miyata et al., 1995), including expression in dopamine-β-dehydroxylase immunoreactive neurons within the NTS. PRV retrograde labeling from IBAT was also found to be expressed in the NTS (Cano et al., 2003). These data suggest a putative role for the NTS in the noradrenergic control of IBAT thermogenesis. Our results showing significant amounts of PRV and MC4R co-localization in the NTS, together with the recent observation that α-MSH fibers are in close proximity to NTS neurons that poly-synaptically associate with BAT in rats (Zheng et al., 2005), further suggest that MC4R signaling in the NTS might contribute to the regulation of IBAT thermogenesis.

In summary, this study indicates which central melanocortin sites innervate IBAT, thereby providing the neuroanatomical substrate for the melanocortin system's regulation of sympathetically-mediated IBAT thermogenesis.

ACKNOWLEDGEMENTS

We gratefully acknowledge Dr. Jeffrey Friedman and Dr. Hongyan Lui for kindly providing the MC4R-GFP mice, Dr. Lynn Enquist for kindly providing us with PRV-Beblue, and Drs. Todd Wisner and David Johnson for their generous help in growing the virus. This work is supported by NIDDK/NIH grants DK62179 (WF), 5R01DK051730 and 5R01DK070332 (RDC).

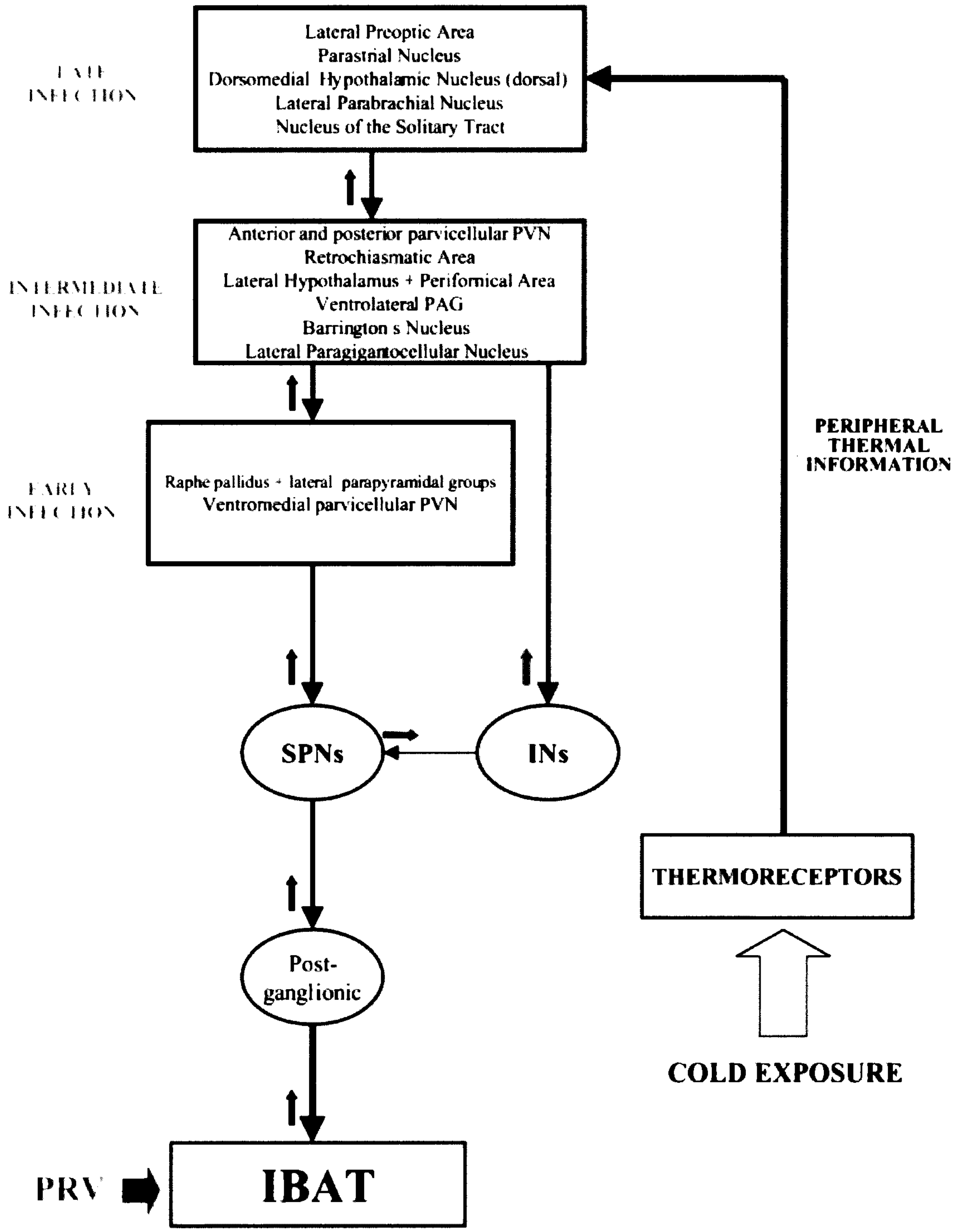

Figure 1. Schematic diagram of the neural circuitry involved in the cold-evoked activation of IBAT thermogenesis. All brain areas included in this diagram were infected after injection of PRV into IBAT and activated by cold exposure, using c-Fos as a marker of activation. Proposed synaptology is based on the temporal progression of viral infection (retrograde transport) and on well-established anatomic connections from previous studies. PRV, pseudorabies virus; SPN, sympathetic pregangionic neuron; INs, interneurons; PVN, paraventricular nucleus; PAG, periaqueductal grey. From (Cano G, 2003)

Area	PRV positive neurons	MC4R positive neurons	%PRV neurons co-expressing MC4R	%MC4R neurons co-expressing PRV
Day 2				
PVH, parvicellular	+/-	+ + +	*	*
Gigantocellular reticular nucleus	+/-	+ + +	*	*
Raphe pallidus	+ /-	+	*	*
Thoracic spinal cord	+	+	58	45
Day 3				
PVH, parvicellular	+/-	+ + +	*	*
Gigantocellular reticular nucleus	+	+ + +	41	26
Raphe pallidus	+	+	40	25
Thoracic spinal cord	+	+	33	43
Rostroventrolateral medulla	+ +	+ +	*	*
Day 4				
PVH, parvicellular	+ + + +	+ + +	20	42
Lateral hypothalamic area	+/-	+ +	*	*
Periaqueductal gray, ventrolateral	+ + +	+ +	15	25
A5 cell group	+ + +	+ +	9	11
Gigantocellular reticular nucleus	+ + + +	+ + +	6	26
Raphe pallidus	+ +	+	47	90
NTS, medial	+ +	+ +	42	56
Rostroventrolateral medulla	+ + +	+ +	12	12
Day 5				
PVH, parvicellular	+ + + +	+ + +	30	72
Lateral hypothalamic area	+ + + +	+ +	10	22
Dorsomedial hypothalamic nucleus dorsal	+ + + +	+ +	9	30
Medial preoptic area	+/-	+ + +	*	*
Periaqueductal gray, ventrolateral	+ + + +	+ +	16	27
Laterodorsal tegmental nucleus	+ +	+ +	73	40
A5 cell group	+ + +	+ +	13	21
Pontine reticular nucleus, ventral	+ +	+ +	12	17
Lateral parabrachial nucleus	+/-	+ + +	*	*
Locus coeruleus	+ + +	+ +	18	31
Gigantocellular reticular nucleus	+ + + +	+ + +	8	50
Raphe pallidus	+ +	+	42	92
NTS, medial	+ +	+ +	33	50
Rostroventrolateral medulla	+ + +	+ +	18	25

[1]Brain areas are listed rostral to caudal. Number of positive neurons per region from a 1:8 set of sections: +/-= 1-5, but not in all mice; + = 1-10; ++ = 11-20; +++ = 21-30; ++++ >30; * some co-expression observed, but percentages were not calculated unless all mice showed co-expression; n=3 for each survival time. PVH, paraventricular hypothalamic nucleus; NTS, nucleus of the solitary tract.

Table 1. Spinal cord and brain regions exhibiting colocalization of PRV-IR and MC4R-GFP-IR at different survival times after PRV injection into IBAT.

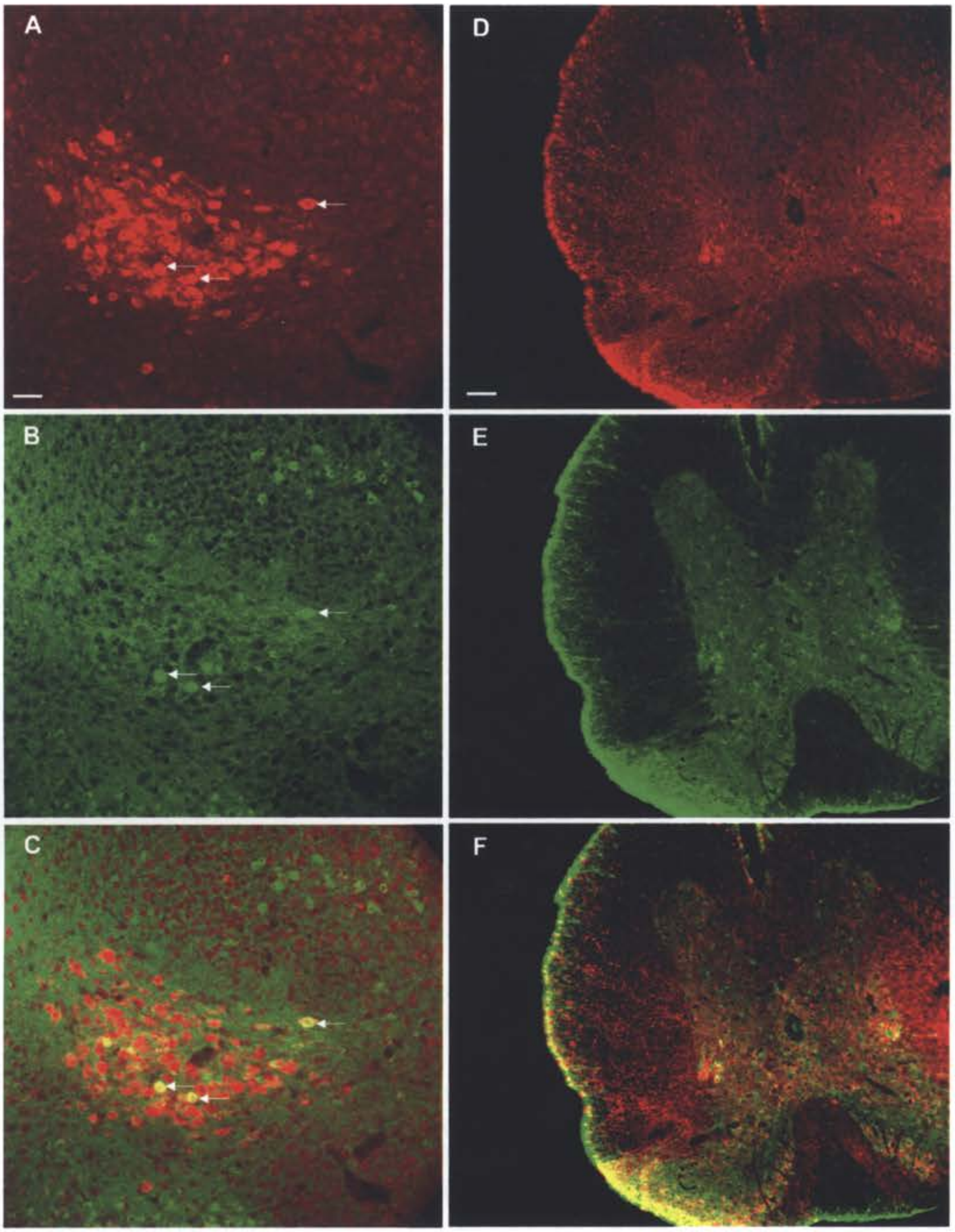

Figure 2: PRV and MC4R are co-expressed in the thoracic spinal cord (D-E) and NTS (A-B). (**A**) PRV infected neurons (red) in the spinal cord two days after injection into IBAT (scale bar represents 50μm and applies to all parts of this figure). (**B**) Same section as (A), depicting MC4R expressing neurons (green). (**C**) Same section as (A), depicting neurons co-expressing PRV and MC4R (yellow). (**D**) PRV infected neurons (red) in the NTS four days after injection into IBAT. (**E**) Same section as (D), depicting MC4R expressing neurons (green). (**F**) Same section as (D), depicting neurons co-expressing PRV and MC4R (yellow).

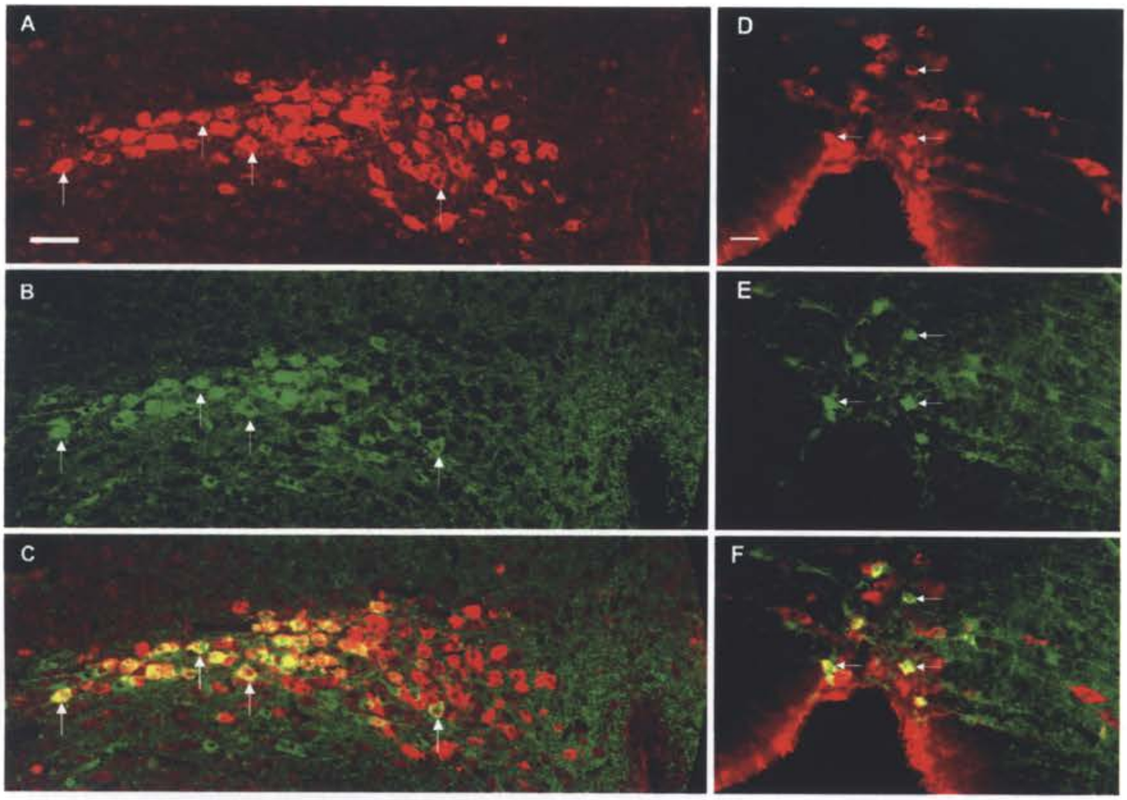

Figure 3: PRV and MC4R are co-expressed in the PVH (A-C) and RPa (D-E). (**A**) PRV infected neurons (red) in the PVH four days after injection into IBAT (scale bar represents 50μm and applies to all parts of this figure). (**B**) Same section as in (A), depicting MC4R expressing neurons (green). (**C**) Same section as in (A), depicting neurons co-expressing PRV and MC4R (yellow). (**D**) PRV infected neurons (red) in the RPa four days after injection into IBAT. (**E**) Same section as in (D), depicting MC4R expressing neurons (green). (**F**) Same section as in (D), depicting neurons co-expressing PRV and MC4R (yellow).

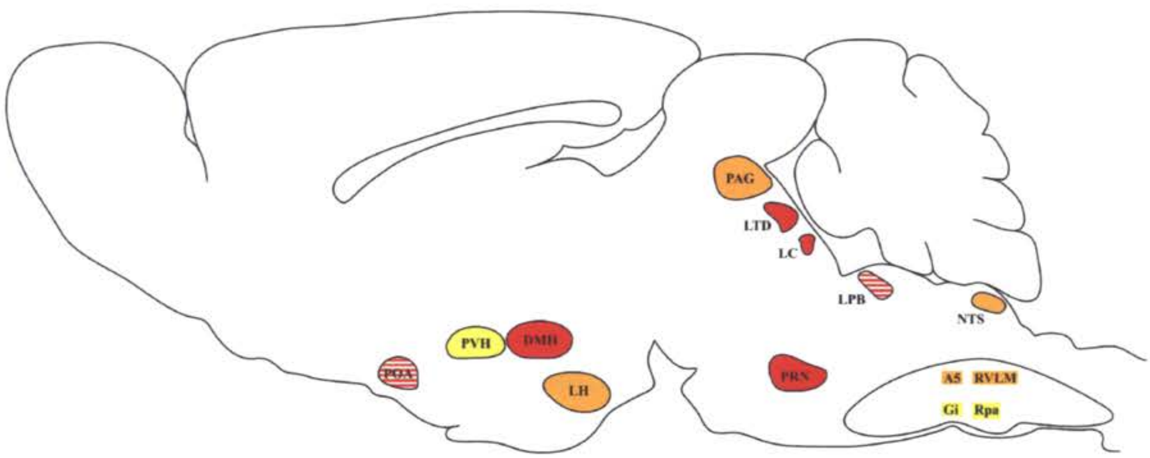

Figure 4. Schematic diagram of brain regions exhibiting co-localization of PRV-IR and MC4R-GFP-IR at different survival times after PRV injection into IBAT in mouse (code: yellow, early survival time; orange, intermediate survival time; red, long survival time; red striped, long survival time, but not in all animals). Because of numerous infected areas in the brainstem, the temporal progression in this region is represented by the shade of the abbreviation. Template adapted from Paxinos and Watson (1998). POA, preoptic area; PVH, paraventricular hypothalamic nucleus; DMH, dorsomedial hypothalamic nucleus; LH, lateral hypothalamic area; PAG, periaqueductal gray; LTD, laterodorsal tegmental nucleus; LC, locus coeruleus; LPB, lateral parabrachial nucleus; NTS, nucleus of the solitary tract; Gi, gigantocellular nucleus; RVLM, rostroventrolateral medulla; RPa, raphe pallidus, PRN, pontine reticular nucleus.

CHAPTER TWO

Physiological role of the central melanocortin system in adaptive thermogenesis of brown adipose tissue

Adriana Voss-Andreae, Kate L.J. Ellacott, Jon G. Murphy, Eduardo A. Nillni, Wei Fan and Roger D. Cone

ABSTRACT

The specific effector pathways used by the melanocortin system in the regulation of energy expenditure are not fully understood. On a moderate fat diet wild-type C57BL/6J mice maintain energy homeostasis while melanocortin-4 receptor null (MC4R-/-) mice on the same background gain weight at a rapid rate as a result of a defect in compensatory responses in both intake and expenditure. In this study, we examine the energy expenditure defect in MC4R-/- mice, focusing on the melanocortin system's role in non-shivering thermogenesis in interscapular brown adipose tissue (IBAT) activity. A high-fat or moderate-fat diet leads to an up-regulation in uncoupling protein-1 (UCP1) in wild-type mice, but not in MC4R-/- or agouti-related peptide (AGRP)-treated mice. This failure to up-regulate UCP1 levels in response to diet is independent of alterations in the hypothalamic-pituitary-thyroid (HPT) axis since MC4R-/- and AGRP-treated mice on a high-fat diet increase their triiodothyronine (T_3) levels in a manner comparable with wild-type controls. Additionally, in comparison with wild-type mice, MC4R-/- mice exposed to 4°C for 4 hours have attenuated uncoupling protein-1 (UCP1) expression levels. However when exposed to 4°C for 5 days , MC4R-/- mice have an increase in UCP1 expression levels similar to wild-type mice. These results suggest that MC4R signaling is critically required for acute high fat-induced and acute cold exposure-induced IBAT thermogenesis.

INTRODUCTION

Melanocortin-4-receptor knockout (MC4R-/-) mice gain more weight than wild-type control animals when placed on a moderate-fat diet due to a combination of increased food intake and a defect in energy expenditure (Butler et al., 2001). MC4R-/- mice also have a profound defect in acute diet-induced thermogenesis caused by a failure to increase their basal and total oxygen consumption in response to an increase in dietary fat, a defect not found in leptin deficient (*Lep*^{ob}/*Lep*^{ob}) mice. The mechanisms underlying the MC4R-/- mouse's inability to coordinate energy intake with energy expenditure remain largely unexplained and may be related to alterations in thermogenesis caused by changes in sympathetic activity, changes in mitochondrial uncoupling protein-1 (UCP1), or a combination of these factors.

Diet-induced thermogenesis (DIT) was initially defined by studies showing that consumption of a high-fat diet induces recruitment of interscapular brown adipose tissue (IBAT), a major thermogenic organ in rodents, accompanied by a large increase in heat production (Brooks et al., 1980; Rothwell and Stock, 1979). These studies first proposed the idea that adaptive non-shivering thermogenesis, a form of thermogenesis found only in BAT, may play a role in resistance to obesity. Numerous studies have since strengthened this hypothesis by demonstrating that a high-fat, or 'cafeteria', diet induces an up-regulation of mitochondrial UCP1 mRNA or protein levels in IBAT (Archer et al., 2005; Li et al., 2004; Margareto et al., 2001; Nedergaard et al., 1984; Portillo et al., 1998; Rippe et al., 2000; Rippe et al., 2003; Surwit et al., 1998). UCP1 is principally expressed in BAT where it disassociates or 'uncouples' the respiratory chain from ATP production.

This mitochondrial uncoupling, regulated by the sympathetic nervous system, and activated in situations such as cold exposure, intake of calorie dense food, arousal from hibernation, and fever, causes an increase in respiration and the dissipatation of resulting oxidation energy as heat.

In addition to DIT, one of the most important functions of BAT in smaller mammals is to sustain normal body temperature during chronic cold exposure and it is the only site of cold-acclimation recruited non-shivering thermogenesis (Cannon and Nedergaard, 2004; Golozoubova et al., 2006; Golozoubova et al., 2001; Nedergaard et al., 2001). Cold exposure stimulates sympathetic activity, which, through the β-adrenoreceptors, mediates an increase in UCP1 expression and thermogenesis in BAT.

Chronic and acute central administration of melanocortin agonists and antagonists cause an increase or decrease, respectively, in UCP1 expression levels, oxygen consumption and IBAT sympathetic nerve activity (Baran et al., 2002; Cettour-Rose and Rohner-Jeanrenaud, 2002; Haynes et al., 1999; Li et al., 2004; Small et al., 2001; Williams et al., 2003; Yasuda et al., 2004; Zhang et al., 2004), suggesting that the melanocortin system is involved in mediating IBAT-induced thermogenesis. The MC4R also appears to mediate at least part of leptin's activation of IBAT through stimulation of UCP1 (Li et al., 2003; Satoh et al., 1998; Ste Marie et al., 2000; Zhang et al., 2005). However, it has not been demonstrated whether the melanocortin system regulates UCP1 under physiological conditions that normally trigger IBAT activation, such as an increase in dietary fat or cold exposure. Given our neuronanatomic results, described in Chapter 1, which demonstrate that MC4R is expressed in regions polysynaptically associated with IBAT, we sought to test the hypothesis that central MC4R signaling plays a critical role in mediating diet-induced and cold-induced IBAT thermogenesis.

Thyroid hormones are known to act synergistically with sympathetic input to activate UCP1 transcription (Lanni et al., 2003). Rats or humans fed a high-fat diet or overfed for a period of weeks have been shown to have an increase in their levels of total T_3 (Almeida et al., 1996; Danforth et al., 1979; Leblanc et al., 1982; Naim et al., 1985; Rabolli and Martin, 1977; Tulp et al., 1982) although it is not entirely clear from these studies whether the increase is a result of increasing dietary fat or the concomitant weight gain. It has also been stipulated that the melanocortin system may play a role in leptin's regulation of the HPT axis (Fekete et al., 2002a). The parvicellular part of the paraventricular hypothalamus (PVHpv) contains a large degree of MC4R and thyrotropin-releasing hormone (TRH) co-expression, as well as containing α-MSH-IR axon varicosities and AGRP-containing axon terminals that are juxtaposed to pro-TRH neurons in both rats and humans (Fekete et al., 2000; Harris et al., 2001; Legradi and Lechan, 1999; Mihaly et al., 2000). Serum TSH is increased with centrally administered α-MSH and decreased with AGRP (Kim et al., 2000). α-MSH also leads to TRH release in hypothalamic explants (Kim et al., 2000). Centrally administered α-MSH is known to increase plasma thyroid hormone levels and AGRP has been shown to significantly suppress circulating levels of T_4 and T_3 and to inhibit the proTRH mRNA content in the PVH of rats (Fekete et al., 2002a). No significant effects of AGRP treatment on T_4 or TRH mRNA levels were observed in MC4R-/- mice, specifically implicating MC4R involvement in AGRP's effects on the HPT axis (Fekete et al., 2004). T_4 levels are normal in MC4R-/- (Fekete et al., 2004), but T_3 measurements in MC4R-/- have not been previously published. AGRP-null mice exhibit an age-dependent lean phenotype correlated with an increase in metabolic rate, locomotor activity, metabolic rate, T_3 and T_4 levels and UCP1 expression (Wortley et al., 2005), although the effect of exogenous AGRP on UCP1 and thyrotropin (TSH) levels is conflicted (Fekete et al., 2002a; Small et al., 2001). We therefore wanted to examine whether the hypothalamic-pituitary-thyroid (HPT) axis mediates the melanocortin system's regulation of UCP1 in response to a high-fat diet.

Here we used alteration of physiological conditions known to result in IBAT recruitment to ascertain whether the central melanocortin system was involved in mediating regulation of UCP1 levels in IBAT. In two separate experiments, MC4R-/- and wild-type mice were either fed high-fat diets or exposed to cold temperatures and Western blotting was used to examine the relative UCP1 protein levels. In order to make sure that results were not due to developmental defects in the MC4R-/- animals, the high-fat diet experiment was also performed on mice injected intracerebroventricularly (ICV) with either AGRP or saline. Because the central melanocortin system has been implicated in the regulation of the HPT axis (Fekete et al., 2002a), we also examined whether the HPT axis mediates any of the central melanocortin system's regulation of UCP1. In this study, we demonstrate that MC4R-/- mice have a defect in their ability to up-regulate UCP1 in response to acute increased dietary fat and short-term, but not long-term, cold exposure.

MATERIALS AND METHODS

Animals

Age-matched male MC4R-/- and wild-type (C57BL/6J strain) mice were individually housed after weaning at approximately 4 weeks and kept in a 12-h light/dark cycle. Wild-type mice were purchased (Jackson Laboratories, Bar Harbor, ME). Mice had *ad libitum* access to Laboratory Rodent Diet (Purina 5001, PMI Nutrition International, Brentwood, MO, composed of 12% fat, 28.0% protein, 49% carbohydrate by calories; 3.04 kcal/g metabolizable energy).

High-fat and moderate-fat diets

At 7.5 weeks of age, MC4R-/- and wild-type mice were switched to a high-fat diet (Research Diets; 60% fat, 20% protein, 20% carbohydrate by calories; 5.24 kcal/g metabolizable energy) or moderate-fat diet (Purina diet 5015; 26% fat calories, 18% protein, 56% carbohydrate; 3.73 kcal/g metabolizable energy) for 48 hours before being euthanized and IBAT immediately dissected as described below. Control animals were maintained on regular chow for the experimental period.

Cold Exposure

5.5-6.5 week old MC4R-/- and wild-type mice (for the 5-day cold experiment) and 7-8 week old mice (for the 4-hour cold experiment) were transferred from the colony room into chambers set at 4°C or 24°C. All animals were maintained in the same 12-hour light/dark cycle with *ad libitum* access to food (Purina 5001, PMI Nutrition International, Brentwood, Missouri) and water. After four hours or 5 days animals were euthanized and immediately dissected as described below.

Thyroid hormone measurements

Blood was collected into serum-collecting tubes (Becton-Dickinson, Franklin Lakes, NJ) immediately after euthanasia. Blood samples were briefly spun down at 4°C and the serum was transferred to fresh tubes. The serum was then frozen in liquid nitrogen and kept frozen until assays were performed. Assays of total T_3 and total T_4 were performed using RIAs and antibodies previously described (Nillni et al., 1995; Perello et al., 2006) using the same serum volumes in duplicate. Procedures and reagents for the thyroid assay were from MP Biomedicals Diagnostic Division (Orangeburg, NY). Briefly, 100μl of total T_3 or T_4 serum standards and samples were added to 1.0 ml of total T_3 or T_4 Tracer Solution (T_3 or T_4 [^{125}I] derivative in Tris buffered saline with bovine albumin, EDTA, blue dye and 0.5% sodium azide) in Antibody-Coated Tubes and incubated in a 37°C water bath for 2.5 hours. The tubes were then aspirated and rinsed with 1.0 ml of deionized water. The tubes were again aspirated and the radioactivity was counted for one minute with a gamma counter. The sensitivities of the T_3 and T_4 assays were 12.5 ng/dl and 1.2μg/dl, and the intra- and inter-assay variability were approximately 5-7% and 10-11% respectively.

Protein extraction and Western blot

Both IBAT pads were removed in each animal and any visible surrounding white adipose tissue carefully dissected out and discarded. The IBAT pads were immediately placed in homogenization solution in 10mM Tris-HCL, 2%SDS, 100mM PMSF, pH 6.8 containing protease inhibitors ('Complete' EDTA-free protease inhibitor cocktail, Roche Diagnostics, Alameda, CA), cut into small pieces and briefly sonicated. Samples were passed through a 0.45μm MCE syringe filter (Millipore, Billerica, MA) and snap frozen in liquid nitrogen until ready to process further. Bicinchoninic acid (BCA) protein assay reagent (Pierce Biotechnology, Rockford, IL) was used to determine protein concentrations and 20μg of each sample was resolved alongside a protein standard (Precision Plus Dual Color, Bio-Rad, Hercules, CA) with 12% SDS-PAGE and electrotransfered to an Imobilon-FL PVDF membrane (Millipore, Billerica, MA). The membrane was blocked with Aquablock (EastCoast Bio, North Berwick, ME) and then incubated overnight 1:100 with guinea-pig anti-human UCP1 antibody, cross-reactive with mouse (Linco Research, St. Charles, MO) and 1:2500 with antibody specific to mouse tubulin E7 ascites (Developmental Studies Hybridoma Bank, University of Iowa) diluted in Aquablock with 0.1% tween. Subsequent immunoblotting was performed in accordance with the Odyssey near infrared imaging platform system (LI-COR Biosciences, Lincoln, NE), and data were captured using the Odyssey scanner. The data using the Odyssey system was densitized with the system software and further processed and normalized using Microsoft Excel.

Quantitative RT-PCR

RNA extraction and reverse transcription.

The following protocol was done using RNase-free equipment and solutions in order to minimize RNA degradation. IBAT was cut up in TRIzol into small pieces with scissors and homogenized using a homogenizor (Branson Sonifier 250; Branson Ultrasonics Corp., Danbury, CT). The RNA was extracted using the TRIzol method according to manufacturer's protocol (Invitrogen, Carlsbad, CA). The RNA was then re-suspended in RNase-free water and 0.5μl RNase inhibitor and heated for 10 minutes at 55°C. An agarose gel was run and O.D. analysis performed in order to confirm the integrity of the RNA. The following was then added to a new tube on ice: 1μg IBAT RNA, 1μl 10xDNaseI reaction buffer, 1μl DNaseI (Amp Grade, 1U/μl; Invitrogen), DEPC-treated water to 10μl. The tube was incubated for 15 minutes at room temperature, followed by addition of 1μl of 25mM EDTA solution. The mixture was incubated at 10 minutes at 65°C to inactivate the DNaseI. 1μl of random hexamer primer (0.2μg/μl; New England BioLabs, Beverly, MA) was added to 10μl of DNase-treated RNA, mixed, and incubated for 5 minutes at 70°C. Tubes were then placed on ice and the following was added: 1μl Ribonuclease inhibitor (20U/μl), 2μl 10mM dNTP mix, and 4μl 5x reaction buffer. Tubes were mixed and incubated for 5 minutes at room temperature. 2μl Moloney murine leukaemia virus reverse transcriptase (20U/μl; New England BioLabs) was then added to the RNA mixture and reverse transcribed under the following conditions: 10 minutes at room temperature, one hour at 37°C, 10 minutes at 70°C and the final cDNA product was chilled on ice.

PCR and Quantitative PCR

In order to make a standard for use in quantitative PCR, PCR was performed with the UCP1 cDNA and the following primers in order to amplify a fragment of UCP1: mouse UCP1 (GenBank U63418) forward position 409-428: 5'GTG AAG GTC AGA ATG CAA GC3'and reverse position 586-605: 5'AGG GCC CCC TTC ATG AGG TC3'(Kogure A, 2002). To 1μl UCP1 cDNA we added 0.4μl primer mix (each primer at 50pmol/μl), 12.5ml 2xPCR Master Mix (containing *Taq* DNA polymerase [recombinant; 0.05 U/μl] in reation buffer, 0.4 mM dNTPs [0.4mM each of dATP, dCTP, dGTP, dTTP], 4mM $MgCl_2$; Fermentas Inc, Hanover, MD) and 10.1µl water. The following PCR conditions (based on primer and template sequence) were programmed on a thermal cycler (GeneAmp PCR System 2400; PerkinElmer Life and Analytical Sciences Inc., Boston, MA) based on primer sequence: denaturing at 95°C for 3 minutes, followed by 40 cycles of denaturing at 95°C for 1 minute, annealing at 60°C for 1 minute, polymerization at 72°C for 1 minute, and after the 40 cycles one final polymerization step at 72°C for 5 minutes. The resulting 197bp UCP1 fragment was run out on a 1% low melt agarose gel and isolated from the gel using a QIAquick PCR Purification Kit according to manufacturer's protocol (Qiagen Inc., Valencia, CA). Quantitative PCR was then performed using the following reaction (per reaction): 2µl 10xPCR buffer, 0.6µl $MgCl_2$ (pre-optimized for the given primers, 2.5mM final concentration), 5µl primer mix (1.5mM final concentration of each UCP1 primer), 0.4µl dNTPs (10mM; containing equimolar concentrations of dATP, dCTP, dGTP and dTTP), 0.2µl Sybr green (50x; Applied Biosystems, Foster city, CA), 0.4µl Platinum *Taq* DNA polymerase (Invitrogen, Carlsbad, CA), gel-isolated UCP1 cDNA (in order to make a standard curve, one of a series of the following serial dilutions was used per reaction: 1:10, 1:100, 1:1000, 1:10,000 and 1:100,000), and water to a final volume of 20µl. The same reaction mixture was also done replacing the UCP1 cDNA with known amounts of the housekeeping gene 18S for quantitation (forward: 5'CCG CAG CTA GGA ATA ATG GA3' and reverse: 5'CCC TCT TAA TCA TGG CCT CA3') and water as a negative control reaction. Duplicates are made of all reactions on 24x5 well PCR plates. A fluorescence temperature cycler (Opticon Continuous Fluorescence Detector; MJ Research Inc., South San Francisco, CA) was used with the following conditions based on optimization for

18S: 95°C for 2 minutes, followed by 40 cycles of denaturing at 95°C for 15 seconds, annealing at 58.6°C for 30 seconds, and a plate read after each cycle. Final melting curves were calculated with a start temperature of 75°C, an ending temperature of 95°C, and a 1°C temperature increment. Standard curves, which allow for the determination of the relative concentration of RNA in the samples, were calculated by plotting the log of the input RNA against the critical threshold (CT) cycle, the cycle in which the fluorescence signal of the sample is greater than the baseline threshold. Amplification products performed in the fluorescence temperature cycler were checked by electrophoresis on 1.5% ethiduim bromide-stained agarose gels to make sure the size of the amplified fragments matched the calculated fragment size for UCP1 (197bp).

ICV injections

Surgical procedures were performed using sterile technique. Adult wild-type C57Bl/6J mice were deeply aenesthetized with a combination of ketamine hydrochoride and isofluorane and implanted with a 25-gauge stainless steel guide cannula with obdurator stylet into the lateral cerebral ventricle under stereotaxic control (coordinates were –0.6 relative to bregma, midline, and 4.75 mm below the surface of the skull). The cannula was secured to the skull with dental cement. Animals were individually housed and allowed to recover for one week with *ad libitum* access to standard low-fat Purina diet 5001. After recovery, 1nmol/injection/day AGRP (83-132) in a 2μl volume or 2μl saline was injected over 1 minute using a polyethylene 0.28mm diameter tubing attached to a Hamilton micro-syringe. The injector was left in place for another minute before removal. At this point, the low-fat chow was switched to the high-fat Research diets for the remainder of the 48-hour experiment. 24 hours after the first injection, a second identical dose was injected. The dose of AGRP was chosen based on efficacy in prior studies (Rossi et al., 1998). The position of the cannulae were verfied at the end of the experiment by dissection. 24 hours after the second injection animals were euthanized and IBAT was removed as described above.

Indirect calorimetry

Eight week-old wild-type and MC4R-/- male mice were acclimated to the oxygen consumption chambers for four days prior to the experiment. Oxygen consumption was measured by indirect calorimetry (Oxymax, Columbus Instruments, Columbus, Ohio). The Oxymax system measures the volume of oxygen at the inlet and outlet ports of the chamber through which a known amount of air flow is circulated. Mice were individually housed in chambers at around 24°C with an airflow of 500m/min and samples were recorded during the middle of the light cycle. The inlet fresh air flow-rate was 0.5liters(l)/minute at a sampling flow rate of 0.4l/minute. Each chamber was sampled for 50 seconds with a resettling time of 150 seconds. On the day of the experiment, animals were placed in the chambers for four hours prior to injections and measurements were taken after the first two hours when animals were at rest. After a subcutaneous injection of the highly specific β_3-adrenergic agonist CL316,243 (1µg/g) or an equal volume of saline, animals were placed back in the chambers and oxygen consumption was assessed 90 minutes post-injection while animals were at rest.

Statistical methods

Results are presented as mean ± standard error (SEM). Data sets were analyzed for significance using a one-way and two-way analysis of variance (ANOVA) followed by

Tukey and Bonferroni *post hoc* testing, respectively, on PRISM software (GraphPad, San Diego, CA). $P<0.05$ was considered statistically significant.

RESULTS

MC4R-/- mice exhibit attenuated UCP1 expression in response to a high-fat (HF) diet

In order to test the hypothesis that the MC4R is involved in regulating IBAT thermogenesis in response to a HF diet, we directly examined whether HF-fed MC4R-/- and AGRP-treated mice exhibit attenuated IBAT function. IBAT function was assessed by measuring UCP1 levels using Western blot technique.

Age-matched male wild-type and MC4R-/- mice that were raised on a low-fat (LF) diet were either continued on the LF diet (Purina 5001, PMI Nutrition International, Brentwood, MO, composed of 23.0%protein, 4.5% fat, 49% carbohydrate with 3.04 kcal/g metabolizable energy), or were placed for 48 hours on a HF diet (Research Diets; 60% fat calories, 20% protein, 20% carbohydrate, 5.24 kcal/g). When comparing the groups using two-way ANOVA, there was a significant effect of genotype on food intake measured by weight consumed ($p=0.008$) and of diet on food intake ($p=0.003$), but no significant interaction between genotype and diet on food intake ($p=0.14$)(LF MC4R-/-, 4.9±0.5g; HF MC4R-/-, 6.9±0.3g; LF wild-type, 4.3±0.6g; HF wild-type, 5.1±0.3g). Using a one-way ANOVA, HF-fed wildtype mice did, however, consume more calories than LF-fed wild-type mice ($p<0.001$), and similarly HF-fed MC4R-/- mice consumed more calories than LF-fed MC4R-/- mice ($p<0.001$) (Figure 1A). Using a two-way ANOVA, there was a significant interaction between genotype and diet on food intake when measured as kcal consumed ($p=0.023$). The effect of genotype on caloric intake ($p=0.002$) and of diet on caloric intake ($p<0.0001$) were also significant (LF MC4R-/-, 14.8±1.4kcal; HF MC4R-/-, 36.1±1.8 kcal; LF wild-type, 13.1±1.7kcal; HF wild-type, 26.5±1.5kcal).

There were no significant differences in body weight between the experimental groups at the start of the study. By one-way ANOVA MC4R-/- mice fed a HF diet did gain significantly more weight (2.6±0.3g) than MC4R-/- mice fed a LF diet (-0.1±0.1g) ($p<0.001$) and than wild-type mice fed either LF (-0.3±0.1g) ($p<0.001$) or HF diets (0.9±0.2g)($p<0.001$)(Figure 1C). Wild-type animals fed HF diets also gained significantly more weight than wild-type animals on a LF diet ($p<0.001$), although to a lesser degree than between the two MC4R-/- groups. By two-way ANOVA, the effects of genotype ($p<0.0001$) and diet ($p<0.0001$) on weight, and the genotype by diet interaction ($p=0.0003$) were significant.

Feed efficiency, or the weight gain per kcal ingested, has been previously shown to be increased for MC4R-/- mice (compared to wild-type controls) on a moderate-fat diet (Butler et al., 2001), suggesting that the increase in weight gain observed in MC4R-/- mice is not solely due to hyperphagia. In this study, a one-way ANOVA reveals that MC4R-/- mice similarly have a significantly higher feed efficiency after 48 hours on a HF diet than wild-type mice fed the same diet ($p<0.01$)(LF MC4R-/-, -8.7±10.7mg/kcal; HF MC4R-/-, 72.8±6.4mg/kcal; LF wild-type, -24.2±9.6mg/kcal; wild-type HF, 32.5±7.9mg/kcal) (Figure 1E). Interestingly, these results show that HF-fed wild-type mice also have a significant increase in feed efficiency over LF-fed wild-type mice ($p<0.001$). However, the difference in feed efficiency between MC4R-/- mice fed LF and HF diets was nonetheless found to be greater than the difference between wild-type mice fed LF and HF diets. By two-way ANOVA, the effects of diet ($p<0.0001$) and genotype ($p=0.003$) on feed efficiency were significant, whereas the diet by genotype interaction ($p=0.16$) was not.

After 48 hours, a one-way ANOVA reveals that the relative UCP1 protein levels in HF fed wild-type animals were 4.3±0.8 fold higher (n=11) than in LF fed wild-type animals (n=12) ($p<0.001$)(Figure 2A). Relative UCP1 protein levels in MC4R-/- mice that were fed LF (1.5±0.3, n=10) or HF (1.0±0.1, n=12) diets were not significantly different from each other or from wild-type animals fed a LF diet. By two-way ANOVA, the effect of genotype ($p=0.001$) and diet ($p=0.0014$) on UCP1 levels as well as the interaction between the two ($p<0.0001$) were significant.

A smaller experiment was carried out with a moderate fat (MF) diet (Purina diet 5015; 11% fat calories, 17.0% protein, 53.5% carbohydrate, 3.73 kcal/g metabolizable energy) for 48 hours. By one-way ANOVA, UCP1 protein levels in MF fed wild-type mice (2.0±0.3) were higher than in LF fed wild-type mice (1.0±0.2) ($p<0.05$), although to a lesser degree than with HF fed mice, while again no significant difference was detected between LF fed MC4R-/- (1.1±0.3) and MF fed MC4R-/- (1.0±0.3) (Figure 3A). By two-way ANOVA, the effect of genotype ($p=0.07$) and diet ($p=0.06$) on UCP1 levels were not significant whereas the interaction between the two ($p=0.04$) was significant.

Quantitative real-time PCR (RT-PCR) was used to measure the relative levels of UCP1 mRNA in the same animals. Although MF fed wild-type mice (1.4±0.3) had a trend toward higher UCP1 mRNA levels than LF fed wild-type mice (1.0±0.2) using one-way ANOVA, no significant difference was detected amongst any of the groups, LF MC4R-/- (0.7±0.2) and MF MC4R-/- (0.7±0.2) (Figure 3B). By two-way ANOVA, the effect of genotype ($p=0.03$) was significant, while the effect of diet ($p=0.4$) and the interaction between the two ($p=0.3$) were not significant.

AGRP-treatment attenuates UCP1 protein levels in response to a HF diet

In order to further confirm our findings, we repeated the above protocol, however this time we used a pharmacological approach in place of a genetic one. Age-matched male mice were fed a LF or HF diet while being treated with AGRP (*83-132*) or saline for two days. As expected from previous studies, using one-way ANOVA, AGRP-treated mice consumed more food in grams or calories than wild-type controls ($p<0.001$)(LF saline, 8.0±0.4g, 24.4±1.2kcal; HF saline, 7.3±0.3g, 38.5±1.6kcal; LF AGRP, 10.2±0.3g, 31.1±0.8kcal; HF AGRP, 10.8±0.5g, 57.8±3.0kcal) (Figure 1B). By two-way ANOVA, there was a significant effect of drug treatment ($p<0.0001$) and diet ($p<0.0001$) on calories consumed, and the interaction between them ($p=0.002$). In AGRP-treated animals, by one-way ANOVA, HF saline animals gained more weight than LF saline animals ($p<0.01$) and HF AGRP animals gained more weight than LF AGRP animals ($p<0.001$) (LF saline, -0.2±0.3g; HF saline, 0.9±0.2g; LF AGRP, 1.7±0.2g; HF AGRP, 3.6±0.2g) (Figure 1D). In addition LF AGRP animals gained more weight than LF saline animals ($p<0.001$). By two-way ANOVA, the effect of both drug treatment ($p<0.0001$) and diet ($p<0.0001$) on weight were significant, but not the drug treatment by diet interaction ($p=0.09$).

By one-way ANOVA HF saline had a higher feed efficiency than LF saline ($p<0.05$) and LF AGRP had a higher feed efficiency than LF saline ($p<0.001$) (LF saline, -16.25±14.77mg/kcal; HF saline, 20.68±4.7mg/kcal; LF AGRP, 53.3±7.6mg/kcal; HF AGRP, 66.1±4.5mg/kcal) (Figure 1F). HF saline animals also had a higher feed efficiency than HF saline ($p<0.01$). By two-way ANOVA we observed a significant effect of drug treatment ($p<0.0001$) on feed efficiency in AGRP-treated mice and saline-treated controls. The effect of diet ($p=0.005$) on feed efficiency is also significant, but not the interaction between drug treatment and diet on feed efficiency ($p=0.15$).

By one-way ANOVA, AGRP-treated animals fed a HF diet had similar UCP1 levels (0.6±0.1. n=13) to LF saline (1.0±0.1, n=11) and LF AGRP (0.9±0.1, n=11), but significantly lower relative levels of UCP1 protein than the HF fed saline treated control group (2.8±0.8, n=14)($p<0.05$)(Figure 2B). By two-way ANOVA, the effect of diet alone on UCP1 levels was not significant ($p=0.09$), but the effect of drug treatment ($p=0.01$) and the drug treatment by diet interaction ($p=0.03$) were significant.

Up-regulation of UCP1 by the central melanocortin system in response to an acute HF diet does not appear to be mediated by the HPT axis

By one-way ANOVA, total T_3 levels were modestly, yet significantly, elevated in both HF fed wild-type mice (105.8±6.5 ng/dl, n=11) ($p<0.01$) and MC4R-/- mice (110.5±6.2 ng/dl, n=12) ($p<0.05$) compared with LF fed wild-type (74.5±2.6 ng/dl, n=12) and MC4R-/- mice (85.0±7.6 ng/dl, n=8) (Figure 4A). By two-way ANOVA, the effect of diet on total T_3 levels was significant ($p<0.0001$), however there was no effect of genotype on T_3 levels (p=0.21) or a genotype by diet interaction (p=0.62).

By one-way ANOVA, total T_3 levels were also significantly elevated ($p<0.0001$) in both HF fed AGRP-treated (98.1±8.2, n=8) ($p<0.05$) and saline-treated mice (117.3±6.2, n=8)($p<0.01$) compared with LF fed AGRP-treated (73.0±3.9, n=7) and saline-treated mice (78.6±5.5, n=6) (Figure 4B). By two-way ANOVA, the effect of drug treatment (p=0.06) and the drug treatment by diet interaction (p=0.3) were not significant, whereas the effect of diet was significant ($p<0.0001$).

By one-way ANOVA, total T_4 levels in MC4R-/- and wild-type mice were no significant differences between any two indivdual groups (Figure 4C). However, by two-way ANOVA, total T_4 levels were significant for diet (p=0.01) with HF-fed animals having lower T_4 levels (LF wild-type, 3.4±0.2μg/dl, n=9; LF MC4R-/-, 3.3±0.3μg/dl, n=6) than LF-fed animals (HF wild-type, 2.9±0.2μg/dl, n=8; HF MC4R-/-, 2.6±0.2μg/dl, n=4), but not significantly different between the groups for genotype (p=0.28) or genotype by diet interaction (p=0.72).

Effect of cold exposure on UCP1 levels in MC4R-/- and wild-type mice

In order to test the hypothesis that the MC4R is involved in regulating IBAT thermogenesis in response to cold exposure, we examined whether MC4R-/- and wild-type mice exposed to 4°C had attenuated IBAT function. IBAT function was assessed by measuring UCP1 levels using Western blot technique.

Age-matched lean male and female wild-type and MC4R-/- were placed at room temperature (24°C) or exposed to cold (4°C) for four hours. Males and females were pooled together for analysis after observing no significant difference between them. After four hours, using a one-way ANOVA, the relative UCP1 levels in cold-exposed wild-type mice (1.9 ± 0.1, n=8) were significantly higher than for cold-exposed MC4R-/- mice (1.0 ± 0.1, n=9) ($p<0.01$) or wild-type (1 ± 0.1, n=8) ($p<0.001$) and MC4R-/- (1.1 ± 0.2, n=8) ($p<0.01$) mice kept at room temperature (Figure 5A). By two-way ANOVA, the effect of cold exposure on UCP1 ($p=0.006$), the effect of genotype on UCP1 ($p=0.013$) and the cold exposure by genotype interaction ($p=0.002$) were significant.

In another experiment, age-matched lean male wild-type and MC4R-/- were placed at room temperature (24°C) or exposed to cold (4°C) for five days. After five days of cold exposure, using one-way ANOVA, MC4R-/- mice (3.2 ± 0.1, n=4) had an increase in their relative UCP1 levels compared with MC4R-/- mice (1.4 ± 0.2, n=4) at room temperature

($p<0.001$), similar to the increase observed between wild-type at cold exposure (2.1±0.2, n=4) and wild-type kept at room temperature (1±0.1, n=4) ($p<0.01$)(Figure 5B). MC4R-/- mice with cold exposure had an even larger increase in UCP1 levels compared with wild-type mice under the same conditions ($p<0.01$). By two-way ANOVA, the effect of cold exposure on UCP1 levels ($p<0.0001$) and the effect of genotype on UCP1 levels were significant ($p=0.0005$). However, the effect of cold exposure on genotype ($p=0.03$) was not significant. We also measured the relative UCP1 mRNA levels from the IBAT of the same animals using RT-PCR and obtained similar results. By one-way ANOVA, wild-type (1.9±0.1) and MC4R-/- (1.7±0.2) mice exposed to cold for 5 days had an increase in UCP1 mRNA compared with wild-type (1.0±0.1)($p<0.05$) and MC4R-/- (0.9±0.1) ($p<0.05$) mice kept at room temperature respectively (Figure 5C). By two-way ANOVA, the effect of temperature on UCP1 mRNA levels was significant ($p=0.0002$), whereas the effect of genotype ($p=0.55$) and the temperature by genotype interaction ($p=0.83$) were not significant.

Failure to increase thermogenesis in MC4R-/- mice is not due to a peripheral sympathetic defect

In order to examine whether the attenuation we observed in the MC4R-/- mouse's ability to up-regulate UCP1 in response to a high-fat diet or an acute cold challenge was due to a general defect in peripheral sympathetic responsiveness, we injected MC4R-/- mice and wild-type mice with either saline (MC4R-/- n=8, wild-type n=8) or a β_3-adrenergic agonist. By one-way ANOVA, both wild-type (42.7±5.0%, n=4) and MC4R-/- (39.5±4.2%, n=4) mice injected with the β_3-adrenergic agonist exhibited a significant increase above basal oxygen consumption compared to saline-injected MC4R-/- (2.5±1.9%, n=4)($p<0.001$) and wild-type (0.5±0.6%)($p<0.001$) controls respectively (Figure 6).

DISCUSSION

Central MC4R signaling is critically required in diet-induced UCP1 up-regulation in IBAT

Basal and total oxygen consumption in MC4R-/- mice, in contrast to wild-type C57BL/6J mice, is not up-regulated when animals are fed a moderate-fat diet (Butler et al., 2001). Diet is a powerful regulator of adaptive thermogenesis (Dulloo and Jacquet, 2001; Leibel et al., 1995; Shibata and Bukowiecki, 1987; Wadden et al., 1990) and BAT is arguably the most important site of adaptive thermogenesis in rodents (Cannon and Nedergaard, 2004). Furthermore, it has been shown that a high-fat, or 'cafeteria', diet induces an up-regulation of mitochondrial UCP1 mRNA or protein levels in IBAT (Archer et al., 2005; Li et al., 2004; Margareto et al., 2001; Nedergaard et al., 1984; Portillo et al., 1998; Rippe et al., 2000; Rippe et al., 2003; Surwit et al., 1998). We therefore wanted to examine whether the thermogenic defect observed in MC4R-/- mice (Butler et al., 2001) was due to an inability to up-regulate UCP1 in response to a high-fat diet. Our results demonstrate that MC4R-/- and AGRP-treated wild-type mice have a defect in their ability to up-regulate UCP1 protein expression in IBAT in response to a two day high-fat diet. These data indicate that central MC4R signaling is critically required for acute diet-induced thermogenesis in IBAT and suggest that attenuated IBAT thermogenic function could account for at least part of the decrease in basal oxygen consumption and increased

obesity observed in MC4R-/- animals fed a moderate-fat or high-fat diet. Interestingly, we found that AGRP treatment in mice does not affect UCP1 levels when they are fed a normal low-fat diet, which differed from previous studies in rats showing that AGRP treatment increases (Fekete et al., 2002a) or decreases (Small et al., 2001) UCP1. These varying results may be due to the different methodologies, such as species and size of animal used, as well as time course, dose and method used for AGRP administration. For instance we used mice in our study, whereas Fekete et al. used Sprague Dawley rats and Small et al. used Wistar rats. In our study, daily administration of AGRP was injected ICV into the third ventricle for two days, whereas Small et al. looked at ICV injections of AGRP into the third ventricle for 7 days, and Fekete et al. used ICV administration of AGRP into the lateral ventricle via osmotic minipumps for 3 days. However, it is clear from our results that AGRP-treated mice, in contrast to saline-treated control mice, were unable to increase UCP1 expression when switched from a low-fat to a high-fat diet.
We observed a more moderate increase in UCP1 levels in wild-type mice when they were fed the same moderate-fat diet used in used in previously published results (Butler et al., 2001)(Purina diet 5015, 11% fat, 17% protein, 53.5% carbohydrate, 3.73 kcal/g metabolizable energy) rather than the high-fat diet (Research Diets; 60% fat calories, 20% protein, 20% carbohydrate, 5.24 kcal/g). There were no differences in UCP1 levels between moderate-fat fed MC4R-/- mice, low-fat fed MC4R-/- mice and low-fat fed wild-type mice (data not shown).

Putative mechanisms underlying MC4R signaling-dependent up-regulation of UCP1 in response to a high-fat diet

In rodents, thyroid hormones act synergistically with the SNS to regulate UCP1 expression (Bianco et al., 1988; Cassard-Doulcier et al., 1994; Lanni et al., 2003; Rabelo et al., 1995; Rim and Kozak, 2002). One of the major roles of the HPT axis in warm-blooded animlas is the regulation of energy expenditure, primarily via increased thermogenesis. Animals in a state of negative energy balance, such as occurs with fasting, have reduced serum T_3 and T_4 levels (Ahima et al., 1996; Blake et al., 1991; Kinlaw et al., 1985; Kok et al., 2005; Rondeel et al., 1992) as well as reduced TRH mRNA levels in the PVH (Blake et al., 1991; Harris et al., 2001; van Haasteren et al., 1995), which leads to the conservation of energy by reducing metabolic rate (Blake et al., 1991). Conversly, a state of positive energy balance, such as feeding with a calorie-dense chow (Danforth et al., 1979) and/or a chronic increase in dietary fat (Almeida et al., 1996; Leblanc et al., 1982; Naim et al., 1985; Rabolli and Martin, 1977; Tulp et al., 1982) has been shown to increase both the NE turnover in rodents (Schwartz et al., 1983) and serum T_3 levels (Almeida et al., 1996; Danforth et al., 1979; Leblanc et al., 1982; Naim et al., 1985; Rabolli and Martin, 1977; Tulp et al., 1982). TRH neurons in the PVH express MC4R and are densely innervated by α-MSH-containing and AGRP-containing axon terminals in both rats and humans (Fekete et al., 2000; Harris et al., 2001; Legradi and Lechan, 1999; Mihaly et al., 2000). Furthermore, the melanocortin system has also been implicated in the regulation of the HPT axis (Fekete et al., 2000; Fekete et al., 2004; Fekete et al., 2002a). For instance, ICV infusion of α-MSH (Fekete et al., 2000) or leptin (Fekete et al., 2006) into fasted rats completely restores pro-TRH mRNA levels in the PVH to normal fed levels. ICV α-MSH in fasted rats also restores thyroid hormones to 50% of fed levels (Fekete et al., 2000) and increases phosphorylation of the transcription factor cAMP response element binding protein (CREB) in TRH neurons in the PVH

(Sarkar et al., 2002). Additionally, AGRP inhibits proTRH mRNA levels in the PVH of wild-type controls but not MC4R-/- mice, suggesting that AGRP signaling to TRH hypophysiotropic neurons is mediated by the MC4R (Fekete et al., 2004). These studies led to our hypothesis that perhaps there may be a defect in the MC4R-HPT axis that contributes to the inability of MC4R-/- to up-regulate UCP1 expression in BAT in response to a high-fat diet. We therefore examined the effect of a high-fat diet on thyroid hormone levels in MC4R-/- and AGRP-treated mice and found, contrary to our original hypothesis, that MC4R-/- and AGRP-treated mice exhibit the same increase in total T_3 hormone levels as wild-type controls when switched from a low-fat to a high-fat diet. Interestingly, we also found that total T_4 levels in high-fat fed MC4R-/- and wild-type mice are decreased, which is likely related to the observed increases in T_3, as T_4 is converted to T_3, the more biologically active form. Overall, these results suggest that the central melanocortin-mediated regulation of the HPT axis does not appear to be involved in the DIT–induced up-regulation of UCP1. Our study cannot, however, completely rule out the possibility that the HPT axis is involved in mediating the melanocortin system's effects on UCP1 regulation. It is, for instance, possible that wild-type mice have higher free T_3 levels (the more biologically active form) than MC4R-/- mice and that we did not detect this difference by measuring only the total T_3, which is comprised mostly of the less active plasma protein-bound T_3. However, free T_4 and T_3 are generally considered to be in equilibrium with the protein-bound hormones in both plasma and tissue and thus total serum thyroid hormone levels are thought to be reflective of the relative free thyroid hormone levels.

The most likely mechanism of action underlying the MC4R-/- animal's inability to up-regulate UCP1 in IBAT is, therefore, a defect in sympathetic outflow to IBAT in response to a high-fat diet. However, one study observed that after 24-hours on a moderate fat diet wild-type mice display comparable NE-turnover in IBAT to that of wild-type mice on a low-fat diet, suggesting that changes in sympathetic activity in IBAT is not involved in DIT in this model (Butler et al., 2001), although it remains nevertheless quite possible that a difference was not detected because of the limited time frame in which the experiment was performed. In contrast, multiple studies have found that a high-fat diet does lead to increases in UCP1 levels (Archer et al., 2005; Li et al., 2004; Margareto et al., 2001; Nedergaard et al., 1984; Portillo et al., 1998; Rippe et al., 2000; Rippe et al., 2003; Surwit et al., 1998). Further studies are needed to clarify the effect of DIT and the role of the central melanocortin system on sympathetic outflow to BAT.

Our results demonstrating that MC4R-/- mice have the same increase in oxygen consumption as wild-type animals after injection of a β_3-adrenergic agonist, strongly suggest that the defect observed in MC4R-/- mice is not due to a peripheral defect in sympathetic responsiveness.

Effect of cold exposure on the melanocortin system's regulation of UCP1

UCP1 plays a central role in sustaining normal body temperatures of rodents and other mammals during cold exposure. Therefore, in order to examine the hypothesis that the melanocortin system is involved in the regulation of UCP1 under physiological conditions that normally stimulate BAT recruitment, we exposed MC4R-/- and wild-type mice to cold temperatures (4°C) and compared their UCP1 levels.

One of the central arguments raised against the hypothesis that attenuated IBAT function in MC4R-/- mice accounts for part of their increased obesity, stems from the observation that MC4R-/- mice, unlike Lep^{ob}/Lep^{ob} mice (Trayhurn et al., 1977), are able to thermoregulate at 4°C, and it has been therefore argued that they have no defect in BAT recruitment (Butler et al., 2001). However, even UCP1-ablated animals, although cold-sensitive in the first hours, are able by 24 hours to thermoregulate during cold exposure by compensating for the lack of non-shivering thermogenesis with shivering thermogenesis (Golozoubova et al., 2001). Thus the ability of MC4R-/- animals to maintain their core body temperature under chronic cold conditions may involve mechanisms other than non-shivering thermogenesis. Our finding that MC4R-/- mice exposed to 4°C for 4 hours were unable to up-regulate UCP1 expression indicates that MC4R signaling is also critically required for an acute cold-induced IBAT thermogenesis and provides further evidence that MC4R-/- mice do indeed have some defect in their ability to induce non-shivering thermogenesis. However, after a 5-day cold exposure MC4R-/- mice regain their ability to induce UCP1. One interpretation could be that the melanocortin system is involved in, or necessary, only for the short-term regulation of UCP1 and that other compensatory mechanisms are activated upon longer periods of cold exposure that do not require central MC4R signaling. It is also possible that animals may differentially regulate UCP1 in response to cold and dietary fat, and that even though BAT recruitment in MC4R-/- mice may remain in tact during long-term exposure to cold temperatures, they do not have the ability to recruit BAT in response to increased dietary fat. The mechanisms underlying the differences in the melanocortin system's ability to regulate UCP1 during short-term and long-term cold exposure remain to be understood.

ACKNOWLEDGEMENTS

This work was supported by NIDDK/NIH grants DK62179 (WF), DK070332 and DK051730 (RDC), DK58148 and NS045231 (EAN). Eduardo Nillni collaborated with us on the thyroid assays, Kate L.J. Ellacott assisted with the IBAT dissections and Jon G. Murphy assisted with the cannulations and with the dissections. We also thank Ronald C. Stuart, Ilia G. Halatchev, Ken Gruber and Paul Kievit for their help.

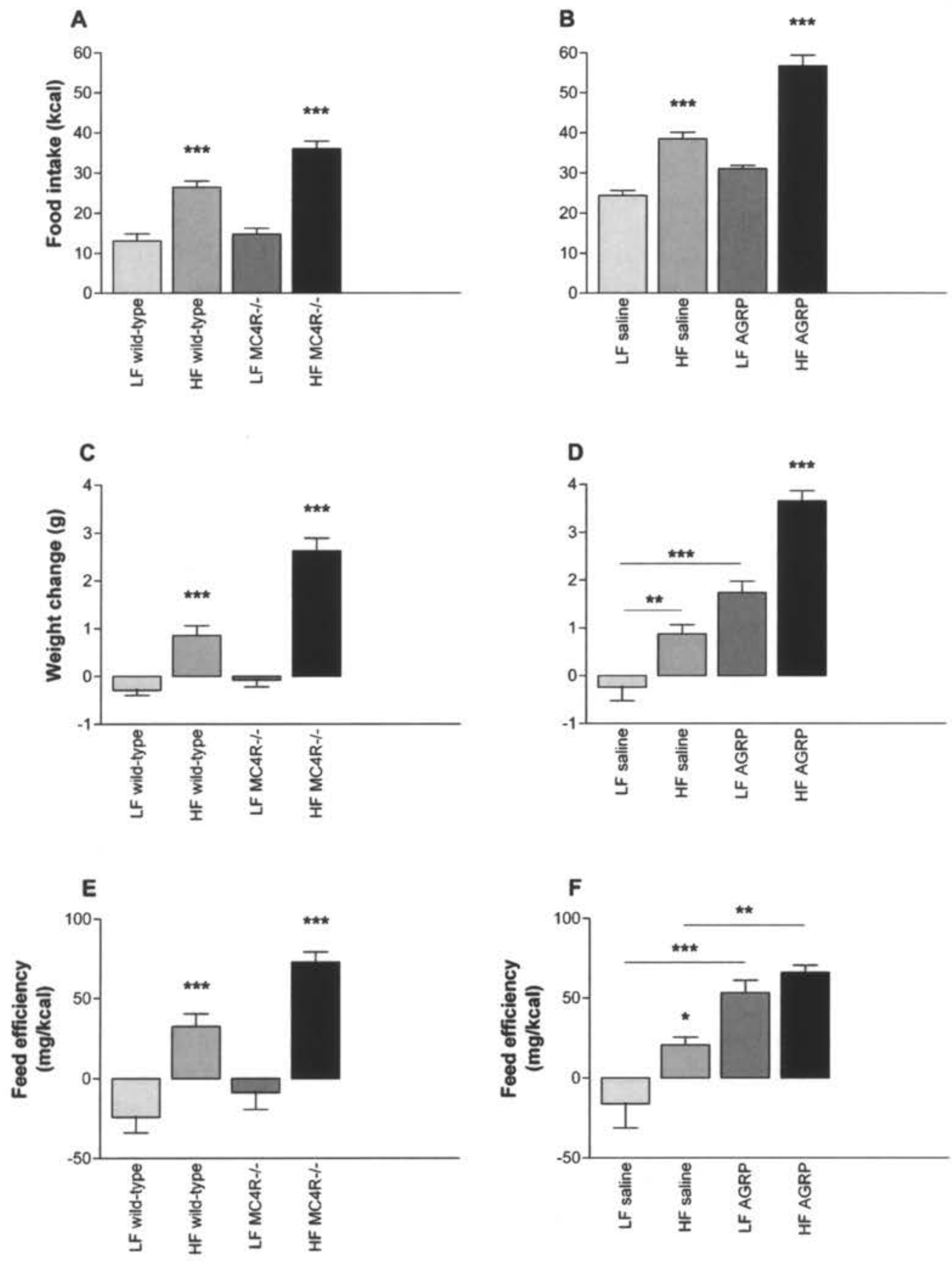

Figure 1: Total 2-day food intake, weight change and feed efficiency in 7.5 week-old male MC4R-/- and AGRP-treated mice given a low-fat (LF) or high-fat (HF) diet. (**A**) MC4R-/- mice on a HF diet have a higher caloric intake compared with HF-fed wild-type mice. (**B**) Similarly, AGRP-treated mice on a HF diet have a higher caloric intake compared with HF-fed saline-treated controls. (**C**) MC4R-/- mice gain more weight than wild-type mice when switched from a LF to a HF diet. (**D**) AGRP-treated mice gain more weight than wild-type mice when switched from a LF to a HF diet. Increased feed efficiency in MC4R-/- mice (**E**) and AGRP-treated mice (**F**). n= 10-14 for each group. By one-way ANOVA: *, P<0.05;**, P<0.01;***, P<0.001.

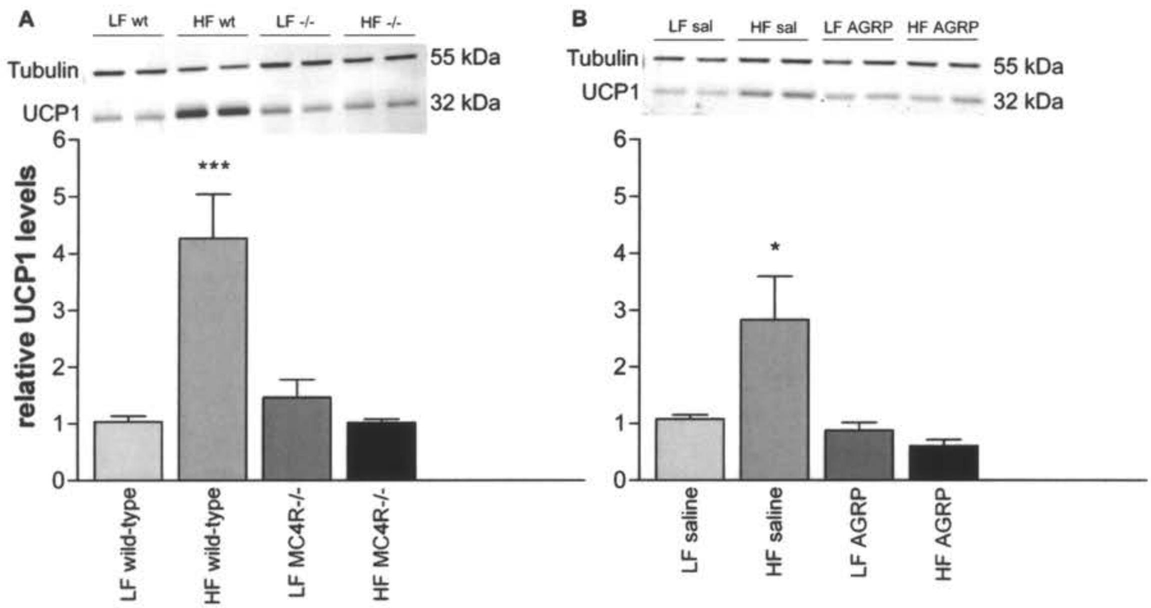

Figure 2: Lean male MC4R-/- and AGRP-treated mice have attenuated UCP1 protein levels in response to a high-fat (HF) diet. UCP1 (32kDa) is normalized with respect to tubulin (55kDa) for each animal, and the four sets of animals within each experiment are further normalized to either low-fat (LF)-fed wild-type (A) or saline-treated (B) mice. Representative Western blot results for two animals from each group are shown above the bar graphs. The bar graphs indicate the mean values for each group. (**A**) UCP1 protein levels are induced 4-fold by a HF diet in wild-type mice. After a HF diet, MC4R-/- mice (n=12) do not exhibit the increase in UCP1 levels found in wild-type mice (n=11). UCP1 levels are the same in MC4R-/- (n=10) and wild-type mice (n=12) fed a LF diet. (**B**) UCP1 protein levels are induced 2.5 fold by a HF diet in wild-type mice treated with ICV saline. After a HF diet, mice treated ICV with AGRP (n=13) do not exhibit the increase in UCP1 levels found in saline-treated mice (n=14). UCP1 levels are the same in AGRP-treated (n=11) and saline-treated mice (n=11) fed a LF diet. By one-way ANOVA: *, $P<0.05$; ***, $P<0.0001$.

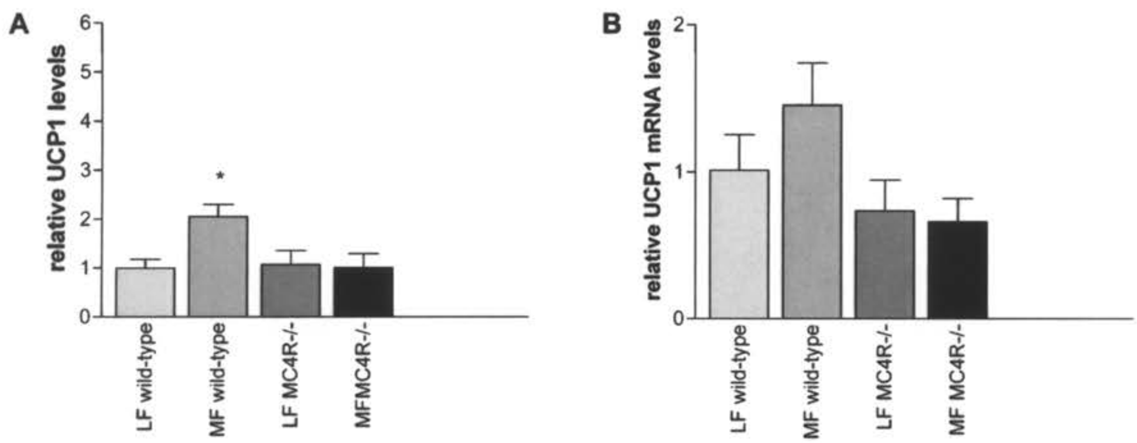

Figure 3: Lean male MC4R-/- mice have attenuated UCP1 protein and mRNA levels in response to a 2-day moderate-fat (MF) diet. UCP1 protein and mRNA levels are normalized to tubulin and 18S, respectively, for each animal, and the four sets of animals within each experiment are further normalized to low-fat (LF)-fed wild-type mice. (**A**) UCP1 protein levels are induced 2-fold by a MF diet in wild-type mice. After a MF diet, MC4R-/- mice (n=5) do not exhibit the increase in UCP1 levels found in wild-type mice (n=6). UCP1 levels are the same in MC4R-/- (n=5) and wild-type mice (n=6) fed a LF diet. (**B**) UCP1 mRNA levels are increased, although not significantly, in wild-type mice (n=5) after a MF diet in comparison with wild-type mice on a LF diet (n=6). UCP1 mRNA levels are the same in MC4R-/- (n=5) and wild-type mice (n=5) fed a LF diet. By one-way ANOVA: *, P<0.05.

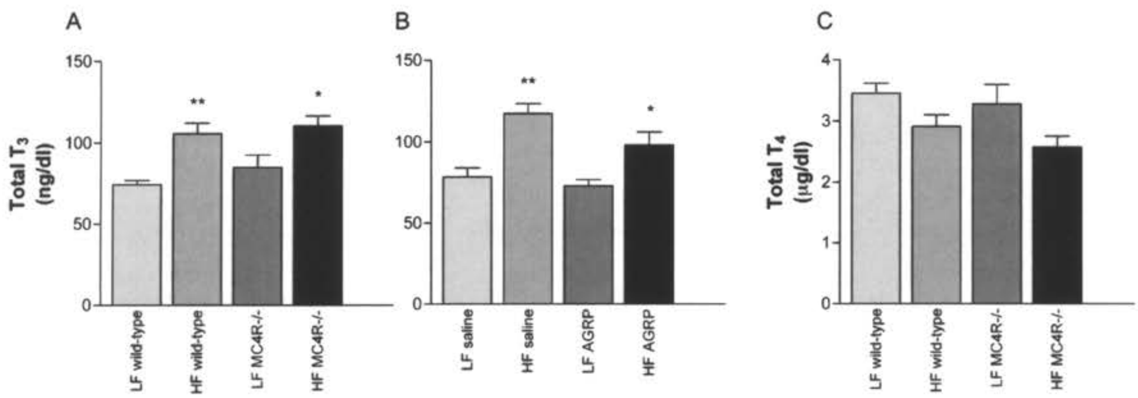

Figure 4: MC4R-/- and AGRP-treated mice have normally elevated total T_3 serum hormone levels in response to a 2-day high-fat (HF) diet. (**A**) Total T_3 levels are elevated in MC4R-/- (n=12) and wild-type (n=11) mice fed a high-fat diet compared to MC4R-/- (n=8) and wild-type (n=12) mice fed a low-fat (LF) diet. (**B**) Total T_3 levels are elevated in HF-fed AGRP-treated (n=8) and saline-treated (n=8) mice compared to AGRP-treated (n=7) and saline treated (n=6) mice fed a LF diet. (**C**) Total T_4 levels are reduced, but not significantly, in MC4R-/- (n=4) and wild-type mice (n=8) fed a HF diet compared to MC4-/- (n=6) and wild-type (n=9) mice fed a LF diet. By one-way ANOVA: *, $P<0.05$; **, $P<0.01$.

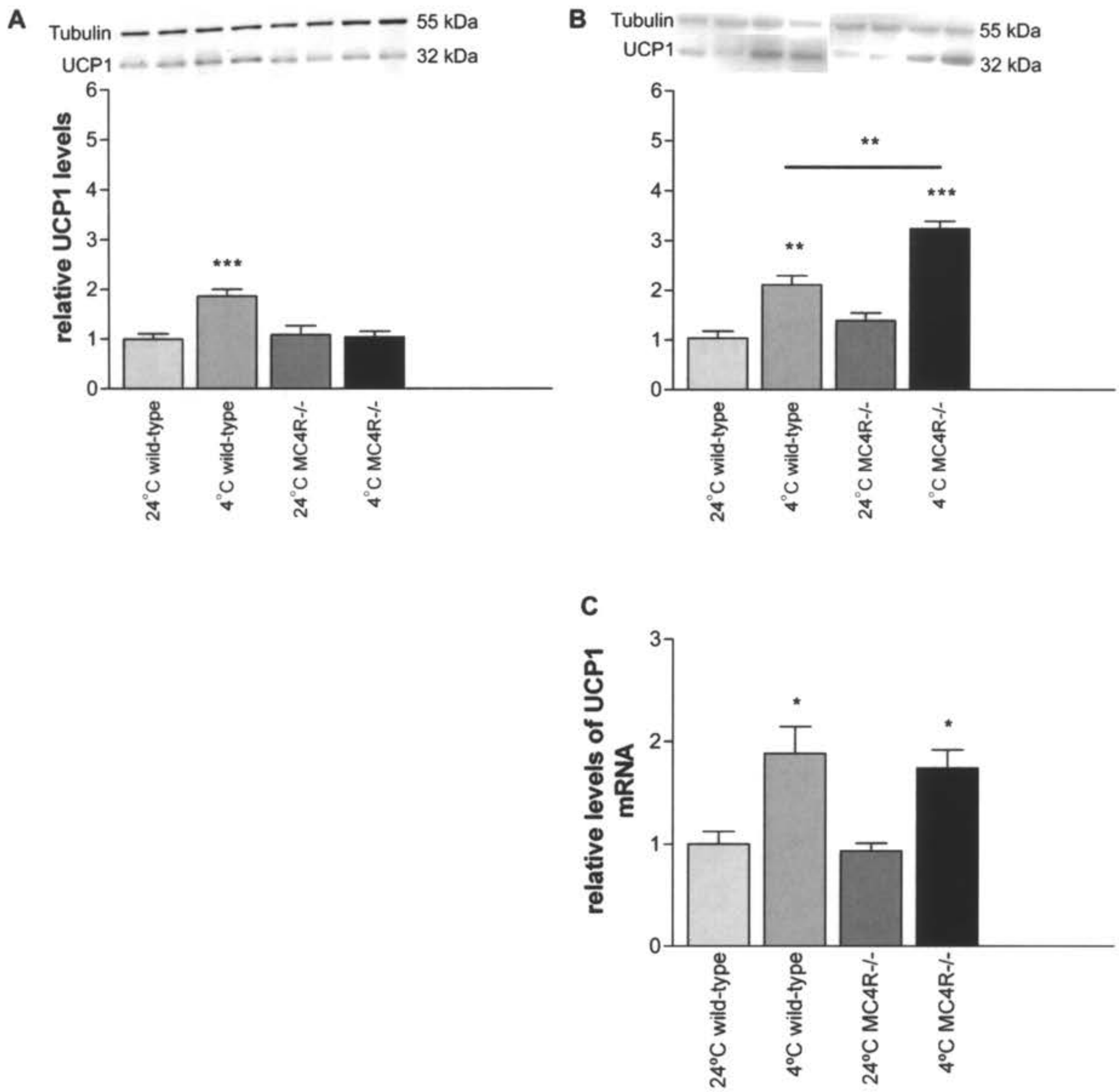

Figure 5. Lean male and MC4R-/- mice fail to increase UCP1 protein levels in response to 4 hours of cold exposure (A), but are able to up-regulate UCP1 protein and mRNA levels after a 5-day cold exposure (B) and (C). UCP1 protein (32kDa) and mRNA levels are normalized with respect to tubulin (55kDa) or 18S, respectively, for each animal, and the four sets of animals within each experiment are further normalized to 24°C wild-type mice. Representative Western blot results for two animals from each group are shown above the bar graphs in (A) and (B). The bar graphs indicate the mean values for each group. (**A**) After exposure to 4°C for 4 hours, 7-8 week old MC4R-/- mice (n=9) do not exhibit the almost 2-fold increase in UCP1 protein levels observed in age-matched wild-type mice (n=8). UCP1 levels are the same in MC4R-/- (n=9) and wild-type mice at 24°C (n=8). (**B**) After exposure to 4°C for 5 days, 5.5-6.5 week old MC4R-/- mice (n=4) up-regulate UCP1 levels, as do age-matched wild-type mice (n=4). UCP1 levels are the same in MC4R-/- (n=4) and wild-type mice (n=4) after 5 days at 24°C. (**C**) UCP1 mRNA levels are increased almost 2-fold wild-type mice (n=5) and in MC4R-/- mice after 5 days at 4°C (n=5) when compared with control wild-type (n=5) and MC4R-/- (n=5) mice at 24°C. By one-way ANOVA: *, $P<0.05$. ; **, $P<0.01$; ***, $P<0.0001$.

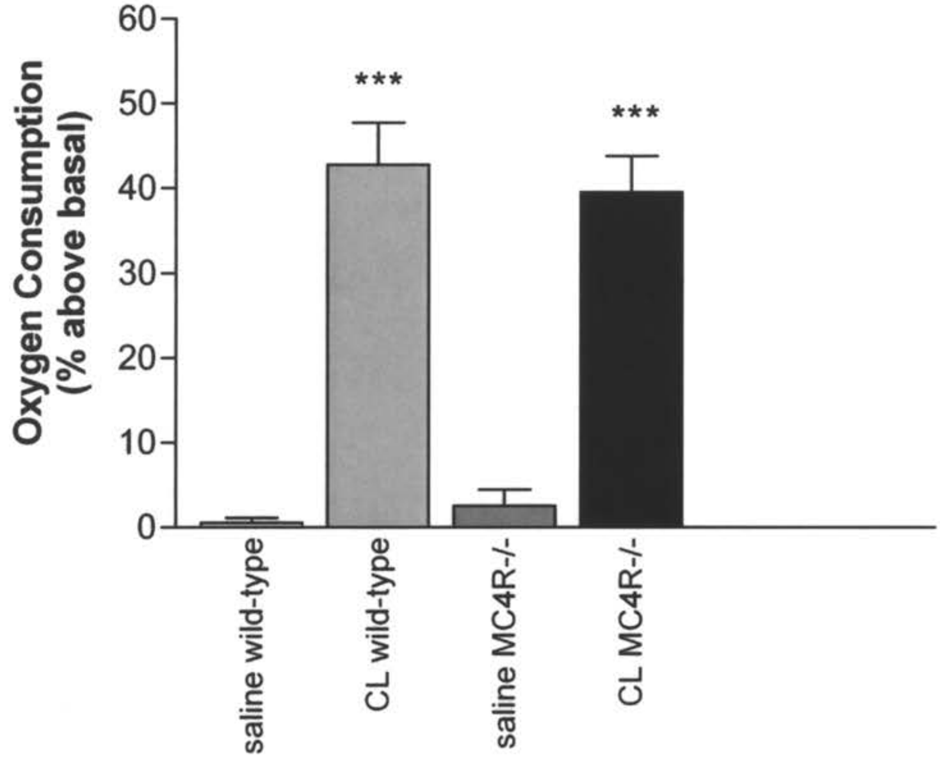

Figure 6: MC4R-/- exhibit normal increase in energy expenditure in response to peripheral injection of the β_3-adrenergic agonist CL316,243 (CL) at a dose of 1μg/g. MC4R-/- (n=4) and wild-type (n=4) mice have a large increase in oxygen consumption 90 minutes post-injection with CL, when compared with saline-injected wild-type (n=4) and MC4R-/- (n=4) controls. By one-way ANOVA: ***, P<0.001.

CHAPTER THREE

Melanocortin-4 Receptor and glutamic acid decarboxylase colocalize in sexually dimorphic nuclei in the mouse brain

Adriana Voss-Andreae and Roger D. Cone

ABSTRACT

The melanocortin-4 receptor (MC4R) has been shown to play a critical role in the regulation of energy homeostasis in rodents and humans. Deletion of the MC4R or overexpression of the endogenous antagonist of the MC4R, agouti related peptide (AGRP), conversely result in the stimulation of feeding and decrease in energy expenditure. Central melanocortin receptor agonists can also cause an inhibition of feeding when administered solely into the paraventricular hypothalamic nucleus (PVH) and intraPVH NPY administration antagonizes melanocortin agonist actions. Melanocortin agonists and NPY/AGRP also elicit opposing GABAergic responses in electrophysiological assays using whole cell patch recording from certain medial parvocellular PVH neurons. Regulation of GABA release was thus proposed to be one mechanism by which multiple afferent signals, such as those carried by POMC and NPY/AGRP fibers, could be integrated at downstream adipostatic effector sites. To determine whether POMC and NPY/AGRP neurons modulate GABA release by directly contacting MC4R positive GABA interneurons or whether they indirectly modulate GABA release, we characterized co-expression of the MC4R and glutamic acid decarboxylase (GAD), a marker of GABAergic neurons, by using double *in situ* hybridization. We found that MC4R co-localized with GAD in a limited number of nuclei, but no co-localization was found in the PVH. Remarkably, most GABAergic MC4R neurons were found in sexually dimorphic nuclei, such as the medial amygdala, preoptic area, anteroventral periventricular nucleus of the hypothalamus and the bed nucleus of the stria terminalis, suggesting a mechanism by which melanocortin signaling mediates its observed sexually divergent effects on energy homeostasis.

INTRODUCTION

The paraventricular hypothalamus (PVH) expresses the melanocortin-4 receptor (MC4R) and receives dense pro-opiomelanocortin (POMC) and neuropeptide Y(NPY)/agouti related peptide (AGRP) projections from the arcuate nucleus (ARC) (Cowley et al., 1999; Haskell-Luevano et al., 1999; Kishi et al., 2003; Mountjoy et al., 1994). Microinjection of NPY and melanocortin ligands into the PVH influences feeding behavior (Cowley et al., 1999). These and other observations led to the hypothesis that ARC POMC and NPY/AGRP projections act on the same MC4R-containing neurons in the PVH, thus integrating orexigenic and anorexigenic signals (Cowley et al., 1999). In support of this hypothesis, microinjection of the central MC3R and MC4R agonist melanotan II (MTII), into the PVH of rats results in a potent inhibition of feeding which is blocked by pre-injection of the MC3R and MC4R antagonist SHU9119 (Cowley et al., 1999). SHU9119 administered alone stimulates feeding. Furthermore, opposing synaptic responses are mediated, at least in part, by $GABA_A$ receptors. Bath application of MTII and α-MSH causes a dose-dependent increase in the amplitude of the GABA-evoked currents, which can be blocked by pre-treatment with SHU9119 or AGRP respectively. NPY causes a decrease in these same currents. These observations taken together suggest a model whereby ARC POMC and NPY/AGRP neurons project to PVH GABA interneurons where they modulate GABA release. These GABAergic interneurons may thus integrate orexigenic and anorexigenic information, thereby providing an example of a cellular mechanism underlying the adipostat (Figure 1).

While it is likely that GABA release is modulated in part by α-melanocortin stimulating hormone (α-MSH) acting on the MC4R in PVH GABAergic neurons, it has not yet been determined whether MC4Rs directly modulate GABA release from GABAergic neurons in the PVH, or whether they indirectly influence GABA release, for example by exciting neurons that then synapse onto the GABAergic neurons. Although there are very few GABAergic neurons in the PVH, neuroanatomical tracing studies combined with detection of the GABA synthesizing enzyme, glutamic acid decarboxylase (GAD), revealed that GABAergic projections to the PVH originate from several, diffusely distributed local sources (Roland and Sawchenko, 1993), including the anterior perifornical region, the anterior hypothalamic area immediately ventral to the PVH, the perinuclear GABAergic cell cluster, the medial nucleus of the amygdala (MeA), the bed nucleus of the tria terminalis (BST), the medial preoptic area (MPO) and the suprachiasmatic nucleus (SCH). These results are consistent with electrophysiologic data showing the local origins of inhibitory GABAergic inputs to the parvocellular neurons of the PVH (Boudaba et al., 1996; Tasker and Dudek, 1993). A number of different types of PVH neurons that have been shown to co-express the MC4R (Liu et al., 2003) are also known to be under GABAergic control, such as hypophysiotropic thyrotropin-releaseing hormone (TRH) neurons (Fekete et al., 2002b), corticotropin-releasing hormone (CRH) neurons (Cullinan, 2000; Cullinan and Wolfe, 2000; Miklos and Kovacs, 2002) and magnocellular oxytocin neurons (Richards et al., 2005). A subpopulation of CRH neurons are themselves GABAergic (Meister et al., 1988; Meister et al., 1987). In addition, about one-third of ARC POMC neurons in mice are colocalized with GAD and release GABA (Hentges et al., 2004).

In addition to learning more about the α-MSH-responsive GABAergic currents in the PVH, we also wanted to determine the extent to which MC4R signaling may act through regulating GABA release in other hypothalamic or extrahypothalamic regions. We therefore looked for areas of co-expression of GAD, the enzyme responsible for the synthesis of GABA and therefore a marker for GABAergic neurons, and the MC4R in the PVH and other regions in the adult mouse brain using double *in situ* hybridization histochemistry.

MATERIALS AND METHODS

Animals and Tissue Collection

Five age-matched 10-week old adult male C57Bl/6J mice were housed in a light and temperature-controlled environment using a 12-hour light/dark cycle with *ad libitum* access to food and water. Mice were deeply anesthetized with an intraperitoneal injection of Tribromoethanol (1ml/100g body weight) before cardiac puncture and transcardial perfusion with diethylpyrocarbonate (DEPC)-treated 0.9% normal saline followed by 200ml of chilled 4% paraformaldehyde in borate buffer, pH 9.5. The brains were immediately removed and placed in the same fixative solution with 20% sucrose at 4°C overnight. After freezing the brains were cut using a frozen sledge-microtome into 25μm coronal sections. Each brain was cut in a 1:4 series and the sections stored free-floating in wells containing DEPC-treated 0.02M potassium phosphate-buffered saline (KPBS) with 0.25% paraformaldehyde. Sections were then placed in DEPC-treated KPBS, mounted onto gelatin-poly-L-lysine coated slides, and dried overnight in a vacuum dessicator. A 1:4 series of sections were pre-hybridized for 30 minutes at 37°C in DEPC-treated TE buffer (100mM Tris, pH 8.0, 50mM EDTA) with proteinase K (10mg/ml) followed by a brief rinse in TE buffer and pre-equilibration in 0.1M triethanolamine (TE), pH 8.0, for 3 minutes. Then sections were acetylated for 10 minutes in 0.1M TEA with 0.0025% acetic anhydride, rinsed twice for 2 minutes in 2X SSC (NaCl/NaCitrate), dehydrated in ascending ethanol concentrations, and vacuum dried for 2 hours. A series of sections was processed for each animal using double *in situ* hybridization histochemistry with ^{33}P probes for MC4R mRNA and digoxigenin probes for GAD 65 and GAD67 mRNA.

In Situ Hybridization

Preperation of cRNA probes

Antisense MC4R was prepared by linearizing pBluescriptII KS phagmid containing 400bp of the rat MC4R (kindly provided by Dr. Joel Elmquist, Touchstone Center for Diabetes Research, University of Texas Southwestern Medical Center, TX) with KpnI. 1μg of linearized vector was transcribed into a [^{33}P] cRNA probe with T3 RNA polymerase for 1.5 hours at 37°C in a reaction with [^{33}P] UTP using an *in vitro* transcription kit protocol (Promega, Madison, WI) and purified from unincorporated [^{33}P] -labelled nucleotides on a Sephadex G-50 NICK column (Amersham Biosciences) Antisense GAD65 was prepared by linearizing pBluescript II containing 238bp of the rat GAD65 with DraII, and antisense GAD67 was prepared by linearizing pGEM-T (Promega) containing 220bp of the rat GAD67 with NotI (both vectors kindly provided by Dr. Sergio Ojeda, Oregon National Primate Research Center/OHSU, OR). 1μg of linearized vector was transcribed into a digoxigenin-labeled cRNA probe with T3 polymerase (for GAD65) or T7 polymerase (for GAD67) for 1.5 hours at 37°C in a reaction with Dig-UTP using an in vitro transcription kit protocol (Roche Diagnostics, Basel, Switzerland), and then ethanol precipitated and resuspended in DEPC-treated water. The GAD65 and GAD67 probes were combined 50:50 into one GAD cRNA probe solution.

Hybridization

Sections were hybridized for 20 hours at 58°C with ^{33}P-labeled MC4R (2.5×10^{7} cpm/ml) and digoxigenin-labeled GAD probes (labeled amount derived from 1μg, diluted 1:10) in 65% formamide, 13% dextran sulfate, 13mM Tris, pH 8.0, 1.3mM EDTA, 1.3x Denhardt's solution. Sections were then rinsed 4 times in 4xSSC for 5 minutes, digested with RNase (20mg/ml) for 20 minutes at 37°C, desalted in a series of washes 5-10 minutes each from 2xSSC with 1mM dithiothreitol (DTT) to 0.1xSSC with 1mM DTT for 30 minutes at 65°C. Sections were then incubated overnight in LSSC (2xSSC, 0.05% Trition X-100, 2% normal goat serum) at room temperature on a shaker, washed twice for 5 minutes in buffer 1 (100mM Tris-HCl, pH 7.5, 150 mM NaCl), incubated in sheep anti-digoxigenin primary antisera conjugated to alkaline phosphatase (1:1000; Roche Molecular Biochemicals, Basel, Switzerland) for 5 hours, washed in buffer 1 and buffer 2 (100mM Tris-HCl, pH 9.5, 100 mM NaCl, 50mM $MgCl_2$) and incubated in a nitroblue tetrazolium chloride, 5-bromo-4chloro-3-indolyl-phosphate (NBT/BCIP; Roche Molecular Biochemicals) chromagen solution overnight. Sections were then rinsed twice in buffer 3 (10mM Tris-HCl, pH 8.1, 1mM EDTA) for 10 minutes, then washed 3x 5 minute and 1x 30minute in 0.02M KPBS, dehydrated in ascending ethanol concentrations, and vacuum dried for 30 minutes.

Autoradiography and Analysis

Sections were dipped in 3% parlodian (Fisher Scientific, Rockville, MD) in isoamyl acetate, air dried, dipped in K5 photographic emulsion (Kodak, Rochester, NY), dried in a dark lightly humidified chamber for 4 hours, and stored in desiccated, light-tight boxes at 4°C for 3 weeks. Slides were then developed with D-19 developer (Kodak). A number of adjacent sections were stained with thionin to view the morphology, dehydrated in ascending ethanol concentrations, cleared in xylene, and vacuum dried for 30 minutes. All the sections were coverslipped with DPX. Sections were analyzed with a Zeiss Axioplan photomicroscope. Double-labeled cells were determined using two combined methods (Elias et al., 1999; Kishi et al., 2003). Neurons were considered positively double-labeled if the silver grains overlying the digoxigenin-labeled cell bodies were 5x above background hybridization and approximately conformed to the shape of the digoxigenin-labeled cells. Background was calculated as the mean number of silver grains overlying a counting grid (100 μm^2) in the internal capsule.

RESULTS

GAD and MC4R were both expressed widely throughout the brain, but were found to be co-localized in only a small number of regions examined. The cerebral cortex and brainstem were not examined in this study. The PVH expressed small amounts of MC4R and had very weak GAD expression with no observed co-localization, including in the medial parvicellular division. In addition, no co-expression of GAD and MC4R was observed in the GABAergic cell cluster adjacent to the PVH. The highest amounts of co-localization were found in the MeA (primarily in the anteroventral, anterodorsal and posterodorsal regions; Figure 2A), the preoptic area (POA; primarily, the medial and central parts), the lateral septal nucleus (LSD; primarily caudal, dorsal zone, dorsal region). Moderate amounts of co-localization were found in the SCH, the BST (primarily the anterolateral area of the anterolateral division, the principal nucleus, the intrafascicular and transverse nuclei of the posterior division) and the lateral septal nucleus, ventral (LSV; Figure 2B). A lesser degree of co-localization was also found in the anteroventral periventricular nucleus of the hypothalamus (AVPV) and the dorsolateral nucleus of the anterior division of the BST.

DISCUSSION

There are two major inhibitory mechanisms regulating the activity of the hypothalamo-pituitary-adrenocortical (HPA) axis: hormonal negative feedback and neural inhibition by GABAergic neurons (Davis and Hadley, 1978; Jones et al., 1976; Kovacs et al., 2004). Furthermore, GABAergic neurons comprise at least half of the hypothalamic neuronal population (Decavel and Van den Pol, 1990; Decavel and van den Pol, 1992). We show that GAD and MC4R mRNA are not co-localized in the GABAergic interneurons surrounding the PVH, indicating that the MC4R is not expressed in GABAergic fibers extending into the PVH. It is, therefore, probable that POMC neurons from the ARC do not directly contact MC4R expressing dense shell of GABA interneurons in the PVH, but instead indirectly modulate GABA release. One possibility is that the ARC POMC neurons excite intermediary neurons, which in turn excite PVH GABA interneurons.

Perhaps some of these GABAergic interneurons are located in the areas where we found co-localization of GAD 65/67 and MC4R mRNA, such the MeA, the BST, the MPO and the SCH, since GABAergic projections to the PVH are known to originate from these areas. Further studies are needed to determine where these GABAergic interneurons are located and to further characterize them. Subsequently, another group performed dual-label immunohistochemistry for GAD67 and GFP in MC4R-GFP mice and similarly found that a few GFP-IR cells producing GAD67 were scattered in the BST, as well as the perifornical area, and also found no co-expression in the PVH (Liu et al., 2003). Co-expression of MC4R-GFP-IR and GAD67-IR was also observed in a few scattered neurons in the caudate-putamen and in the cerebral cortex (Liu et al., 2003), brain regions which were not included in our study. However, unlike in our study, Liu et al. did not observe co-expression in the MeA, POA, suprachiasmatic nucleus, AVPV, lateral septal nuclei. Although our study used both GAD65 and GAD67 as well as MC4R mRNA probes, whereas Liu et al. used antibodies to GAD67 and MC4R-GFP, which may account for some of the differences, the reason for the discrepancies between the two studies remains unclear.

Neurons of the Arc and PVH send and receive projections from many of the other sites where we found co-expression of GAD and MC4R, including the BST, the POA, the AVPV, the MeA and the lateral septal nucleus. Many of the areas that we found to co-express GAD and MC4R mRNA are known to be sexually dimorphic and contain high levels of sex steroids and their receptors, in particular estrogen and progesterone. The AVPV and mPOA, for instance, contain some of the highest levels of estrogen receptor expression in the entire CNS. Widespread sexual dimorphisms have been described in the rat brain, primarily within forebrain circuits that directly influence reproductive function, such as the BST (Polston et al., 2004). The principal nucleus of the BST (BSTp), replete with sex steroid receptors, receives projections from the MeA, an area known to process pheromonal and viscerosensory information associated with reproduction, and sends projections of dimorphic density to the AVPV, which plays an important role in the regulation of LH and prolactin (Gu et al., 2003; Hutton et al., 1998). Many of these dimporphic nuclei also contain peptides involved in energy regulation (Bloch et al., 1993; Elias et al., 2001; Iqbal et al., 2001; Micevych et al., 1988; Polston and Simerly, 2003; Takatsu et al., 2001). Overall, these dimorphic nuclei are thought to be critical players in the integration of multiple endocrine, autonomic and visceromotor functions essential to survival, including drinking and feeding behavior, metabolism, reproductive and maternal behaviors and stress responses. It would therefore be interesting to further explore whether these nuclei that co-express GAD and MC4R mRNA are involved in dimorphically mediating energy homeostatic mechanisms and whether they help form part of the link between energy regulation and reproductive function.

GABA is the major inhibitory neurotransmitter regulating reproductive function and is abundantly expressed in the MeA, BST, DMH and POA (Flugge et al., 1986; Herbison et al., 1992; Okamura et al., 1990; Stefanova et al., 1998). GABA release in the AVPV and other preoptic areas are directly modulated by estrogen. For example, GABAergic neurons in the POA, which express the estrogen receptor, are important in the regulation of GnRH release (Mansky et al., 1982; Wagner et al., 2001). Many of these nuclei dimorphically express GAD, and sex steroids acting in these nuclei, in particular estrogen, have been shown to alter neuronal GABA synthesis and turnover, $GABA_A$

receptor density, as well as affecting GABA transporter function, thus potentially allowing estrogen to differentially affect GABAergic neuronal downstream targets (Demling et al., 1985; Grattan and Selmanoff, 1994; Herbison, 1997; Herbison et al., 1995; Herbison and Fenelon, 1995; Searles et al., 2000).

Arc POMC and NPY/AGRP neurons also send projections to GnRH neurons (Chowen et al., 1990; Leranth et al., 1988; Turi et al., 2003). In hypothalamic neuronal cell culture of GT1-1 cells, which express MC4R, α-MSH is able to stimulate GnRH release (Khong et al., 2001), and MC3R/MC4R agonists and antagonists can regulate GnRH pulse generator activity in female goats and monkeys (Matsuyama et al., 2005; Vulliemoz et al., 2005). Energy homeostasis and reproductive function are intimately linked with one another, for instance, nutritional deprivation interferes with a functional reproductive system. In light of our findings, it would therefore be interesting to examine whether MC4R-containing GABAergic neurons project directly onto GnRH neurons, or whether, influenced by sex steroids such as estrogen, they dimorphically regulate ingestive behavior and metabolism.

The BST and POA, areas where we found high levels of GAD and MC4R co-expression, are also known to be important regions in regulating central stress circuits and GAD mRNA in these brain regions has been shown to be regulated by stress (Bowers et al., 1998). GABAergic neurons synapse onto corticotropin-releasing hormone (CRH) neurons in the PVH and are thought to play an important role in regulating their neurosecrection (Miklos and Kovacs, 2002). Additionally, there is evidence to suggest that the MC4R may play a role in regulating the effects of stress on feeding behavior. For instance, A^y and MC4R-/- mice appear to be hypersensitive to stress and transiently lose weight in response to mild stressors (De Souza et al., 2000). Central administration of CRH induces sex-dependent anorectic effects (Heinrichs and Richard, 1999; Rivest et al., 1989) and a subset of CRH neurons in the PVH express the MC4R and CRH acts as a downstream mediator of melanocortin signaling (Lu et al., 2003; Sarkar et al., 2002). Interestingly, MC4R-/- mice are hypersensitive to ICV administered CRH (De Souza et al., 2000; Marsh et al., 1999). Based on these data together with our results, one could speculate that some of the regulation of the CRH stress axis may be occurring through MC4R-expressing GABAergic neurons in dimorphic nuclei.

Estrogen is known to have strong centrally driven anorectic effects in rats leading to a decrease in meal size, total food intake, body weight and fat mass (Blaustein and Wade, 1976; Heine et al., 2000; Lacasa et al., 1991; Richard, 1986; Wade, 1975). It is well established that a sexual dimorphism exists in the body composition of humans and that females have a smaller lean body mass and a larger fat body mass (with less deep subcutaneous abdominal fat) than males beginning at puberty, sustained throughout adulthood, and increasing at menopause (Durnin and Womersley, 1974; O'Sullivan et al., 2001; Rebuffe-Scrive et al., 1987; Smith et al., 2001). Estrogen/androgen therapy in both obese and non-obese postmenopausal women causes a significant decrease in visceral adipose tissue compared to controls (Dobs et al., 2002; Sites et al., 2001). Additionally, in female ovariectomized rats, estrogen treatment leads to reduced food intake, body weight and increased physical activity (Asarian and Geary, 2002). Estrogen is also able to modulate leptin receptor expression levels in the hypothalamus and in adipose tissue

(Meli et al., 2004) and POMC mRNA levels in the Arc (Chowen et al., 1990), providing further evidence for a link between sex steroids and energy homeostasis.

Transgenic mice that ubiquitously express agouti (A^{vy}) and MC4R-/- mice show phenotypic differences between males and females. For example, transgenic agouti obese female mice develop a greater obesity than transgenic males relative to control wild-type mice, and while both males and females become hyperinsulinemic, only the males become clearly hyperglycemic (Klebig et al., 1995). Ubiquitously expressed agouti can block the action of α-MSH on the central melanocortin receptors, with a particularly high specific affinity for the MC4R. In younger animals, around twelve weeks old, A^{vy} females have three fold higher levels of plasma insulin than A^{vy} males (Frigeri et al., 1983; Yen et al., 1994). In addition, A^{vy} males are hyperglycemic whereas A^{vy} females tend to be normoglycemic, males exhibit a greater degree of insulin resistance and glucose intolerance than females. Similarly, MC4R-/- males are hyperglycemic whereas females are normoglycemic, and in comparison to sex-matched controls, females become significantly more hyperinsulinemic than males (Huszar et al., 1997). Also serum leptin levels, mean length and increase in body weight are greater in females. Therefore, it would be interesting to further study whether the co-localization of the MC4R and GAD found in sexually dimorphic nuclei indeed plays a role in regulating the sexually dimorphic phenotypes found in these melanocortin-disrupted models of rodent obesity, and if so, whether the central melanocortin system plays a role in dimorphically regulating energy homeostatic mechanisms.

ACKNOWLEDGMENTS

We wish to thank Melissa Kirigiti for her technical advice, Dr. Richard B. Simerly for his valuable discussions on dimorphic anatomy, Dr. Joel Elmquist (Touchstone Center for Diabetes Research, University of Texas Southwestern Medical Center) for providing us with the template for the MC4R probe and Dr. Sergio Ojeda (Oregon National Primate Research Center/OHSU) for providing us with the templates for both of the GAD probes. This work is supported by NIDDK/NIH grants 5R01DK070332 and 5R01DK051730 (RDC).

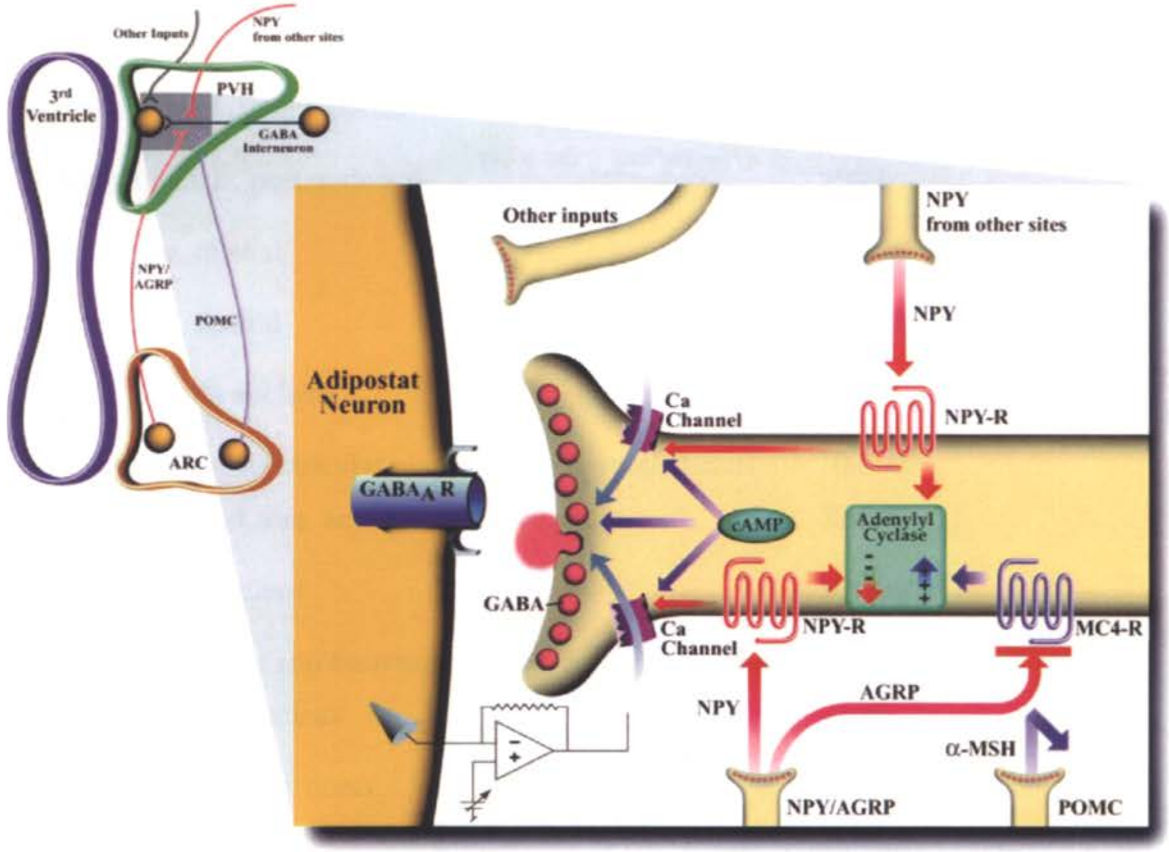

Figure 1. Model for the integration of α-MSH, NPY, and AGRP signals at GABergic neurons upstream of the adipostat. (Top left) arcuate POMC neurons and NPY/AGRP neurons project to GABAergic interneurons in the PVH. These neurons provide inhibitory input to the adipostat neurons. (Inset) melanocortin receptors in the GABAergic interneurons may directly regulate GABA release via their opposing action on adenylyl cyclase. From (Cowley et al., 1999)

Areas of co-localization	Percent of GAD neurons that are MC4R positive
Medial amygdala, anteroventral	70-90%
Medial amygdala, anterodorsal	70-90%
Medial amygdala, posterodorsal	>90%
Preoptic area, medial	50-70%
Preoptic area, central	50-70%
Suprachiasmatic nucleus	10-30%
Anteroventral periventricular nucleus of the hypothalamus	10-30%
BST, anterolateral area, anterolateral division	30-50%
BST, principal nucleus	10-30%
BST, intrafascicular and transverse nuclei, posterior division	30-50%
BST, dorsolateral nucleus	<10%
Lateral septal nucleus, dorsal	50-70%
Lateral septal nucleus, ventral	30-50%

Table 1: Brain regions exhibiting colocalization of GAD65/67 and MC4R mRNA by double *in situ* hybridization.

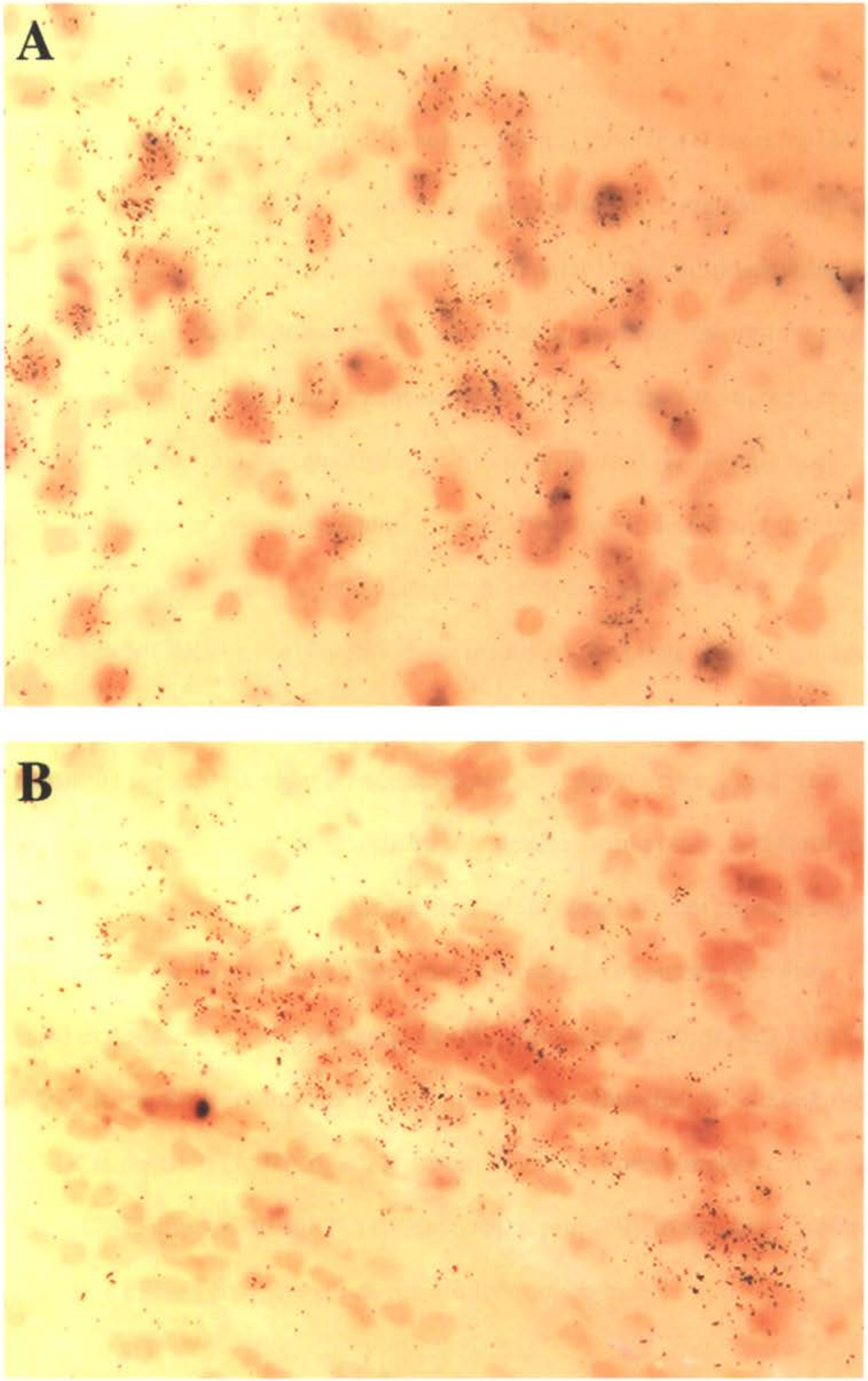

Figure 2: Representative examples of colocalization of GAD65/67 (digoxin-labeled) and MC4R (silver grains) mRNA by double *in situ* hybridization in sexually dimorphic brain regions. (A) Medial amygdala, anterodorsal; (B) Lateral septal nucleus, ventral.

SUMMARY AND CONCLUDING REMARKS

In summary, we demonstrated that specific subsets of melanocortin-4 receptor (MC4R)-expressing neurons in the CNS that are anatomically positioned to regulate sympathetic outflow are poly-synaptically associated with interscapular brown adipose tissue (IBAT) and that MC4R-/- mice have a defect in their ability to up-regulate uncoupling protein-1 (UCP1) in response to increased dietary fat and short-, but not long-term, cold exposure. Our results also indicate that the hypothalamic-pituitary-thyroid (HPT) axis does not mediate the melanocortin system's regulation of UCP1 levels in IBAT and that the thermogenic defect is not due to a general defect in peripheral sympathetic responsiveness in MC4R-/- mice. Overall these results suggest that MC4R signaling is critically required for acute cold exposure-induced and high fat-induced IBAT thermogenesis. This study provides a neuroanatomic and physiological basis for the regulation of non-shivering thermogenesis by the melanocortin system and furthers our insight into a potential mechanism by which the melanocortin system regulates energy expenditure in response to an increase in dietary fat and cold exposure. We also demonstrated that there is no co-expression of (glutamic acid decarboxylase) GAD and MC4R mRNA in the PVH, indicating that POMC neurons from the Arc do not directly contact MC4R expressing GABA interneurons in the PVH. Surprisingly we did, however, find GAD and MC4R mRNA co-expression primarily in sexually dimorphic nuclei. A number of important questions remain for further study:

Are the differences we observed between wild-type and MC4R-/- animals, with respect to the regulation of IBAT, representative of a general alteration of sympathetic circuitry or are they specific to BAT?

The first brain regions infected after IBAT inoculation with PRV are areas known to provide dominant supraspinal innervation of sympathetic preganglionic neurons in the IML of the spinal cord: the A5 region, the rostral ventrolateral medulla (RVLM), the caudal raphe nuclei and the PVH (Cano et al., 2003), suggesting they are common to neural circuits controlling the sympathetic outflow to different tissues. A recent study, in which PRV was injected into white adipose tissue (WAT) depots of adult male Siberian hamsters, used combined *in situ* hybridization/immunohistochemistry to look for co-expression of PRV-IR and MC4R mRNA 6 days post-injection. The study found all of the same sites of co-expression as in our anatomical IBAT study as well as many more sites (Song et al., 2005). However, it is difficult to directly compare the results of our study with the Song et al. study for a number of reasons. For instance, Song et al. looked only at one long survival time, making it difficult to compare the hierarchical circuitry. Song et al. also looked at MC4R mRNA (as opposed to protein expression in our study), and most importantly, although WAT is both sympathetically and parasympathetically innervated, no distinctions were made between them in their study. It will be important to address whether the differences we observed between wild-type and MC4R-/- animals, with respect to the regulation of IBAT, are specific to this organ or are representative of a general alteration of sympathetic circuitry. Physiological studies provide evidence for a variety of factors that may account for regional differences in these common sympathetic areas, including density of projections to sympathetic preganglionic neurons and subnuclear specificity. For instance, a larger number of infected neurons are observed in the raphe nuclei after PRV injection into IBAT (Cano et al., 2003) than after injection into kidney or spleen (Cano et al., 2000). Additionally, following PRV-inoculation of parasympathetically denervated pancreas in the rat, second neurons not only label in the RVLM, RPa, PVH and A5 regions, but also in the locus coeruleus, LH, zone incerta, retrochiasmatic area and prefrontal cortex, and not in the gigantocellular reticular nucleus (Buijs et al., 2001).

Physiological experiments also highlight differences in response to sympathetic inputs between organ systems. For example, stimulation of the RVLM causes sympathetically mediated increases in arterial pressure associated with vasoconstriction, but does not affect sympathetically mediated changes in piloerection, gastric motility, papillary diameter or IBAT activation (Morrison, 1999). In addition, disinhibition of the RVLM increases splanchnic sympathetic nerve activity and vasomotor tone, but not IBAT sympathetic nerve activity, whereas disinhibition of the rostral RPa greatly increases IBAT sympathetic nerve activity, but not splanchnic sympathetic nerve activity or vasomotor tone (Morrison, 1999; Sved et al., 2001). These and other studies suggest that there exists discrete regulation of selective sympathetic outputs by specific regions in addition to orchestrated global sympathetic responses.

Studies using stimulus-evoked expression of early response genes, such as *c-fos*, have also been used to examine differences in the regulation of sympathetic outflow to different targets by determining whether specific neuronal populations are activated by a given stimulus. For example, rats exposed to cold temperatures for four hours showed high levels of c-Fos expression in the PVH and RPa, but not in the RVLM (Cano et al., 2003). PVH and RPa are also amongst the first brain regions to be infected with PRV after injection into IBAT (Cano et al., 2003; Oldfield et al., 2002). Taken together, this strongly suggests that the PVH and RPa contain sympathetic premotor neurons responsible for the final central output to IBAT preganglionic neurons in response to cold exposure. It is also evident from these studies that in addition to a temporal analysis of PRV labeling, it is important to correlate any anatomical findings with physiological ones in order to determine their relative importance in the overall circuitry. Therefore it would be interesting to further correlate our neuroanatomical findings with neuronal activity mapping studies examining whether c-Fos and MC4R are co-expressed in the same areas as PRV and MC4R after acute cold exposure or a high-fat diet. However, one limitation of such c-Fos studies is that c-Fos is only a marker of neuronal activation and not inhibition. It would also be interesting to further characterize the PRV and MC4R co-expressing neurons in terms of their neurochemical phenotype to gain greater insight into potential downstream mediators.

Is the central melanocortin system involved in the long-term regulation of DIT?

In our study we demonstrate that after a two day high-fat diet wild-type mice are able to upregulate UCP1, whereas MC4R-/- mice lack this ability, suggesting that intact MC4R signaling is required for the regulation of IBAT thermogenesis in response to an acute increase in dietary fat. In addition, numerous studies have demonstrated that UCP1 is up-regulated in wild-type mice after a long-term high-fat diet (Archer et al., 2005; Li et al., 2004; Margareto et al., 2001; Nedergaard et al., 1984; Portillo et al., 1998; Rippe et al., 2000; Rippe et al., 2003; Surwit et al., 1998), but it still remains to be determined whether the central melancortin system is also involved in this up-regulation of UCP1 after a long-term high-fat diet. Our experiments were constrained by the fact that UCP1 is upregulated by obesity itself, and therefore a longer period of high-fat feeding, which would have led to obesity in either the genetic or pharmacologic melanocortin blockade models, would have confounded our UCP1 results. This therefore remains an important unanswered question that is difficult to address, although pair-feeding experiments might help shed some light on this topic. One study demonstrated that diet-induced obese rats fed a chronic high-fat diet not only had increased BAT UCP1 protein levels, but also had further increases in UCP1 levels after 6 days of ICV MTII treatment (Li et al., 2004). This suggests that after a long-term high-fat diet the central melanocortin system has the ability to up-regulate UCP1, but does not address whether it is critically required.

What is the mechanism underlying the melanocortin system's regulation of UCP1?

Butler et al. found no difference in NE turnover in IBAT of wild-type mice fed either low-fat or moderate-fat diets for 24 hours (Butler et al., 2001), and our results suggest that the HPT axis may not be involved in mediating the increase in UCP1 levels. Therefore, the underlying mechanism by which the melanocortin system up-regulates UCP1 remains unknown. However, as discussed above, by far the most likely mechanism is through the central regulation of sympathetic outflow, since it is the principal control mechanism for BAT thermogenesis and our neuroanatomical study demonstrates that the MC4R is expressed in regions polysynaptically associated with IBAT that are also known to be important in controlling sympathetic outflow. As mentioned previously, it is also possible that a difference in NE turnover was not detected in the Butler et al. study because of the limited time frame in which the experiment was performed (NE turnover was measured at 0 hours and 4 hrs). In addition, contrary to the NE turnover results from

Butler et al., numerous studies have demonstrated that UCP1 is up-regulated in wild-type mice after a long-term high-fat diet (Archer et al., 2005; Li et al., 2004; Margareto et al., 2001; Nedergaard et al., 1984; Portillo et al., 1998; Rippe et al., 2000; Rippe et al., 2003; Surwit et al., 1998) and at least one study demonstrated an increased NE turnover in the IBAT and heart of rats in response to a 5-day increase in dietary fat or sucrose in rodents (Schwartz et al., 1983). The NE turnover was measured at 0, 2, 6, 12 and 24 hours, with the first significant difference detected at 24 hours (Schwartz et al., 1983). Thus it may be worth repeating the NE turnover experiment.

It is also important to note that our study cannot completely rule out the possibility that the HPT axis is involved in mediating the melanocortin system's effects on UCP1 regulation. It is, for instance, possible that wild-type mice have lower free T_3 levels (the more active form) than MC4R-/- mice and that we did not detect this difference by measuring only the total T_3, which is comprised mostly of the less active plasma protein-bound T_3. However, most thyroid studies measure total thyroid hormone levels because measuring free T_3 levels is technically challenging and generally free T_4 and T_3 are in equilibrium with the protein-bound hormones in both plasma and tissue (McPhee et al., 1997) and thus total serum thyroid hormone levels are reflective of the relative free thyroid hormone levels.

Are animal studies of BAT thermogenesis relevant to humans?

Although our data suggests that the central melanocortin system is an important regulator of DIT-induced IBAT thermogenesis in mice, it is unclear whether this has any relevance to humans, who do not have any significant depots of BAT past infancy. However, although UCP1, which exists almost exclusively in the mitochondria of brown adipocytes, has been found only in very small amounts in adult humans, its homologues, UCP2 and UCP3, which are 56% identical at the amino acid level, are expressed in a number of tissues in mammals, including humans. UCP2 is present in several tissues (Fleury et al., 1997) and UCP3 is expressed mostly in skeletal muscle (Boss et al., 1997). Skeletal muscle activity accounts for a major component of the resting energy expenditure in humans, and skeletal muscle and liver mitochondrial proton leak account for approximately 20% of resting metabolic rate in rat (Rolfe and Brand, 1996; Rolfe et al., 1994). It would, therefore, be interesting to further explore whether the melanocortin system regulates these homologues and what role, if any, they may have in affecting energy homeostasis. It is important to point out that UCP2 and UCP3 gene knockout mice have normal body weight, energy expenditure, responses to high-fat feeding and cold tolerance (Arsenijevic et al., 2000; Gong et al., 1997; Vidal-Puig et al., 2000). Nonetheless, UCP2 and UCP3 mediated proton leak does affect the intracellular bioenergetic status of the cell. Recent studies have demonstrated that mice overexpressing UCP3 are leaner, and have a substantial decrease in adipose mass, lower fasting plasma glucose and insulin levels (Clapham et al., 2000; Costford et al., 2006; Horvath et al., 2003), a larger increase in oxygen consumption and less weight gain on a high-fat diet in comparison with wild-type animals (Son et al., 2004). Although the physiological role of UCP3 is not yet fully elucidated, it is generally thought that, at least under physiological conditions, the UCP homologues do not generally mediate adaptive thermogenesis or energetic inefficiency in the same way that UCP1 does, but rather facilitate fatty acid oxidation and minimize the production of reactive oxygen species (Bezaire et al., 2005; MacLellan et al., 2005). UCP2 has also been shown to be a negative regulator of insulin secretion (Zhang et al., 2001). Therefore, although the UCP homologues might be thermogenic under specific conditions and are relevant to energy metabolism, diabetes treatment and possibly obesity treatment, the mechanisms of the UCP homologues appear to be quite different (Brand and Esteves, 2005).

The human UCP1 gene has been cloned, sequenced and mapped to the long arm of chromosome 4(q31)(Cassard et al., 1990). Studies of genetic variants of the human UCP1 gene and their link to human obesity phenotypes have been mixed, with some studies showing a relationship (Cassard-Doulcier et al., 1996; Clement et al., 1996; Fumeron et al., 1996; Kogure et al., 1998; Oberkofler et al., 1997; Oppert et al., 1994) and other studies finding no links (Gagnon et al., 1998; Hayakawa et al., 1999; Schaffler et al., 1999; Valve et al., 1998). Overall, polymorphisms in UCP1 do not appear to be a major contributor to the development of obesity, but the presence of a minor variant allele is related to an increase propensity to gain weight over time, particularly in individuals with a higher risk for obesity (Del Mar Gonzalez-Barroso et al., 2000).

BAT is probably essential for the survival of human newborns, but not for adults who have a larger surface area:volume ratio, as well as clothing and shelter protecting us from cold exposure. Other adult primates show cold-acclimation-induced BAT recruitment (Chaffee et al., 1975; Genin et al., 2003) and there is no reason to believe that adult humans could not recruit BAT under certain physiological or pathophysiological conditions, although there has not been much experimental evidence. However, humans with pheochromocytoma, a condition characterized by very high adrenergic activation, are able to regain UCP1-containing BAT (Bouillaud et al., 1988; Ricquier et al., 1982).

Adult humans have also recently been shown to have brown adipocytes within white adipose depots and UCP1 mRNA has been detected in human white adipose tissue (WAT) (Cinti, 2005; Garruti and Ricquier, 1992; Oberkofler et al., 1997).

Is there any potential therapeutic potential for the treatment of human obesity through increased sympathetically-mediated BAT thermogenesis?

Since the thermogenic capacity of recruited BAT has been estimated to be 500 watts/kg, even very small quantities (on the order of 50g) of BAT in an adult human would be enough to have significant effects on energy balance (Stock, 1989). It has been demonstrated that adenovirus-mediated expression of human PPAR-γ co-activator (PGC-1) alpha, a UCP1 transcriptional co-activator, can increase the expression of UCP1, respiratory chain protein and fatty acid oxidation enzymes in human subcutaneous white adipocytes, leading to the suggestion that increased substrate utilization in white adipose tissue through conversion into BAT or through the acquisition of BAT-like features could be a conceivable strategy for the treatment of obesity (Tiraby et al., 2003).

The sympathetic nervous system is considered to be the regulator of adaptive thermogenesis: Cold exposure and increased caloric intake lead to increased sympathetic nerve activity, exogenous administration of adrenergic agonists leads to increased energy expenditure, BAT is sympathetically innervated and wholly depends on intact sympathetic innervation for its thermogenic activity (Lowell and Bachman, 2003). Unlike the other β-adrenoreceptors, which are widely expressed, the β_3-adrenoreceptor is expressed primarily in adipocytes in rodents and in brown adipocytes in humans (Krief et al., 1993; Weyer et al., 1998). In rodents, treatment with a β_3-adrenoreceptor agonist is associated with increased UCP1-expressing BAT within WAT depots (Champigny et al., 1991; Collins et al., 1997; Fisher et al., 1998; Himms-Hagen et al., 1994; Oana et al., 2005; Sasaki et al., 1998) Multiple studies in different animal models have demonstrated the potent anti-obesity and antihyperglycemic properties of β_3-adrenoreceptor agonists (Arch et al., 1984; Collins et al., 1997; Collins and Surwit, 1996; Himms-Hagen et al., 1994; Oana et al., 2005; Sasaki et al., 1998). β_3-adrenoreceptor can also be found in human adipose tissue, but at much lower levels than in rodents, with the largest amount of expression in brown adipocytes found clustered amongst white fat cells, particularly within intra-abdominal depots (Krief et al., 1993; Weyer et al., 1998). The visceral location of brown adipocytes make it difficult to quantify their relative abundance and more large studies need to be done in order to more accurately determine the extent of brown adipocytes remaining in adult humans and whether β_3-adrenoreceptor agonists can modulate lipolysis in human adipocytes. In primates, as in rodents and dogs, treatment with selective β_3-adrenoreceptor agonists lead to increased metabolic rate, decreased fat mass and the appearance of brown adipocytes within typically white adipose depots (Fisher et al., 1998).

A very recently published study demonstrates that bile acids can also increase energy expenditure in BAT via induction of the cAMP-dependent thyroid hormone activating enzyme DII, thereby preventing obesity and insulin resistance in mice (Watanabe et al., 2006). Whether treatment of adult humans with β_3-adrenoreceptor agonists can lead to the recruitment of thermogenically active brown adipocytes and whether it or other activators of BAT thermogenesis can ultimately be used as a treatment for human obesity remains to be determined.

REFERENCES

Ahima, R. S., Prabakaran, D., Mantzoros, C., Qu, D., Lowell, B., Maratos-Flier, E., and Flier, J. S. (1996). Role of leptin in the neuroendocrine response to fasting. Nature *382*, 250-252.

Almeida, N. G., Levitsky, D. A., and Strupp, B. (1996). Enhanced thermogenesis during recovery from diet-induced weight gain in the rat. Am J Physiol *271*, R1380-1387.

Amendt, K., Czachurski, J., Dembowsky, K., and Seller, H. (1979). Bulbospinal projections to the intermediolateral cell column: a neuroanatomical study. J Auton Nerv Syst *1*, 103-107.

Amir, S. (1990a). Activation of brown adipose tissue thermogenesis by chemical stimulation of the posterior hypothalamus. Brain Res *534*, 303-308.

Amir, S. (1990b). Intra-ventromedial hypothalamic injection of glutamate stimulates brown adipose tissue thermogenesis in the rat. Brain Res *511*, 341-344.

Amir, S. (1990c). Stimulation of the paraventricular nucleus with glutamate activates interscapular brown adipose tissue thermogenesis in rats. Brain Res *508*, 152-155.

Amir, S., and De Blasio, E. (1991). Activation of brown adipose tissue thermogenesis by chemical stimulation of the hypothalamic supraoptic nucleus. Brain Res *563*, 349-352.

Amir, S., Shizgal, P., and Rompre, P. P. (1989). Glutamate injection into the suprachiasmatic nucleus stimulates brown fat thermogenesis in the rat. Brain Res *498*, 140-144.

Anand, B. K., and Brobeck, J. R. (1951a). Hypothalamic control of food intake in rats and cats. Yale J Biol Med *24*, 123-140.

Anand, B. K., and Brobeck, J. R. (1951b). Localization of a "feeding center" in the hypothalamus of the rat. Proc Soc Exp Biol Med *77*, 323-324.

Arase, K., Sakaguchi, T., and Bray, G. A. (1987). Lateral hypothalamic lesions and activity of the sympathetic nervous system. Life Sci *41*, 657-662.

Arch, J. R., Ainsworth, A. T., Ellis, R. D., Piercy, V., Thody, V. E., Thurlby, P. L., Wilson, C., Wilson, S., and Young, P. (1984). Treatment of obesity with thermogenic beta-adrenoceptor agonists: studies on BRL 26830A in rodents. Int J Obes *8 Suppl 1*, 1-11.

Archer, Z. A., Rayner, D. V., Duncan, J. S., Bell, L. M., and Mercer, J. G. (2005). Introduction of a high-energy diet acutely up-regulates hypothalamic cocaine and amphetamine-regulated transcript, Mc4R and brown adipose

tissue uncoupling protein-1 gene expression in male Sprague-Dawley rats. J Neuroendocrinol *17*, 10-17.
Argeson, A. C., Nelson, K. K., and Siracusa, L. D. (1996). Molecular basis of the pleiotropic phenotype of mice carrying the hypervariable yellow (Ahvy) mutation at the agouti locus. Genetics *142*, 557-567.
Arsenijevic, D., Onuma, H., Pecqueur, C., Raimbault, S., Manning, B. S., Miroux, B., Couplan, E., Alves-Guerra, M. C., Goubern, M., Surwit, R., *et al.* (2000). Disruption of the uncoupling protein-2 gene in mice reveals a role in immunity and reactive oxygen species production. Nat Genet *26*, 435-439.
Asarian, L., and Geary, N. (2002). Cyclic estradiol treatment normalizes body weight and restores physiological patterns of spontaneous feeding and sexual receptivity in ovariectomized rats. Horm Behav *42*, 461-471.
Aston-Jones, G., and Card, J. P. (2000). Use of pseudorabies virus to delineate multisynaptic circuits in brain: opportunities and limitations. J Neurosci Methods *103*, 51-61.
Aston-Jones, G., Chen, S., Zhu, Y., and Oshinsky, M. L. (2001). A neural circuit for circadian regulation of arousal. Nat Neurosci *4*, 732-738.
Aston-Jones, G., Shipley, M. T., Chouvet, G., Ennis, M., van Bockstaele, E., Pieribone, V., Shiekhattar, R., Akaoka, H., Drolet, G., Astier, B., and et al. (1991). Afferent regulation of locus coeruleus neurons: anatomy, physiology and pharmacology. Prog Brain Res *88*, 47-75.
Bachman, E. S., Dhillon, H., Zhang, C. Y., Cinti, S., Bianco, A. C., Kobilka, B. K., and Lowell, B. B. (2002). betaAR signaling required for diet-induced thermogenesis and obesity resistance. Science *297*, 843-845.
Bado, A., Levasseur, S., Attoub, S., Kermorgant, S., Laigneau, J. P., Bortoluzzi, M. N., Moizo, L., Lehy, T., Guerre-Millo, M., Le Marchand-Brustel, Y., and Lewin, M. J. (1998). The stomach is a source of leptin. Nature *394*, 790-793.
Baffi, J. S., and Palkovits, M. (2000). Fine topography of brain areas activated by cold stress. A fos immunohistochemical study in rats. Neuroendocrinology *72*, 102-113.
Bagnol, D., Lu, X. Y., Kaelin, C. B., Day, H. E., Ollmann, M., Gantz, I., Akil, H., Barsh, G. S., and Watson, S. J. (1999). Anatomy of an endogenous antagonist: relationship between Agouti-related protein and proopiomelanocortin in brain. J Neurosci *19*, RC26.
Bahouth, S. W. (1991). Thyroid hormones transcriptionally regulate the beta 1-adrenergic receptor gene in cultured ventricular myocytes. J Biol Chem *266*, 15863-15869.

Ball, E. G., and Jungas, R. L. (1961). On the action of hormones which accelerate the rate of oxygen consumption and fatty acid release in rat adipose tissue in vitro. Proc Natl Acad Sci U S A *47*, 932-941.
Bamshad, M., Song, C. K., and Bartness, T. J. (1999). CNS origins of the sympathetic nervous system outflow to brown adipose tissue. Am J Physiol *276*, R1569-1578.
Baran, K., Preston, E., Wilks, D., Cooney, G. J., Kraegen, E. W., and Sainsbury, A. (2002). Chronic central melanocortin-4 receptor antagonism and central neuropeptide-Y infusion in rats produce increased adiposity by divergent pathways. Diabetes *51*, 152-158.
Bernardis, L. L., and Bellinger, L. L. (1993). The lateral hypothalamic area revisited: neuroanatomy, body weight regulation, neuroendocrinology and metabolism. Neurosci Biobehav Rev *17*, 141-193.
Bewick, G. A., Gardiner, J. V., Dhillo, W. S., Kent, A. S., White, N. E., Webster, Z., Ghatei, M. A., and Bloom, S. R. (2005). Post-embryonic ablation of AgRP neurons in mice leads to a lean, hypophagic phenotype. Faseb J *19*, 1680-1682.
Bezaire, V., Spriet, L. L., Campbell, S., Sabet, N., Gerrits, M., Bonen, A., and Harper, M. E. (2005). Constitutive UCP3 overexpression at physiological levels increases mouse skeletal muscle capacity for fatty acid transport and oxidation. Faseb J *19*, 977-979.
Bianco, A. C., Kieffer, J. D., and Silva, J. E. (1992). Adenosine 3',5'-monophosphate and thyroid hormone control of uncoupling protein messenger ribonucleic acid in freshly dispersed brown adipocytes. Endocrinology *130*, 2625-2633.
Bianco, A. C., Sheng, X. Y., and Silva, J. E. (1988). Triiodothyronine amplifies norepinephrine stimulation of uncoupling protein gene transcription by a mechanism not requiring protein synthesis. J Biol Chem *263*, 18168-18175.
Blake, N. G., Eckland, D. J., Foster, O. J., and Lightman, S. L. (1991). Inhibition of hypothalamic thyrotropin-releasing hormone messenger ribonucleic acid during food deprivation. Endocrinology *129*, 2714-2718.
Blaustein, J. D., and Wade, G. N. (1976). Ovarian influences on the meal patterns of female rats. Physiol Behav *17*, 201-208.
Bloch, G. J., Eckersell, C., and Mills, R. (1993). Distribution of galanin-immunoreactive cells within sexually dimorphic components of the medial preoptic area of the male and female rat. Brain Res *620*, 259-268.
Boss, O., Samec, S., Paoloni-Giacobino, A., Rossier, C., Dulloo, A., Seydoux, J., Muzzin, P., and Giacobino, J. P. (1997). Uncoupling protein-3: a new member of the mitochondrial carrier family with tissue-specific expression. FEBS Lett *408*, 39-42.

Bouchard, C., and Perusse, L. (1993). Genetics of obesity. Annu Rev Nutr *13*, 337-354.
Bouchard, C., Tremblay, A., Despres, J. P., Nadeau, A., Lupien, P. J., Theriault, G., Dussault, J., Moorjani, S., Pinault, S., and Fournier, G. (1990). The response to long-term overfeeding in identical twins. N Engl J Med *322*, 1477-1482.
Boudaba, C., Szabo, K., and Tasker, J. G. (1996). Physiological mapping of local inhibitory inputs to the hypothalamic paraventricular nucleus. J Neurosci *16*, 7151-7160.
Bouillaud, F., Villarroya, F., Hentz, E., Raimbault, S., Cassard, A. M., and Ricquier, D. (1988). Detection of brown adipose tissue uncoupling protein mRNA in adult patients by a human genomic probe. Clin Sci (Lond) *75*, 21-27.
Bowers, G., Cullinan, W. E., and Herman, J. P. (1998). Region-specific regulation of glutamic acid decarboxylase (GAD) mRNA expression in central stress circuits. J Neurosci *18*, 5938-5947.
Branco, M., Ribeiro, M., Negrao, N., and Bianco, A. C. (1999). 3,5,3'-Triiodothyronine actively stimulates UCP in brown fat under minimal sympathetic activity. Am J Physiol *276*, E179-187.
Brand, M. D., and Esteves, T. C. (2005). Physiological functions of the mitochondrial uncoupling proteins UCP2 and UCP3. Cell Metab *2*, 85-93.
Bray, G. A. (1984). Hypothalamic and genetic obesity: an appraisal of the autonomic hypothesis and the endocrine hypothesis. Int J Obes *8 Suppl 1*, 119-137.
Brent, G. A. (1994). The molecular basis of thyroid hormone action. N Engl J Med *331*, 847-853.
Broberger, C., De Lecea, L., Sutcliffe, J. G., and Hokfelt, T. (1998a). Hypocretin/orexin- and melanin-concentrating hormone-expressing cells form distinct populations in the rodent lateral hypothalamus: relationship to the neuropeptide Y and agouti gene-related protein systems. J Comp Neurol *402*, 460-474.
Broberger, C., and Hokfelt, T. (2001). Hypothalamic and vagal neuropeptide circuitries regulating food intake. Physiol Behav *74*, 669-682.
Broberger, C., Johansen, J., Johansson, C., Schalling, M., and Hokfelt, T. (1998b). The neuropeptide Y/agouti gene-related protein (AGRP) brain circuitry in normal, anorectic, and monosodium glutamate-treated mice. Proc Natl Acad Sci U S A *95*, 15043-15048.
Brooks, S. L., Rothwell, N. J., Stock, M. J., Goodbody, A. E., and Trayhurn, P. (1980). Increased proton conductance pathway in brown adipose tissue mitochondria of rats exhibiting diet-induced thermogenesis. Nature *286*, 274-276.

Buijs, R. M., Chun, S. J., Niijima, A., Romijn, H. J., and Nagai, K. (2001). Parasympathetic and sympathetic control of the pancreas: a role for the suprachiasmatic nucleus and other hypothalamic centers that are involved in the regulation of food intake. J Comp Neurol *431*, 405-423.
Bultman, S. J., Michaud, E. J., and Woychik, R. P. (1992). Molecular characterization of the mouse agouti locus. Cell *71*, 1195-1204.
Butler, A. A. (2006). The melanocortin system and energy balance. Peptides *27*, 281-290.
Butler, A. A., Kesterson, R. A., Khong, K., Cullen, M. J., Pelleymounter, M. A., Dekoning, J., Baetscher, M., and Cone, R. D. (2000). A unique metabolic syndrome causes obesity in the melanocortin-3 receptor-deficient mouse. Endocrinology *141*, 3518-3521.
Butler, A. A., Marks, D. L., Fan, W., Kuhn, C. M., Bartolome, M., and Cone, R. D. (2001). Melanocortin-4 receptor is required for acute homeostatic responses to increased dietary fat. Nat Neurosci *4*, 605-611.
Cannon, B., and Nedergaard, J. (2004). Brown adipose tissue: function and physiological significance. Physiol Rev *84*, 277-359.
Cannon B, N. J. (2004). Brown Adipose Tissue: Function and Physiological Significance. Physiol Rev *84*, 277-359.
Cano, G., Card, J. P., Rinaman, L., and Sved, A. F. (2000). Connections of Barrington's nucleus to the sympathetic nervous system in rats. J Auton Nerv Syst *79*, 117-128.
Cano G, P. A., Schiltz JC, Card PJ, Morrison SF, and Sved AF (2003). Anatomical Substrates for the Central Control of Sympathetic Outflow to Interscapular Adipose Tissue during Cold Exposure. J Comp Neurol *460*, 303-326.
Cano, G., Passerin, A. M., Schiltz, J. C., Card, J. P., Morrison, S. F., and Sved, A. F. (2003). Anatomical substrates for the central control of sympathetic outflow to interscapular adipose tissue during cold exposure. J Comp Neurol *460*, 303-326.
Cao, W. H., Fan, W., and Morrison, S. F. (2004). Medullary pathways mediating specific sympathetic responses to activation of dorsomedial hypothalamus. Neuroscience *126*, 229-240.
Card, J. P., Rinaman, L., Lynn, R. B., Lee, B. H., Meade, R. P., Miselis, R. R., and Enquist, L. W. (1993). Pseudorabies virus infection of the rat central nervous system: ultrastructural characterization of viral replication, transport, and pathogenesis. J Neurosci *13*, 2515-2539.
Carvalho, S. D., Kimura, E. T., Bianco, A. C., and Silva, J. E. (1991). Central role of brown adipose tissue thyroxine 5'-deiodinase on thyroid hormone-dependent thermogenic response to cold. Endocrinology *128*, 2149-2159.

Cassard, A. M., Bouillaud, F., Mattei, M. G., Hentz, E., Raimbault, S., Thomas, M., and Ricquier, D. (1990). Human uncoupling protein gene: structure, comparison with rat gene, and assignment to the long arm of chromosome 4. J Cell Biochem *43*, 255-264.
Cassard-Doulcier, A. M., Bouillaud, F., Chagnon, M., Gelly, C., Dionne, F. T., Oppert, J. M., Bouchard, C., Chagnon, Y., and Ricquier, D. (1996). The Bcl I polymorphism of the human uncoupling protein (ucp) gene is due to a point mutation in the 5'-flanking region. Int J Obes Relat Metab Disord *20*, 278-279.
Cassard-Doulcier, A. M., Larose, M., Matamala, J. C., Champigny, O., Bouillaud, F., and Ricquier, D. (1994). In vitro interactions between nuclear proteins and uncoupling protein gene promoter reveal several putative transactivating factors including Ets1, retinoid X receptor, thyroid hormone receptor, and a CACCC box-binding protein. J Biol Chem *269*, 24335-24342.
Cechetto, D. F., and Saper, C. B. (1988). Neurochemical organization of the hypothalamic projection to the spinal cord in the rat. J Comp Neurol *272*, 579-604.
Center for Disease Control and Prevention, C. (2004). Behavior Risk Factor Surveillance System Survey Data (Atlanta, Georgia:, U.S. Department of Health and Human Services, CDC).
Cerri, M., and Morrison, S. F. (2005). Activation of lateral hypothalamic neurons stimulates brown adipose tissue thermogenesis. Neuroscience *135*, 627-638.
Cettour-Rose, P., and Rohner-Jeanrenaud, F. (2002). The leptin-like effects of 3-d peripheral administration of a melanocortin agonist are more marked in genetically obese Zucker (fa/fa) than in lean rats. Endocrinology *143*, 2277-2283.
Chaffee, R. R., Allen, J. R., Arine, R. M., Fineg, A. J., Rochelle, R. H., and Rosander, J. (1975). Studies on thermogenesis in brown adipose tissue in temperature-acclimated Macaca mulatta. Comp Biochem Physiol A *50*, 303-306.
Champigny, O., Ricquier, D., Blondel, O., Mayers, R. M., Briscoe, M. G., and Holloway, B. R. (1991). Beta 3-adrenergic receptor stimulation restores message and expression of brown-fat mitochondrial uncoupling protein in adult dogs. Proc Natl Acad Sci U S A *88*, 10774-10777.
Chang, F. C., and Scott, T. R. (1984). Conditioned taste aversions modify neural responses in the rat nucleus tractus solitarius. J Neurosci *4*, 1850-1862.
Chen, A. S., Marsh, D. J., Trumbauer, M. E., Frazier, E. G., Guan, X. M., Yu, H., Rosenblum, C. I., Vongs, A., Feng, Y., Cao, L., *et al.* (2000a).

Inactivation of the mouse melanocortin-3 receptor results in increased fat mass and reduced lean body mass. Nat Genet *26*, 97-102.
Chen, A. S., Metzger, J. M., Trumbauer, M. E., Guan, X. M., Yu, H., Frazier, E. G., Marsh, D. J., Forrest, M. J., Gopal-Truter, S., Fisher, J., *et al.* (2000b). Role of the melanocortin-4 receptor in metabolic rate and food intake in mice. Transgenic Res *9*, 145-154.
Chen, H., Charlat, O., Tartaglia, L. A., Woolf, E. A., Weng, X., Ellis, S. J., Lakey, N. D., Culpepper, J., Moore, K. J., Breitbart, R. E., *et al.* (1996). Evidence that the diabetes gene encodes the leptin receptor: identification of a mutation in the leptin receptor gene in db/db mice. Cell *84*, 491-495.
Chen, P., Williams, S. M., Grove, K. L., and Smith, M. S. (2004). Melanocortin 4 receptor-mediated hyperphagia and activation of neuropeptide Y expression in the dorsomedial hypothalamus during lactation. J Neurosci *24*, 5091-5100.
Chen, W., Kelly, M. A., Opitz-Araya, X., Thomas, R. E., Low, M. J., and Cone, R. D. (1997). Exocrine gland dysfunction in MC5-R-deficient mice: evidence for coordinated regulation of exocrine gland function by melanocortin peptides. Cell *91*, 789-798.
Cheung, C. C., Clifton, D. K., and Steiner, R. A. (1997). Proopiomelanocortin neurons are direct targets for leptin in the hypothalamus. Endocrinology *138*, 4489-4492.
Chhajlani, V., and Wikberg, J. E. (1992). Molecular cloning and expression of the human melanocyte stimulating hormone receptor cDNA. FEBS Lett *309*, 417-420.
Chowen, J. A., Argente, J., Vician, L., Clifton, D. K., and Steiner, R. A. (1990). Pro-opiomelanocortin messenger RNA in hypothalamic neurons is increased by testosterone through aromatization to estradiol. Neuroendocrinology *52*, 581-588.
Cinti, S. (2005). The adipose organ. Prostaglandins Leukot Essent Fatty Acids *73*, 9-15.
Clapham, J. C., Arch, J. R., Chapman, H., Haynes, A., Lister, C., Moore, G. B., Piercy, V., Carter, S. A., Lehner, I., Smith, S. A., *et al.* (2000). Mice overexpressing human uncoupling protein-3 in skeletal muscle are hyperphagic and lean. Nature *406*, 415-418.
Clement, K., Ruiz, J., Cassard-Doulcier, A. M., Bouillaud, F., Ricquier, D., Basdevant, A., Guy-Grand, B., and Froguel, P. (1996). Additive effect of A->G (-3826) variant of the uncoupling protein gene and the Trp64Arg mutation of the beta 3-adrenergic receptor gene on weight gain in morbid obesity. Int J Obes Relat Metab Disord *20*, 1062-1066.
Coleman, D. L. (1973). Effects of parabiosis of obese with diabetes and normal mice. Diabetologia *9*, 294-298.

Coleman, D. L. (1978). Obese and diabetes: two mutant genes causing diabetes-obesity syndromes in mice. Diabetologia *14*, 141-148.
Coleman, D. L., and Hummel, K. P. (1969). Effects of parabiosis of normal with genetically diabetic mice. Am J Physiol *217*, 1298-1304.
Collins, S., Daniel, K. W., Petro, A. E., and Surwit, R. S. (1997). Strain-specific response to beta 3-adrenergic receptor agonist treatment of diet-induced obesity in mice. Endocrinology *138*, 405-413.
Collins, S., Kuhn, C. M., Petro, A. E., Swick, A. G., Chrunyk, B. A., and Surwit, R. S. (1996). Role of leptin in fat regulation. Nature *380*, 677.
Collins, S., and Surwit, R. S. (1996). Pharmacologic manipulation of ob expression in a dietary model of obesity. J Biol Chem *271*, 9437-9440.
Commins, S. P., Marsh, D. J., Thomas, S. A., Watson, P. M., Padgett, M. A., Palmiter, R., and Gettys, T. W. (1999a). Norepinephrine is required for leptin effects on gene expression in brown and white adipose tissue. Endocrinology *140*, 4772-4778.
Commins, S. P., Watson, P. M., Frampton, I. C., and Gettys, T. W. (2001). Leptin selectively reduces white adipose tissue in mice via a UCP1-dependent mechanism in brown adipose tissue. Am J Physiol Endocrinol Metab *280*, E372-377.
Commins, S. P., Watson, P. M., Padgett, M. A., Dudley, A., Argyropoulos, G., and Gettys, T. W. (1999b). Induction of uncoupling protein expression in brown and white adipose tissue by leptin. Endocrinology *140*, 292-300.
Cone, R. D. (2005). Anatomy and regulation of the central melanocortin system. Nature Neuroscience *8*, 571-578.
Costford, S. R., Chaudhry, S. N., Salkhordeh, M., and Harper, M. E. (2006). Effects of the Presence, Absence and Overexpression of Uncoupling Protein-3 on Adiposity and Fuel Metabolism in Congenic Mice. Am J Physiol Endocrinol Metab.
Cowley, M. A., Pronchuk, N., Fan, W., Dinulescu, D. M., Colmers, W. F., and Cone, R. D. (1999). Integration of NPY, AGRP, and melanocortin signals in the hypothalamic paraventricular nucleus: evidence of a cellular basis for the adipostat. Neuron *24*, 155-163.
Cowley, M. A., Smart, J. L., Rubinstein, M., Cerdan, M. G., Diano, S., Horvath, T. L., Cone, R. D., and Low, M. J. (2001). Leptin activates anorexigenic POMC neurons through a neural network in the arcuate nucleus. Nature *411*, 480-484.
Cullinan, W. E. (2000). GABA(A) receptor subunit expression within hypophysiotropic CRH neurons: a dual hybridization histochemical study. J Comp Neurol *419*, 344-351.

Cullinan, W. E., and Wolfe, T. J. (2000). Chronic stress regulates levels of mRNA transcripts encoding beta subunits of the GABA(A) receptor in the rat stress axis. Brain Res *887*, 118-124.
Danforth, E., Jr., Horton, E. S., O'Connell, M., Sims, E. A., Burger, A. G., Ingbar, S. H., Braverman, L., and Vagenakis, A. G. (1979). Dietary-induced alterations in thyroid hormone metabolism during overnutrition. J Clin Invest *64*, 1336-1347.
Davies, P. S., Day, J. M., and Lucas, A. (1991). Energy expenditure in early infancy and later body fatness. Int J Obes *15*, 727-731.
Davis, M. D., and Hadley, M. E. (1978). Pars intermedia electrical potentials: changes in spike frequency induced by regulatory factors of melanocyte stimulating hormone (MSH) secretion. Neuroendocrinology *26*, 277-282.
De Souza, J., Butler, A. A., and Cone, R. D. (2000). Disproportionate inhibition of feeding in A(y) mice by certain stressors: a cautionary note. Neuroendocrinology *72*, 126-132.
Decavel, C., and Van den Pol, A. N. (1990). GABA: a dominant neurotransmitter in the hypothalamus. J Comp Neurol *302*, 1019-1037.
Decavel, C., and van den Pol, A. N. (1992). Converging GABA- and glutamate-immunoreactive axons make synaptic contact with identified hypothalamic neurosecretory neurons. J Comp Neurol *316*, 104-116.
Del Mar Gonzalez-Barroso, M., Ricquier, D., and Cassard-Doulcier, A. M. (2000). The human uncoupling protein-1 gene (UCP1): present status and perspectives in obesity research. Obes Rev *1*, 61-72.
DeLany, J. P., Harsha, D. W., Kime, J. C., Kumler, J., Melancon, L., and Bray, G. A. (1995). Energy expenditure in lean and obese prepubertal children. Obes Res *3 Suppl 1*, 67-72.
Demling, J., Fuchs, E., Baumert, M., and Wuttke, W. (1985). Preoptic catecholamine, GABA, and glutamate release in ovariectomized and ovariectomized estrogen-primed rats utilizing a push-pull cannula technique. Neuroendocrinology *41*, 212-218.
Dewasmes, G., Loos, N., Delanaud, S., Dewasmes, D., and Geloen, A. (2003). Activation of brown adipose tissue thermogenesis increases slow wave sleep in rat. Neurosci Lett *339*, 207-210.
Dobs, A. S., Nguyen, T., Pace, C., and Roberts, C. P. (2002). Differential effects of oral estrogen versus oral estrogen-androgen replacement therapy on body composition in postmenopausal women. J Clin Endocrinol Metab *87*, 1509-1516.
Duhl, D. M., Stevens, M. E., Vrieling, H., Saxon, P. J., Miller, M. W., Epstein, C. J., and Barsh, G. S. (1994a). Pleiotropic effects of the mouse lethal yellow (Ay) mutation explained by deletion of a maternally expressed

gene and the simultaneous production of agouti fusion RNAs. Development *120*, 1695-1708.
Duhl, D. M., Vrieling, H., Miller, K. A., Wolff, G. L., and Barsh, G. S. (1994b). Neomorphic agouti mutations in obese yellow mice. Nat Genet *8*, 59-65.
Dulloo, A. G., and Jacquet, J. (2001). An adipose-specific control of thermogenesis in body weight regulation. Int J Obes Relat Metab Disord *25 Suppl 5*, S22-29.
Durnin, J. V., and Womersley, J. (1974). Body fat assessed from total body density and its estimation from skinfold thickness: measurements on 481 men and women aged from 16 to 72 years. Br J Nutr *32*, 77-97.
el Hadri, K., Pairault, J., and Feve, B. (1996). Triiodothyronine regulates beta 3-adrenoceptor expression in 3T3-F442A differentiating adipocytes. Eur J Biochem *239*, 519-525.
Elias, C. F., Aschkenasi, C., Lee, C., Kelly, J., Ahima, R. S., Bjorbaek, C., Flier, J. S., Saper, C. B., and Elmquist, J. K. (1999). Leptin differentially regulates NPY and POMC neurons projecting to the lateral hypothalamic area. Neuron *23*, 775-786.
Elias CF, L. C., Kelly J, Aschkenasi C, Ahima RS, Couceyro PR, Kuhar MJ, Saper CB, Elmquist JK (1998). Leptin activates hypothalamic CART neurons projecting to the spinal cord. Neuron *21*, 1375-1385.
Elias, C. F., Lee, C. E., Kelly, J. F., Ahima, R. S., Kuhar, M., Saper, C. B., and Elmquist, J. K. (2001). Characterization of CART neurons in the rat and human hypothalamus. J Comp Neurol *432*, 1-19.
Elias, C. F., Saper, C. B., Maratos-Flier, E., Tritos, N. A., Lee, C., Kelly, J., Tatro, J. B., Hoffman, G. E., Ollmann, M. M., Barsh, G. S., *et al.* (1998). Chemically defined projections linking the mediobasal hypothalamus and the lateral hypothalamic area. J Comp Neurol *402*, 442-459.
Ellacott, K. L., and Cone, R. D. (2004). The central melanocortin system and the integration of short- and long-term regulators of energy homeostasis. Recent Prog Horm Res *59*, 395-408.
Elmquist, J. K. (2001). Hypothalamic pathways underlying the endocrine, autonomic, and behavioral effects of leptin. Physiol Behav *74*, 703-708.
Emorine, L. J., Marullo, S., Briend-Sutren, M. M., Patey, G., Tate, K., Delavier-Klutchko, C., and Strosberg, A. D. (1989). Molecular characterization of the human beta 3-adrenergic receptor. Science *245*, 1118-1121.
Enerback, S., Jacobsson, A., Simpson, E. M., Guerra, C., Yamashita, H., Harper, M. E., and Kozak, L. P. (1997). Mice lacking mitochondrial uncoupling protein are cold-sensitive but not obese. Nature *387*, 90-94.

Fan, W., Boston, B. A., Kesterson, R. A., Hruby, V. J., and Cone, R. D. (1997). Role of melanocortinergic neurons in feeding and the agouti obesity syndrome. Nature *385*, 165-168.
Fan, W., Voss-Andreae, A., Cao, W. H., and Morrison, S. F. (2005). Regulation of thermogenesis by the central melanocortin system. Peptides *26*, 1800-1813.
Farooqi, I. S., Keogh, J. M., Yeo, G. S., Lank, E. J., Cheetham, T., and O'Rahilly, S. (2003). Clinical spectrum of obesity and mutations in the melanocortin 4 receptor gene. N Engl J Med *348*, 1085-1095.
Farooqi, I. S., Yeo, G. S., Keogh, J. M., Aminian, S., Jebb, S. A., Butler, G., Cheetham, T., and O'Rahilly, S. (2000). Dominant and recessive inheritance of morbid obesity associated with melanocortin 4 receptor deficiency. J Clin Invest *106*, 271-279.
Fathi, Z., Iben, L. G., and Parker, E. M. (1995). Cloning, expression, and tissue distribution of a fifth melanocortin receptor subtype. Neurochem Res *20*, 107-113.
Fekete, C., Kelly, J., Mihaly, E., Sarkar, S., Rand, W. M., Legradi, G., Emerson, C. H., and Lechan, R. M. (2001). Neuropeptide Y has a central inhibitory action on the hypothalamic-pituitary-thyroid axis. Endocrinology *142*, 2606-2613.
Fekete, C., Legradi, G., Mihaly, E., Huang, Q. H., Tatro, J. B., Rand, W. M., Emerson, C. H., and Lechan, R. M. (2000). alpha-Melanocyte-stimulating hormone is contained in nerve terminals innervating thyrotropin-releasing hormone-synthesizing neurons in the hypothalamic paraventricular nucleus and prevents fasting-induced suppression of prothyrotropin-releasing hormone gene expression. J Neurosci *20*, 1550-1558.
Fekete, C., Marks, D. L., Sarkar, S., Emerson, C. H., Rand, W. M., Cone, R. D., and Lechan, R. M. (2004). Effect of Agouti-related protein in regulation of the hypothalamic-pituitary-thyroid axis in the melanocortin 4 receptor knockout mouse. Endocrinology *145*, 4816-4821.
Fekete, C., Sarkar, S., Rand, W. M., Harney, J. W., Emerson, C. H., Bianco, A. C., and Lechan, R. M. (2002a). Agouti-related protein (AGRP) has a central inhibitory action on the hypothalamic-pituitary-thyroid (HPT) axis; comparisons between the effect of AGRP and neuropeptide Y on energy homeostasis and the HPT axis. Endocrinology *143*, 3846-3853.
Fekete, C., Singru, P. S., Sanchez, E., Sarkar, S., Christoffolete, M. A., Riberio, R. S., Rand, W. M., Emerson, C. H., Bianco, A. C., and Lechan, R. M. (2006). Differential effects of central leptin, insulin, or glucose administration during fasting on the hypothalamic-pituitary-thyroid axis and feeding-related neurons in the arcuate nucleus. Endocrinology *147*, 520-529.

Fekete, C., Wittmann, G., Liposits, Z., and Lechan, R. M. (2002b). GABAergic innervation of thyrotropin-releasing hormone-synthesizing neurons in the hypothalamic paraventricular nucleus of the rat. Brain Res *957*, 251-258.
Fisher, M. H., Amend, A. M., Bach, T. J., Barker, J. M., Brady, E. J., Candelore, M. R., Carroll, D., Cascieri, M. A., Chiu, S. H., Deng, L., *et al.* (1998). A selective human beta3 adrenergic receptor agonist increases metabolic rate in rhesus monkeys. J Clin Invest *101*, 2387-2393.
Fleury, C., Neverova, M., Collins, S., Raimbault, S., Champigny, O., Levi-Meyrueis, C., Bouillaud, F., Seldin, M. F., Surwit, R. S., Ricquier, D., and Warden, C. H. (1997). Uncoupling protein-2: a novel gene linked to obesity and hyperinsulinemia. Nat Genet *15*, 269-272.
Flugge, G., Oertel, W. H., and Wuttke, W. (1986). Evidence for estrogen-receptive GABAergic neurons in the preoptic/anterior hypothalamic area of the rat brain. Neuroendocrinology *43*, 1-5.
Foster, D. O., and Frydman, M. L. (1979). Tissue distribution of cold-induced thermogenesis in conscious warm- or cold-acclimated rats reevaluated from changes in tissue blood flow: the dominant role of brown adipose tissue in the replacement of shivering by nonshivering thermogenesis. Can J Physiol Pharmacol *57*, 257-270.
Freedman, D. S., Dietz, W. H., Srinivasan, S. R., and Berenson, G. S. (1999). The relation of overweight to cardiovascular risk factors among children and adolescents: the Bogalusa Heart Study. Pediatrics *103*, 1175-1182.
Friedrich, M. J. (2002). Epidemic of obesity expands its spread to developing countries. Jama *287*, 1382-1386.
Frigeri, L. G., Wolff, G. L., and Robel, G. (1983). Impairment of glucose tolerance in yellow (Avy/A) (BALB/c X VY) F-1 hybrid mice by hyperglycemic peptide(s) from human pituitary glands. Endocrinology *113*, 2097-2105.
Froguel, P., and Boutin, P. (2001). Genetics of pathways regulating body weight in the development of obesity in humans. Exp Biol Med (Maywood) *226*, 991-996.
Fumeron, F., Durack-Bown, I., Betoulle, D., Cassard-Doulcier, A. M., Tuzet, S., Bouillaud, F., Melchior, J. C., Ricquier, D., and Apfelbaum, M. (1996). Polymorphisms of uncoupling protein (UCP) and beta 3 adrenoreceptor genes in obese people submitted to a low calorie diet. Int J Obes Relat Metab Disord *20*, 1051-1054.
Funahashi, H., Yamada, S., Kageyama, H., Takenoya, F., Guan, J. L., and Shioda, S. (2003). Co-existence of leptin- and orexin-receptors in feeding-regulating neurons in the hypothalamic arcuate nucleus-a triple labeling study. Peptides *24*, 687-694.

Fyda, D. M., Cooper, K. E., and Veale, W. L. (1991). Modulation of brown adipose tissue-mediated thermogenesis by lesions to the nucleus tractus solitarius in the rat. Brain Res *546*, 203-210.
Gagnon, J., Lago, F., Chagnon, Y. C., Perusse, L., Naslund, I., Lissner, L., Sjostrom, L., and Bouchard, C. (1998). DNA polymorphism in the uncoupling protein 1 (UCP1) gene has no effect on obesity related phenotypes in the Swedish Obese Subjects cohorts. Int J Obes Relat Metab Disord *22*, 500-505.
Gantz, I., Konda, Y., Tashiro, T., Shimoto, Y., Miwa, H., Munzert, G., Watson, S. J., DelValle, J., and Yamada, T. (1993a). Molecular cloning of a novel melanocortin receptor. J Biol Chem *268*, 8246-8250.
Gantz, I., Miwa, H., Konda, Y., Shimoto, Y., Tashiro, T., Watson, S. J., DelValle, J., and Yamada, T. (1993b). Molecular cloning, expression, and gene localization of a fourth melanocortin receptor. J Biol Chem *268*, 15174-15179.
Gantz, I., Shimoto, Y., Konda, Y., Miwa, H., Dickinson, C. J., and Yamada, T. (1994). Molecular cloning, expression, and characterization of a fifth melanocortin receptor. Biochem Biophys Res Commun *200*, 1214-1220.
Garruti, G., and Ricquier, D. (1992). Analysis of uncoupling protein and its mRNA in adipose tissue deposits of adult humans. Int J Obes Relat Metab Disord *16*, 383-390.
Genin, F., Nibbelink, M., Galand, M., Perret, M., and Ambid, L. (2003). Brown fat and nonshivering thermogenesis in the gray mouse lemur (Microcebus murinus). Am J Physiol Regul Integr Comp Physiol *284*, R811-818.
Golozoubova, V., Cannon, B., and Nedergaard, J. (2006). UCP1 is essential for adaptive adrenergic nonshivering thermogenesis. Am J Physiol Endocrinol Metab.
Golozoubova, V., Hohtola, E., Matthias, A., Jacobsson, A., Cannon, B., and Nedergaard, J. (2001). Only UCP1 can mediate adaptive nonshivering thermogenesis in the cold. Faseb J *15*, 2048-2050.
Gong, D. W., He, Y., Karas, M., and Reitman, M. (1997). Uncoupling protein-3 is a mediator of thermogenesis regulated by thyroid hormone, beta3-adrenergic agonists, and leptin. J Biol Chem *272*, 24129-24132.
Goran, M. I., Shewchuk, R., Gower, B. A., Nagy, T. R., Carpenter, W. H., and Johnson, R. K. (1998). Longitudinal changes in fatness in white children: no effect of childhood energy expenditure. Am J Clin Nutr *67*, 309-316.
Goto, K., Inui, A., Takimoto, Y., Yuzuriha, H., Asakawa, A., Kawamura, Y., Tsuji, H., Takahara, Y., Takeyama, C., Katsuura, G., and Kasuga, M. (2003). Acute intracerebroventricular administration of either carboxyl-

terminal or amino-terminal fragments of agouti-related peptide produces a long-term decrease in energy expenditure in rats. Int J Mol Med *12*, 379-383.
Graham, M., Shutter, J. R., Sarmiento, U., Sarosi, I., and Stark, K. L. (1997). Overexpression of Agrt leads to obesity in transgenic mice. Nat Genet *17*, 273-274.
Grattan, D. R., and Selmanoff, M. (1994). Castration-induced decrease in the activity of medial preoptic and tuberoinfundibular GABAergic neurons is prevented by testosterone. Neuroendocrinology *60*, 141-149.
Green, E. D., Maffei, M., Braden, V. V., Proenca, R., DeSilva, U., Zhang, Y., Chua, S. C., Jr., Leibel, R. L., Weissenbach, J., and Friedman, J. M. (1995). The human obese (OB) gene: RNA expression pattern and mapping on the physical, cytogenetic, and genetic maps of chromosome 7. Genome Res *5*, 5-12.
Griffiths, M., and Payne, P. R. (1976). Energy expenditure in small children of obese and non-obese parents. Nature *260*, 698-700.
Griffiths, M., Payne, P. R., Stunkard, A. J., Rivers, J. P., and Cox, M. (1990). Metabolic rate and physical development in children at risk of obesity. Lancet *336*, 76-78.
Grill, H. J., Schwartz, M. W., Kaplan, J. M., Foxhall, J. S., Breininger, J., and Baskin, D. G. (2002). Evidence that the caudal brainstem is a target for the inhibitory effect of leptin on food intake. Endocrinology *143*, 239-246.
Grkovic, I., and Anderson, C. R. (1997). Calbindin D28K-immunoreactivity identifies distinct subpopulations of sympathetic pre- and postganglionic neurons in the rat. J Comp Neurol *386*, 245-259.
Grodstein, F., Levine, R., Troy, L., Spencer, T., Colditz, G. A., and Stampfer, M. J. (1996). Three-year follow-up of participants in a commercial weight loss program. Can you keep it off? Arch Intern Med *156*, 1302-1306.
Gu, G., Cornea, A., and Simerly, R. B. (2003). Sexual differentiation of projections from the principal nucleus of the bed nuclei of the stria terminalis. J Comp Neurol *460*, 542-562.
Guo, F., Bakal, K., Minokoshi, Y., and Hollenberg, A. N. (2004). Leptin signaling targets the thyrotropin-releasing hormone gene promoter in vivo. Endocrinology *145*, 2221-2227.
Hagan, M. M., Benoit, S. C., Rushing, P. A., Pritchard, L. M., Woods, S. C., and Seeley, R. J. (2001). Immediate and prolonged patterns of Agouti-related peptide-(83--132)-induced c-Fos activation in hypothalamic and extrahypothalamic sites. Endocrinology *142*, 1050-1056.

Hakansson, M. L., Brown, H., Ghilardi, N., Skoda, R. C., and Meister, B. (1998). Leptin receptor immunoreactivity in chemically defined target neurons of the hypothalamus. J Neurosci *18*, 559-572.
Hamann, A., Flier, J. S., and Lowell, B. B. (1996). Decreased brown fat markedly enhances susceptibility to diet-induced obesity, diabetes, and hyperlipidemia. Endocrinology *137*, 21-29.
Hamann, A., Flier, J. S., and Lowell, B. B. (1998). Obesity after genetic ablation of brown adipose tissue. Z Ernahrungswiss *37 Suppl 1*, 1-7.
Hanada, R., Nakazato, M., Matsukura, S., Murakami, N., Yoshimatsu, H., and Sakata, T. (2000). Differential regulation of melanin-concentrating hormone and orexin genes in the agouti-related protein/melanocortin-4 receptor system. Biochem Biophys Res Commun *268*, 88-91.
Haque, M. S., Minokoshi, Y., Hamai, M., Iwai, M., Horiuchi, M., and Shimazu, T. (1999). Role of the sympathetic nervous system and insulin in enhancing glucose uptake in peripheral tissues after intrahypothalamic injection of leptin in rats. Diabetes *48*, 1706-1712.
Harris, M., Aschkenasi, C., Elias, C. F., Chandrankunnel, A., Nillni, E. A., Bjoorbaek, C., Elmquist, J. K., Flier, J. S., and Hollenberg, A. N. (2001). Transcriptional regulation of the thyrotropin-releasing hormone gene by leptin and melanocortin signaling. J Clin Invest *107*, 111-120.
Haskell-Luevano, C., Chen, P., Li, C., Chang, K., Smith, M. S., Cameron, J. L., and Cone, R. D. (1999). Characterization of the neuroanatomical distribution of agouti-related protein immunoreactivity in the rhesus monkey and the rat. Endocrinology *140*, 1408-1415.
Hausberger, F. X. (1959). Parabiosis and transplantation experiments in hereditary obese mice. Anat Rec *130*, 313.
Hayakawa, T., Nagai, Y., Taniguchi, M., Yamashita, H., Takamura, T., Abe, T., Nomura, G., and Kobayashi, K. (1999). Phenotypic characterization of the beta3-adrenergic receptor mutation and the uncoupling protein 1 polymorphism in Japanese men. Metabolism *48*, 636-640.
Haynes, W. G., Morgan, D. A., Djalali, A., Sivitz, W. I., and Mark, A. L. (1999). Interactions between the melanocortin system and leptin in control of sympathetic nerve traffic. Hypertension *33*, 542-547.
Haynes, W. G., Morgan, D. A., Walsh, S. A., Mark, A. L., and Sivitz, W. I. (1997). Receptor-mediated regional sympathetic nerve activation by leptin. J Clin Invest *100*, 270-278.
Hedley, A. A., Ogden, C. L., Johnson, C. L., Carroll, M. D., Curtin, L. R., and Flegal, K. M. (2004). Prevalence of overweight and obesity among US children, adolescents, and adults, 1999-2002. Jama *291*, 2847-2850.

Heine, P. A., Taylor, J. A., Iwamoto, G. A., Lubahn, D. B., and Cooke, P. S. (2000). Increased adipose tissue in male and female estrogen receptor-alpha knockout mice. Proc Natl Acad Sci U S A *97*, 12729-12734.
Heinrichs, S. C., and Richard, D. (1999). The role of corticotropin-releasing factor and urocortin in the modulation of ingestive behavior. Neuropeptides *33*, 350-359.
Hentges, S. T., Nishiyama, M., Overstreet, L. S., Stenzel-Poore, M., Williams, J. T., and Low, M. J. (2004). GABA release from proopiomelanocortin neurons. J Neurosci *24*, 1578-1583.
Herbison, A. E. (1997). Estrogen regulation of GABA transmission in rat preoptic area. Brain Res Bull *44*, 321-326.
Herbison, A. E., Augood, S. J., and McGowan, E. M. (1992). Expression of glutamic acid decarboxylase messenger RNA in rat medial preoptic area neurones during the oestrous cycle and after ovariectomy. Brain Res Mol Brain Res *14*, 310-316.
Herbison, A. E., Augood, S. J., Simonian, S. X., and Chapman, C. (1995). Regulation of GABA transporter activity and mRNA expression by estrogen in rat preoptic area. J Neurosci *15*, 8302-8309.
Herbison, A. E., and Fenelon, V. S. (1995). Estrogen regulation of GABAA receptor subunit mRNA expression in preoptic area and bed nucleus of the stria terminalis of female rat brain. J Neurosci *15*, 2328-2337.
Hermann, D. M., Luppi, P. H., Peyron, C., Hinckel, P., and Jouvet, M. (1997). Afferent projections to the rat nuclei raphe magnus, raphe pallidus and reticularis gigantocellularis pars alpha demonstrated by iontophoretic application of choleratoxin (subunit b). J Chem Neuroanat *13*, 1-21.
Hermanson, O., and Blomqvist, A. (1997). Preproenkephalin messenger RNA-expressing neurons in the rat parabrachial nucleus: subnuclear organization and projections to the intralaminar thalamus. Neuroscience *81*, 803-812.
Hervey, G. R. (1959). The effects of lesions in the hypothalamus in parabiotic rats. J Physiol *145*, 336-352.
Hetherington, A. W., and Ranson, S. W. (1940). Hypothalamic lesions and adiposity in the rat. Anat Rec *78*, 149-172.
Himms-Hagen, J., Cui, J., Danforth, E., Jr., Taatjes, D. J., Lang, S. S., Waters, B. L., and Claus, T. H. (1994). Effect of CL-316,243, a thermogenic beta 3-agonist, on energy balance and brown and white adipose tissues in rats. Am J Physiol *266*, R1371-1382.
Hinney, A., Hohmann, S., Geller, F., Vogel, C., Hess, C., Wermter, A. K., Brokamp, B., Goldschmidt, H., Siegfried, W., Remschmidt, H., *et al.* (2003). Melanocortin-4 receptor gene: case-control study and transmission disequilibrium test confirm that functionally relevant mutations are

compatible with a major gene effect for extreme obesity. J Clin Endocrinol Metab *88*, 4258-4267.
Hoggard, N., Hunter, L., Duncan, J. S., Williams, L. M., Trayhurn, P., and Mercer, J. G. (1997). Leptin and leptin receptor mRNA and protein expression in the murine fetus and placenta. Proc Natl Acad Sci U S A *94*, 11073-11078.
Holt, S. J., and York, D. A. (1988). Effect of lateral hypothalamic lesion on brown adipose tissue of Zucker lean and obese rats. Physiol Behav *43*, 293-299.
Horvath, T. L., Diano, S., Miyamoto, S., Barry, S., Gatti, S., Alberati, D., Livak, F., Lombardi, A., Moreno, M., Goglia, F., *et al.* (2003). Uncoupling proteins-2 and 3 influence obesity and inflammation in transgenic mice. Int J Obes Relat Metab Disord *27*, 433-442.
Hosoya, Y. (1985). Hypothalamic projections to the ventral medulla oblongata in the rat, with special reference to the nucleus raphe pallidus: a study using autoradiographic and HRP techniques. Brain Res *344*, 338-350.
Hosoya, Y., Ito, R., and Kohno, K. (1987). The topographical organization of neurons in the dorsal hypothalamic area that project to the spinal cord or to the nucleus raphe pallidus in the rat. Exp Brain Res *66*, 500-506.
Howes, K. A., Newton, B. W., and Maley, B. E. (1989). Cholecystokinin octapeptide immunoreactivity in the nucleus tractus solitarius of the cat. Peptides *10*, 73-78.
Huszar, D., Lynch, C. A., Fairchild-Huntress, V., Dunmore, J. H., Fang, Q., Berkemeier, L. R., Gu, W., Kesterson, R. A., Boston, B. A., Cone, R. D., *et al.* (1997). Targeted disruption of the melanocortin-4 receptor results in obesity in mice. Cell *88*, 131-141.
Hutton, L. A., Gu, G., and Simerly, R. B. (1998). Development of a sexually dimorphic projection from the bed nuclei of the stria terminalis to the anteroventral periventricular nucleus in the rat. J Neurosci *18*, 3003-3013.
Hwa, J. J., Ghibaudi, L., Gao, J., and Parker, E. M. (2001). Central melanocortin system modulates energy intake and expenditure of obese and lean Zucker rats. Am J Physiol Regul Integr Comp Physiol *281*, R444-451.
Inokuma, K. I., Okamatsu-Ogura, Y., Omachi, A., Matsushita, Y., Kimura, K., Yamashita, H., and Saito, M. (2005). Indispensable role of mitochondrial uncoupling protein 1(UCP1) for anti-obesity effect of {beta}3-adrenergic stimulation. Am J Physiol Endocrinol Metab.
Iqbal, J., Pompolo, S., Sakurai, T., and Clarke, I. J. (2001). Evidence that orexin-containing neurones provide direct input to gonadotropin-releasing hormone neurones in the ovine hypothalamus. J Neuroendocrinol *13*, 1033-1041.

Ito, M., Gomori, A., Ishihara, A., Oda, Z., Mashiko, S., Matsushita, H., Yumoto, M., Sano, H., Tokita, S., Moriya, M., *et al.* (2003). Characterization of MCH-mediated obesity in mice. Am J Physiol Endocrinol Metab *284*, E940-945.
Jacobowitz, D. M., and O'Donohue, T. L. (1978). alpha-Melanocyte stimulating hormone: immunohistochemical identification and mapping in neurons of rat brain. Proc Natl Acad Sci U S A *75*, 6300-6304.
James, P. T., Leach, R., Kalamara, E., and Shayeghi, M. (2001). The worldwide obesity epidemic. Obes Res *9 Suppl 4*, 228S-233S.
Jones, M. T., Hillhouse, E. W., and Burden, J. (1976). Effect on various putative neurotransmitters on the secretion of corticotrophin-releasing hormone from the rat hypothalamus in vitro-a model of the neurotransmitters involved. J Endocrinol *69*, 1-10.
Jonsson, L., Skarphedinsson, J. O., Skuladottir, G. V., Atlason, P. T., Eiriksdottir, V. H., Franzson, L., and Schioth, H. B. (2001). Melanocortin receptor agonist transiently increases oxygen consumption in rats. Neuroreport *12*, 3703-3708.
Joseph, S. A., and Michael, G. J. (1988). Efferent ACTH-IR opiocortin projections from nucleus tractus solitarius: a hypothalamic deafferentation study. Peptides *9*, 193-201.
Kaiyala, K. J., Woods, S. C., and Schwartz, M. W. (1995). New model for the regulation of energy balance and adiposity by the central nervous system. Am J Clin Nutr *62*, 1123S-1134S.
Kanasaki, M., Matsubara, H., Murasawa, S., Masaki, H., Nio, Y., and Inada, M. (1994). cAMP responsive element-mediated regulation of the gene transcription of the alpha 1B adrenergic receptor by thyrotropin. J Clin Invest *94*, 2245-2254.
Kawashima, N., Chaki, S., and Okuyama, S. (2003). Electrophysiological effects of melanocortin receptor ligands on neuronal activities of monoaminergic neurons in rats. Neurosci Lett *353*, 119-122.
Kennedy, G. C. (1953). The role of depot fat in the hypothalamic control of food intake in the rat. Proc R Soc Lond B Biol Sci *140*, 578-596.
Khong, K., Kurtz, S. E., Sykes, R. L., and Cone, R. D. (2001). Expression of functional melanocortin-4 receptor in the hypothalamic GT1-1 cell line. Neuroendocrinology *74*, 193-201.
Kim, M. S., Small, C. J., Stanley, S. A., Morgan, D. G., Seal, L. J., Kong, W. M., Edwards, C. M., Abusnana, S., Sunter, D., Ghatei, M. A., and Bloom, S. R. (2000). The central melanocortin system affects the hypothalamo-pituitary thyroid axis and may mediate the effect of leptin. J Clin Invest *105*, 1005-1011.

King, B. F., Jones, M. V., and Ewart, W. R. (1989). Immunohistochemical localisation of a gastrin-releasing peptide-like material in area postrema, nucleus of the solitary tract and vagal motor nucleus in the brainstem of rat. J Auton Nerv Syst *28*, 97-104.
Kinlaw, W. B., Schwartz, H. L., and Oppenheimer, J. H. (1985). Decreased serum triiodothyronine in starving rats is due primarily to diminished thyroidal secretion of thyroxine. J Clin Invest *75*, 1238-1241.
Kishi, T., Aschkenasi, C. J., Lee, C. E., Mountjoy, K. G., Saper, C. B., and Elmquist, J. K. (2003). Expression of melanocortin 4 receptor mRNA in the central nervous system of the rat. J Comp Neurol *457*, 213-235.
Klebig, M. L., Wilkinson, J. E., Geisler, J. G., and Woychik, R. P. (1995). Ectopic expression of the agouti gene in transgenic mice causes obesity, features of type II diabetes, and yellow fur. Proc Natl Acad Sci U S A *92*, 4728-4732.
Kobayashi, A., and Osaka, T. (2003). Involvement of the parabrachial nucleus in thermogenesis induced by environmental cooling in the rat. Pflugers Arch *446*, 760-765.
Koegler, F. H., and Ritter, S. (1998). Galanin injection into the nucleus of the solitary tract stimulates feeding in rats with lesions of the paraventricular nucleus of the hypothalamus. Physiol Behav *63*, 521-527.
Kogure A, S. N., Takakura Y, Tsunekazu U, Yoshioka K, Nishino H, Yamamoto T, Kawada T, Yoshikawa Y, Yoshida T (2002). Effects of Caffeine on the Uncoupling Protein Family in Obese Yellow KK Mice. Clin Exp Pharmacol Physiol *29*, 391-294.
Kogure, A., Yoshida, T., Sakane, N., Umekawa, T., Takakura, Y., and Kondo, M. (1998). Synergic effect of polymorphisms in uncoupling protein 1 and beta3-adrenergic receptor genes on weight loss in obese Japanese. Diabetologia *41*, 1399.
Kohler, C., Haglund, L., and Swanson, L. W. (1984). A diffuse alpha MSH-immunoreactive projection to the hippocampus and spinal cord from individual neurons in the lateral hypothalamic area and zona incerta. J Comp Neurol *223*, 501-514.
Kok, P., Roelfsema, F., Langendonk, J. G., Frolich, M., Burggraaf, J., Meinders, A. E., and Pijl, H. (2005). High circulating thyrotropin levels in obese women are reduced after body weight loss induced by caloric restriction. J Clin Endocrinol Metab *90*, 4659-4663.
Kovacs, K. J., Miklos, I. H., and Bali, B. (2004). GABAergic mechanisms constraining the activity of the hypothalamo-pituitary-adrenocortical axis. Ann N Y Acad Sci *1018*, 466-476.

Kramer, F. M., Jeffery, R. W., Forster, J. L., and Snell, M. K. (1989). Long-term follow-up of behavioral treatment for obesity: patterns of weight regain among men and women. Int J Obes *13*, 123-136.
Krief, S., Lonnqvist, F., Raimbault, S., Baude, B., Van Spronsen, A., Arner, P., Strosberg, A. D., Ricquier, D., and Emorine, L. J. (1993). Tissue distribution of beta 3-adrenergic receptor mRNA in man. J Clin Invest *91*, 344-349.
Lacasa, D., Agli, B., Pecquery, R., and Giudicelli, Y. (1991). Influence of ovariectomy and regional fat distribution on the membranous transducing system controlling lipolysis in rat fat cells. Endocrinology *128*, 747-753.
Landsberg, L., Saville, M. E., and Young, J. B. (1984). Sympathoadrenal system and regulation of thermogenesis. Am J Physiol *247*, E181-189.
Lanni, A., Moreno, M., Lombardi, A., and Goglia, F. (2003). Thyroid hormone and uncoupling proteins. FEBS Lett *543*, 5-10.
Leblanc, J., Dussault, J., Lupien, D., and Richard, D. (1982). Effect of diet and exercise on norepinephrine-induced thermogenesis in male and female rats. J Appl Physiol *52*, 556-561.
Lee, G. H., Proenca, R., Montez, J. M., Carroll, K. M., Darvishzadeh, J. G., Lee, J. I., and Friedman, J. M. (1996). Abnormal splicing of the leptin receptor in diabetic mice. Nature *379*, 632-635.
Legradi, G., Emerson, C. H., Ahima, R. S., Flier, J. S., and Lechan, R. M. (1997). Leptin prevents fasting-induced suppression of prothyrotropin-releasing hormone messenger ribonucleic acid in neurons of the hypothalamic paraventricular nucleus. Endocrinology *138*, 2569-2576.
Legradi, G., and Lechan, R. M. (1999). Agouti-related protein containing nerve terminals innervate thyrotropin-releasing hormone neurons in the hypothalamic paraventricular nucleus. Endocrinology *140*, 3643-3652.
Leibel, R. L., Rosenbaum, M., and Hirsch, J. (1995). Changes in energy expenditure resulting from altered body weight. N Engl J Med *332*, 621-628.
Leranth, C., MacLusky, N. J., Shanabrough, M., and Naftolin, F. (1988). Immunohistochemical evidence for synaptic connections between pro-opiomelanocortin-immunoreactive axons and LH-RH neurons in the preoptic area of the rat. Brain Res *449*, 167-176.
Li, G., Mobbs, C. V., and Scarpace, P. J. (2003). Central pro-opiomelanocortin gene delivery results in hypophagia, reduced visceral adiposity, and improved insulin sensitivity in genetically obese Zucker rats. Diabetes *52*, 1951-1957.
Li, G., Zhang, Y., Wilsey, J. T., and Scarpace, P. J. (2004). Unabated anorexic and enhanced thermogenic responses to melanotan II in diet-induced obese rats despite reduced melanocortin 3 and 4 receptor expression. J Endocrinol *182*, 123-132.

Lindblom, J., Schioth, H. B., Larsson, A., Wikberg, J. E., and Bergstrom, L. (1998). Autoradiographic discrimination of melanocortin receptors indicates that the MC3 subtype dominates in the medial rat brain. Brain Res *810*, 161-171.
Liu, H., Kishi, T., Roseberry, A. G., Cai, X., Lee, C. E., Montez, J. M., Friedman, J. M., and Elmquist, J. K. (2003). Transgenic mice expressing green fluorescent protein under the control of the melanocortin-4 receptor promoter. J Neurosci *23*, 7143-7154.
Loewy, A. D. (1981). Raphe pallidus and raphe obscurus projections to the intermediolateral cell column in the rat. Brain Res *222*, 129-133.
Loewy, A. D., Franklin, M. F., and Haxhiu, M. A. (1994). CNS monoamine cell groups projecting to pancreatic vagal motor neurons: a transneuronal labeling study using pseudorabies virus. Brain Res *638*, 248-260.
Lonnqvist, F., Arner, P., Nordfors, L., and Schalling, M. (1995). Overexpression of the obese (ob) gene in adipose tissue of human obese subjects. Nat Med *1*, 950-953.
Lowell, B. B., and Bachman, E. S. (2003). Beta-Adrenergic receptors, diet-induced thermogenesis, and obesity. J Biol Chem *278*, 29385-29388.
Lowell, B. B., and Spiegelman, B. M. (2000). Towards a molecular understanding of adaptive thermogenesis. Nature *404*, 652-660.
Lu, D., Willard, D., Patel, I. R., Kadwell, S., Overton, L., Kost, T., Luther, M., Chen, W., Woychik, R. P., Wilkison, W. O., and et al. (1994). Agouti protein is an antagonist of the melanocyte-stimulating-hormone receptor. Nature *371*, 799-802.
Lu, X. Y., Barsh, G. S., Akil, H., and Watson, S. J. (2003). Interaction between alpha-melanocyte-stimulating hormone and corticotropin-releasing hormone in the regulation of feeding and hypothalamo-pituitary-adrenal responses. J Neurosci *23*, 7863-7872.
Lubrano-Berthelier, C., Cavazos, M., Dubern, B., Shapiro, A., Stunff, C. L., Zhang, S., Picart, F., Govaerts, C., Froguel, P., Bougneres, P., *et al.* (2003). Molecular genetics of human obesity-associated MC4R mutations. Ann N Y Acad Sci *994*, 49-57.
Ludwig, D. S., Mountjoy, K. G., Tatro, J. B., Gillette, J. A., Frederich, R. C., Flier, J. S., and Maratos-Flier, E. (1998). Melanin-concentrating hormone: a functional melanocortin antagonist in the hypothalamus. Am J Physiol *274*, E627-633.
Luiten, P. G., ter Horst, G. J., Karst, H., and Steffens, A. B. (1985). The course of paraventricular hypothalamic efferents to autonomic structures in medulla and spinal cord. Brain Res *329*, 374-378.
MacLellan, J. D., Gerrits, M. F., Gowing, A., Smith, P. J., Wheeler, M. B., and Harper, M. E. (2005). Physiological increases in uncoupling protein 3

augment fatty acid oxidation and decrease reactive oxygen species production without uncoupling respiration in muscle cells. Diabetes *54*, 2343-2350.
Maffei, M., Fei, H., Lee, G. H., Dani, C., Leroy, P., Zhang, Y., Proenca, R., Negrel, R., Ailhaud, G., and Friedman, J. M. (1995). Increased expression in adipocytes of ob RNA in mice with lesions of the hypothalamus and with mutations at the db locus. Proc Natl Acad Sci U S A *92*, 6957-6960.
Maffeis, C., Schutz, Y., Grezzani, A., Provera, S., Piacentini, G., and Tato, L. (2001). Meal-induced thermogenesis and obesity: is a fat meal a risk factor for fat gain in children? J Clin Endocrinol Metab *86*, 214-219.
Mansky, T., Mestres-Ventura, P., and Wuttke, W. (1982). Involvement of GABA in the feedback action of estradiol on gonadotropin and prolactin release: hypothalamic GABA and catecholamine turnover rates. Brain Res *231*, 353-364.
Mantzoros, C. S., and Moschos, S. J. (1998). Leptin: in search of role(s) in human physiology and pathophysiology. Clin Endocrinol (Oxf) *49*, 551-567.
Margareto, J., Marti, A., and Martinez, J. A. (2001). Changes in UCP mRNA expression levels in brown adipose tissue and skeletal muscle after feeding a high-energy diet and relationships with leptin, glucose and PPARgamma. J Nutr Biochem *12*, 130-137.
Marsh, D. J., Hollopeter, G., Huszar, D., Laufer, R., Yagaloff, K. A., Fisher, S. L., Burn, P., and Palmiter, R. D. (1999). Response of melanocortin-4 receptor-deficient mice to anorectic and orexigenic peptides. Nat Genet *21*, 119-122.
Masuzaki, H., Ogawa, Y., Sagawa, N., Hosoda, K., Matsumoto, T., Mise, H., Nishimura, H., Yoshimasa, Y., Tanaka, I., Mori, T., and Nakao, K. (1997). Nonadipose tissue production of leptin: leptin as a novel placenta-derived hormone in humans. Nat Med *3*, 1029-1033.
Matsumoto, T., Miyawaki, C., Ue, H., Kanda, T., Yoshitake, Y., and Moritani, T. (2001). Comparison of thermogenic sympathetic response to food intake between obese and non-obese young women. Obes Res *9*, 78-85.
Matsuyama, S., Ohkura, S., Sakurai, K., Tsukamura, H., Maeda, K., and Okamura, H. (2005). Activation of melanocortin receptors accelerates the gonadotropin-releasing hormone pulse generator activity in goats. Neurosci Lett *383*, 289-294.
McPhee, S. J., Vishwanath, L. R., Ganong, W. F., and Lange, J. D. (1997). Pathophysiology of Disease (Stamford, Connecticut, Appelton & Lange).
Meister, B., Hokfelt, T., Geffard, M., and Oertel, W. (1988). Glutamic acid decarboxylase- and gamma-aminobutyric acid-like immunoreactivities in corticotropin-releasing factor-containing parvocellular neurons of the hypothalamic paraventricular nucleus. Neuroendocrinology *48*, 516-526.

Meister, B., Hokfelt, T., and Staines, W. (1987). Presence of glutamic acid decarboxylase in some corticotropin-releasing-factor- (CRF-) containing neurons of the paraventricular nucleus. Acta Physiol Scand *131*, 471-473.
Meli, R., Pacilio, M., Raso, G. M., Esposito, E., Coppola, A., Nasti, A., Di Carlo, C., Nappi, C., and Di Carlo, R. (2004). Estrogen and raloxifene modulate leptin and its receptor in hypothalamus and adipose tissue from ovariectomized rats. Endocrinology *145*, 3115-3121.
Menendez, L., Bester, H., Besson, J. M., and Bernard, J. F. (1996). Parabrachial area: electrophysiological evidence for an involvement in cold nociception. J Neurophysiol *75*, 2099-2116.
Mercer, J. G., Hoggard, N., Williams, L. M., Lawrence, C. B., Hannah, L. T., Morgan, P. J., and Trayhurn, P. (1996). Coexpression of leptin receptor and preproneuropeptide Y mRNA in arcuate nucleus of mouse hypothalamus. J Neuroendocrinol *8*, 733-735.
Micevych, P., Akesson, T., and Elde, R. (1988). Distribution of cholecystokinin-immunoreactive cell bodies in the male and female rat: II. Bed nucleus of the stria terminalis and amygdala. J Comp Neurol *269*, 381-391.
Michaud, E. J., Bultman, S. J., Klebig, M. L., van Vugt, M. J., Stubbs, L. J., Russell, L. B., and Woychik, R. P. (1994a). A molecular model for the genetic and phenotypic characteristics of the mouse lethal yellow (Ay) mutation. Proc Natl Acad Sci U S A *91*, 2562-2566.
Michaud, E. J., van Vugt, M. J., Bultman, S. J., Sweet, H. O., Davisson, M. T., and Woychik, R. P. (1994b). Differential expression of a new dominant agouti allele (Aiapy) is correlated with methylation state and is influenced by parental lineage. Genes Dev *8*, 1463-1472.
Mihaly, E., Fekete, C., Tatro, J. B., Liposits, Z., Stopa, E. G., and Lechan, R. M. (2000). Hypophysiotropic thyrotropin-releasing hormone-synthesizing neurons in the human hypothalamus are innervated by neuropeptide Y, agouti-related protein, and alpha-melanocyte-stimulating hormone. J Clin Endocrinol Metab *85*, 2596-2603.
Miklos, I. H., and Kovacs, K. J. (2002). GABAergic innervation of corticotropin-releasing hormone (CRH)-secreting parvocellular neurons and its plasticity as demonstrated by quantitative immunoelectron microscopy. Neuroscience *113*, 581-592.
Miltenberger, R. J., Mynatt, R. L., Wilkinson, J. E., and Woychik, R. P. (1997). The role of the agouti gene in the yellow obese syndrome. J Nutr *127*, 1902S-1907S.
Minokoshi, Y., Haque, M. S., and Shimazu, T. (1999). Microinjection of leptin into the ventromedial hypothalamus increases glucose uptake in peripheral tissues in rats. Diabetes *48*, 287-291.

Mix, H., Manns, M. P., Wagner, S., Widjaja, A., and Brabant, G. (1999). Expression of leptin and its receptor in the human stomach. Gastroenterology *117*, 509.
Miyata, S., Ishiyama, M., Shido, O., Nakashima, T., Shibata, M., and Kiyohara, T. (1995). Central mechanism of neural activation with cold acclimation of rats using Fos immunohistochemistry. Neurosci Res *22*, 209-218.
Mizuno, T. M., Kleopoulos, S. P., Bergen, H. T., Roberts, J. L., Priest, C. A., and Mobbs, C. V. (1998). Hypothalamic pro-opiomelanocortin mRNA is reduced by fasting and [corrected] in ob/ob and db/db mice, but is stimulated by leptin. Diabetes *47*, 294-297.
Moga, M. M., Saper, C. B., and Gray, T. S. (1990). Neuropeptide organization of the hypothalamic projection to the parabrachial nucleus in the rat. J Comp Neurol *295*, 662-682.
Monda, M., Viggiano, A., and De Luca, V. (2003). Paradoxical [correction of parodoxical] effect of orexin A: hypophagia induced by hyperthermia. Brain Res *961*, 220-228.
Montague, C. T., Farooqi, I. S., Whitehead, J. P., Soos, M. A., Rau, H., Wareham, N. J., Sewter, C. P., Digby, J. E., Mohammed, S. N., Hurst, J. A., *et al.* (1997). Congenital leptin deficiency is associated with severe early-onset obesity in humans. Nature *387*, 903-908.
Morrison, S. F. (1999). RVLM and raphe differentially regulate sympathetic outflows to splanchnic and brown adipose tissue. Am J Physiol *276*, R962-973.
Morrison, S. F. (2001a). Differential control of sympathetic outflow. Am J Physiol Regul Integr Comp Physiol *281*, R683-698.
Morrison, S. F. (2001b). Differential regulation of brown adipose and splanchnic sympathetic outflows in rat: roles of raphe and rostral ventrolateral medulla neurons. Clin Exp Pharmacol Physiol *28*, 138-143.
Morrison, S. F. (2004). Central pathways controlling brown adipose tissue thermogenesis. News Physiol Sci *19*, 67-74.
Mountjoy, K. G., Mortrud, M. T., Low, M. J., Simerly, R. B., and Cone, R. D. (1994). Localization of the melanocortin-4 receptor (MC4-R) in neuroendocrine and autonomic control circuits in the brain. Mol Endocrinol *8*, 1298-1308.
Muroya, S., Funahashi, H., Yamanaka, A., Kohno, D., Uramura, K., Nambu, T., Shibahara, M., Kuramochi, M., Takigawa, M., Yanagisawa, M., *et al.* (2004). Orexins (hypocretins) directly interact with neuropeptide Y, POMC and glucose-responsive neurons to regulate Ca 2+ signaling in a reciprocal manner to leptin: orexigenic neuronal pathways in the mediobasal hypothalamus. Eur J Neurosci *19*, 1524-1534.

Must, A., Spadano, J., Coakley, E. H., Field, A. E., Colditz, G., and Dietz, W. H. (1999). The disease burden associated with overweight and obesity. Jama *282*, 1523-1529.
Naim, M., Brand, J. G., Kare, M. R., and Carpenter, R. G. (1985). Energy intake, weight gain and fat deposition in rats fed flavored, nutritionally controlled diets in a multichoice ("cafeteria") design. J Nutr *115*, 1447-1458.
Narayan, K. M. V., Zhang, P., Kanaya, A. M., Williams, D. E., Engelgau, M. M., Imperatore, G., and Ramachandran, A. (2006). Diabetes: The pandemic and potenial solutions, Disease Control Priorities Porject Partners).
Nedergaard, J., Golozoubova, V., Matthias, A., Shabalina, I., Ohba, K., Ohlson, K., Jacobsson, A., and Cannon, B. (2001). Life without UCP1: mitochondrial, cellular and organismal characteristics of the UCP1-ablated mice. Biochem Soc Trans *29*, 756-763.
Nedergaard, J., Raasmaja, A., and Cannon, B. (1984). Parallel increases in amount of (3H)GDP binding and thermogenin antigen in brown-adipose-tissue mitochondria of cafeteria-fed rats. Biochem Biophys Res Commun *122*, 1328-1336.
Nillni, E. A., Friedman, T. C., Todd, R. B., Birch, N. P., Loh, Y. P., and Jackson, I. M. (1995). Pro-thyrotropin-releasing hormone processing by recombinant PC1. J Neurochem *65*, 2462-2472.
Nillni, E. A., and Sevarino, K. A. (1999). The biology of pro-thyrotropin-releasing hormone-derived peptides. Endocr Rev *20*, 599-648.
Nillni, E. A., Vaslet, C., Harris, M., Hollenberg, A., Bjorbak, C., and Flier, J. S. (2000). Leptin regulates prothyrotropin-releasing hormone biosynthesis. Evidence for direct and indirect pathways. J Biol Chem *275*, 36124-36133.
Nogueira, M. I., de Rezende, B. D., do Vale, L. E., and Bittencourt, J. C. (2000). Afferent connections of the caudal raphe pallidus nucleus in rats: a study using the fluorescent retrograde tracers fluorogold and true-blue. Ann Anat *182*, 35-45.
O'Sullivan, A. J., Martin, A., and Brown, M. A. (2001). Efficient fat storage in premenopausal women and in early pregnancy: a role for estrogen. J Clin Endocrinol Metab *86*, 4951-4956.
Oana, F., Homma, T., Takeda, H., Matsuzawa, A., Akahane, S., Isaji, M., and Akahane, M. (2005). DNA microarray analysis of white adipose tissue from obese (fa/fa) Zucker rats treated with a beta3-adrenoceptor agonist, KTO-7924. Pharmacol Res *52*, 395-400.
Oberkofler, H., Dallinger, G., Liu, Y. M., Hell, E., Krempler, F., and Patsch, W. (1997). Uncoupling protein gene: quantification of expression levels in adipose tissues of obese and non-obese humans. J Lipid Res *38*, 2125-2133.

Okamura, H., Abitbol, M., Julien, J. F., Dumas, S., Berod, A., Geffard, M., Kitahama, K., Bobillier, P., Mallet, J., and Wiklund, L. (1990). Neurons containing messenger RNA encoding glutamate decarboxylase in rat hypothalamus demonstrated by in situ hybridization, with special emphasis on cell groups in medial preoptic area, anterior hypothalamic area and dorsomedial hypothalamic nucleus. Neuroscience *39*, 675-699.
Oldfield, B. J., Giles, M. E., Watson, A., Anderson, C., Colvill, L. M., and McKinley, M. J. (2002). The neurochemical characterisation of hypothalamic pathways projecting polysynaptically to brown adipose tissue in the rat. Neuroscience *110*, 515-526.
Ollmann, M. M., Wilson, B. D., Yang, Y. K., Kerns, J. A., Chen, Y., Gantz, I., and Barsh, G. S. (1997). Antagonism of central melanocortin receptors in vitro and in vivo by agouti-related protein. Science *278*, 135-138.
Oppert, J. M., Vohl, M. C., Chagnon, M., Dionne, F. T., Cassard-Doulcier, A. M., Ricquier, D., Perusse, L., and Bouchard, C. (1994). DNA polymorphism in the uncoupling protein (UCP) gene and human body fat. Int J Obes Relat Metab Disord *18*, 526-531.
Palkovits, M., and Eskay, R. L. (1987). Distribution and possible origin of beta-endorphin and ACTH in discrete brainstem nuclei of rats. Neuropeptides *9*, 123-137.
Palkovits, M., Mezey, E., and Eskay, R. L. (1987). Pro-opiomelanocortin-derived peptides (ACTH/beta-endorphin/alpha-MSH) in brainstem baroreceptor areas of the rat. Brain Res *436*, 323-338.
Penhoat, A., Naville, D., El Mourabit, H., Buronfosse, A., Berberoglu, M., Ocal, G., Tsigos, C., Durand, P., and Begeot, M. (2002). Functional relationships between three novel homozygous mutations in the ACTH receptor gene and familial glucocorticoid deficiency. J Mol Med *80*, 406-411.
Pereira-da-Silva, M., Torsoni, M. A., Nourani, H. V., Augusto, V. D., Souza, C. T., Gasparetti, A. L., Carvalheira, J. B., Ventrucci, G., Marcondes, M. C., Cruz-Neto, A. P., *et al.* (2003). Hypothalamic melanin-concentrating hormone is induced by cold exposure and participates in the control of energy expenditure in rats. Endocrinology *144*, 4831-4840.
Perello, M., Friedman, T., Paez-Espinoza, V., Shen, X., Stuart, R. C., and Nillni, E. A. (2006). Thyroid Hormones Selectively Regulate the Post-translational Processing of ProThyrotropin Releasing Hormone (ProTRH) in the Paraventricular Nucleus of the Hypothalamus. Endocrinology.
Perello M, F. T., Paez-Espinoza V, Shen X, Stuart RC, Nillni EA (2006). Thyroid Hormones Selectively Regulate the Post-translational Processin of ProThyrotropin Releasing Hormone (ProTRH) in the Paraventricular Nucleus of the Hypothalamus. Endocrinology.

Perkins, M. N., Rothwell, N. J., Stock, M. J., and Stone, T. W. (1981). Activation of brown adipose tissue thermogenesis by the ventromedial hypothalamus. Nature *289*, 401-402.
Pierroz, D. D., Ziotopoulou, M., Ungsunan, L., Moschos, S., Flier, J. S., and Mantzoros, C. S. (2002). Effects of acute and chronic administration of the melanocortin agonist MTII in mice with diet-induced obesity. Diabetes *51*, 1337-1345.
Polston, E. K., Gu, G., and Simerly, R. B. (2004). Neurons in the principal nucleus of the bed nuclei of the stria terminalis provide a sexually dimorphic GABAergic input to the anteroventral periventricular nucleus of the hypothalamus. Neuroscience *123*, 793-803.
Polston, E. K., and Simerly, R. B. (2003). Sex-specific patterns of galanin, cholecystokinin, and substance P expression in neurons of the principal bed nucleus of the stria terminalis are differentially reflected within three efferent preoptic pathways in the juvenile rat. J Comp Neurol *465*, 551-559.
Portillo, M. P., Serra, F., Simon, E., del Barrio, A. S., and Palou, A. (1998). Energy restriction with high-fat diet enriched with coconut oil gives higher UCP1 and lower white fat in rats. Int J Obes Relat Metab Disord *22*, 974-979.
Rabelo, R., Schifman, A., Rubio, A., Sheng, X., and Silva, J. E. (1995). Delineation of thyroid hormone-responsive sequences within a critical enhancer in the rat uncoupling protein gene. Endocrinology *136*, 1003-1013.
Rabolli, D., and Martin, R. J. (1977). Effects of diet composition on serum levels of insulin, thyroxine, triiodothyronine, growth hormone, and corticosterone in rats. J Nutr *107*, 1068-1074.
Ravussin, E., Lillioja, S., Knowler, W. C., Christin, L., Freymond, D., Abbott, W. G., Boyce, V., Howard, B. V., and Bogardus, C. (1988). Reduced rate of energy expenditure as a risk factor for body-weight gain. N Engl J Med *318*, 467-472.
Rebuffe-Scrive, M., Lonnroth, P., Marin, P., Wesslau, C., Bjorntorp, P., and Smith, U. (1987). Regional adipose tissue metabolism in men and postmenopausal women. Int J Obes *11*, 347-355.
Rehnmark, S., Nechad, M., Herron, D., Cannon, B., and Nedergaard, J. (1990). Alpha- and beta-adrenergic induction of the expression of the uncoupling protein thermogenin in brown adipocytes differentiated in culture. J Biol Chem *265*, 16464-16471.
Ribeiro, M. O., Carvalho, S. D., Schultz, J. J., Chiellini, G., Scanlan, T. S., Bianco, A. C., and Brent, G. A. (2001). Thyroid hormone--sympathetic interaction and adaptive thermogenesis are thyroid hormone receptor isoform--specific. J Clin Invest *108*, 97-105.

Richard, D. (1986). Effects of ovarian hormones on energy balance and brown adipose tissue thermogenesis. Am J Physiol *250*, R245-249.
Richards, D. S., Villalba, R. M., Alvarez, F. J., and Stern, J. E. (2005). Expression of GABAB receptors in magnocellular neurosecretory cells of male, virgin female and lactating rats. J Neuroendocrinol *17*, 413-423.
Ricquier, D., Nechad, M., and Mory, G. (1982). Ultrastructural and biochemical characterization of human brown adipose tissue in pheochromocytoma. J Clin Endocrinol Metab *54*, 803-807.
Rim, J. S., and Kozak, L. P. (2002). Regulatory motifs for CREB-binding protein and Nfe2l2 transcription factors in the upstream enhancer of the mitochondrial uncoupling protein 1 gene. J Biol Chem *277*, 34589-34600.
Rippe, C., Berger, K., Boiers, C., Ricquier, D., and Erlanson-Albertsson, C. (2000). Effect of high-fat diet, surrounding temperature, and enterostatin on uncoupling protein gene expression. Am J Physiol Endocrinol Metab *279*, E293-300.
Rippe, C., Berger, K., Mei, J., Lowe, M. E., and Erlanson-Albertsson, C. (2003). Effect of long-term high-fat feeding on the expression of pancreatic lipases and adipose tissue uncoupling proteins in mice. Pancreas *26*, e36-42.
Rivest, S., Deshaies, Y., and Richard, D. (1989). Effects of corticotropin-releasing factor on energy balance in rats are sex dependent. Am J Physiol *257*, R1417-1422.
Roberts, S. B., and Leibel, R. L. (1998). Excess energy intake and low energy expenditure as predictors of obesity. Int J Obes Relat Metab Disord *22*, 385-386.
Roberts, S. B., Savage, J., Coward, W. A., Chew, B., and Lucas, A. (1988). Energy expenditure and intake in infants born to lean and overweight mothers. N Engl J Med *318*, 461-466.
Rocchini, A. P. (2002). Childhood obesity and a diabetes epidemic. N Engl J Med *346*, 854-855.
Roland, B. L., and Sawchenko, P. E. (1993). Local origins of some GABAergic projections to the paraventricular and supraoptic nuclei of the hypothalamus in the rat. J Comp Neurol *332*, 123-143.
Rolfe, D. F., and Brand, M. D. (1996). Contribution of mitochondrial proton leak to skeletal muscle respiration and to standard metabolic rate. Am J Physiol *271*, C1380-1389.
Rolfe, D. F., Hulbert, A. J., and Brand, M. D. (1994). Characteristics of mitochondrial proton leak and control of oxidative phosphorylation in the major oxygen-consuming tissues of the rat. Biochim Biophys Acta *1188*, 405-416.
Rondeel, J. M., Heide, R., de Greef, W. J., van Toor, H., van Haasteren, G. A., Klootwijk, W., and Visser, T. J. (1992). Effect of starvation and

subsequent refeeding on thyroid function and release of hypothalamic thyrotropin-releasing hormone. Neuroendocrinology *56*, 348-353.
Rossi, M., Kim, M. S., Morgan, D. G., Small, C. J., Edwards, C. M., Sunter, D., Abusnana, S., Goldstone, A. P., Russell, S. H., Stanley, S. A., *et al.* (1998). A C-terminal fragment of Agouti-related protein increases feeding and antagonizes the effect of alpha-melanocyte stimulating hormone in vivo. Endocrinology *139*, 4428-4431.
Rothwell, N. J., and Stock, M. J. (1979). A role for brown adipose tissue in diet-induced thermogenesis. Nature *281*, 31-35.
Rothwell, N. J., and Stock, M. J. (1982). Effect of chronic food restriction on energy balance, thermogenic capacity, and brown-adipose-tissue activity in the rat. Biosci Rep *2*, 543-549.
Rothwell, N. J., and Stock, M. J. (1984). Effects of denervating brown adipose tissue on the responses to cold, hyperphagia and noradrenaline treatment in the rat. J Physiol *355*, 457-463.
Rouru, J., Cusin, I., Zakrzewska, K. E., Jeanrenaud, B., and Rohner-Jeanrenaud, F. (1999). Effects of intravenously infused leptin on insulin sensitivity and on the expression of uncoupling proteins in brown adipose tissue. Endocrinology *140*, 3688-3692.
Sahakian, B. J., Trayhurn, P., Wallace, M., Deeley, R., Winn, P., Robbins, T. W., and Everitt, B. J. (1983). Increased weight gain and reduced activity in brown adipose tissue produced by depletion of hypothalamic noradrenaline. Neurosci Lett *39*, 321-326.
Sakaguchi, T., Takahashi, M., and Bray, G. A. (1988). Lateral hypothalamus and sympathetic firing rate. Am J Physiol *255*, R507-512.
Saper, C. B., Loewy, A. D., Swanson, L. W., and Cowan, W. M. (1976). Direct hypothalamo-autonomic connections. Brain Res *117*, 305-312.
Sarkar, S., Legradi, G., and Lechan, R. M. (2002). Intracerebroventricular administration of alpha-melanocyte stimulating hormone increases phosphorylation of CREB in TRH- and CRH-producing neurons of the hypothalamic paraventricular nucleus. Brain Res *945*, 50-59.
Sasaki, N., Uchida, E., Niiyama, M., Yoshida, T., and Saito, M. (1998). Anti-obesity effects of selective agonists to the beta 3-adrenergic receptor in dogs. II. Recruitment of thermogenic brown adipocytes and reduction of adiposity after chronic treatment with a beta 3-adrenergic agonist. J Vet Med Sci *60*, 465-469.
Satoh, N., Ogawa, Y., Katsuura, G., Numata, Y., Masuzaki, H., Yoshimasa, Y., and Nakao, K. (1998). Satiety effect and sympathetic activation of leptin are mediated by hypothalamic melanocortin system. Neurosci Lett *249*, 107-110.

Scarpace, P. J., and Matheny, M. (1998). Leptin induction of UCP1 gene expression is dependent on sympathetic innervation. Am J Physiol *275*, E259-264.
Scarpace, P. J., Matheny, M., Pollock, B. H., and Tumer, N. (1997). Leptin increases uncoupling protein expression and energy expenditure. Am J Physiol *273*, E226-230.
Schaffler, A., Palitzsch, K. D., Watzlawek, E., Drobnik, W., Schwer, H., Scholmerich, J., and Schmitz, G. (1999). Frequency and significance of the A-->G (-3826) polymorphism in the promoter of the gene for uncoupling protein-1 with regard to metabolic parameters and adipocyte transcription factor binding in a large population-based Caucasian cohort. Eur J Clin Invest *29*, 770-779.
Schaner, P., Todd, R. B., Seidah, N. G., and Nillni, E. A. (1997). Processing of prothyrotropin-releasing hormone by the family of prohormone convertases. J Biol Chem *272*, 19958-19968.
Schwartz, J. H., Young, J. B., and Landsberg, L. (1983). Effect of dietary fat on sympathetic nervous system activity in the rat. J Clin Invest *72*, 361-370.
Schwartz, M. W., Seeley, R. J., Woods, S. C., Weigle, D. S., Campfield, L. A., Burn, P., and Baskin, D. G. (1997). Leptin increases hypothalamic pro-opiomelanocortin mRNA expression in the rostral arcuate nucleus. Diabetes *46*, 2119-2123.
Searles, R. V., Yoo, M. J., He, J. R., Shen, W. B., and Selmanoff, M. (2000). Sex differences in GABA turnover and glutamic acid decarboxylase (GAD(65) and GAD(67)) mRNA in the rat hypothalamus. Brain Res *878*, 11-19.
Seeley, R. J., Yagaloff, K. A., Fisher, S. L., Burn, P., Thiele, T. E., van Dijk, G., Baskin, D. G., and Schwartz, M. W. (1997). Melanocortin receptors in leptin effects. Nature *390*, 349.
Segal, K. R., Edano, A., and Tomas, M. B. (1990). Thermic effect of a meal over 3 and 6 hours in lean and obese men. Metabolism *39*, 985-992.
Segal, K. R., Lacayanga, I., Dunaif, A., Gutin, B., and Pi-Sunyer, F. X. (1989). Impact of body fat mass and percent fat on metabolic rate and thermogenesis in men. Am J Physiol *256*, E573-579.
Segal-Lieberman, G., Bradley, R. L., Kokkotou, E., Carlson, M., Trombly, D. J., Wang, X., Bates, S., Myers, M. G., Jr., Flier, J. S., and Maratos-Flier, E. (2003). Melanin-concentrating hormone is a critical mediator of the leptin-deficient phenotype. Proc Natl Acad Sci U S A *100*, 10085-10090.
Shibata, H., and Bukowiecki, L. J. (1987). Regulatory alterations of daily energy expenditure induced by fasting or overfeeding in unrestrained rats. J Appl Physiol *63*, 465-470.

Shimada, M., Tritos, N. A., Lowell, B. B., Flier, J. S., and Maratos-Flier, E. (1998). Mice lacking melanin-concentrating hormone are hypophagic and lean. Nature *396*, 670-674.

Shutter, J. R., Graham, M., Kinsey, A. C., Scully, S., Luthy, R., and Stark, K. L. (1997). Hypothalamic expression of ART, a novel gene related to agouti, is up-regulated in obese and diabetic mutant mice. Genes Dev *11*, 593-602.

Silva, J. E., and Larsen, P. R. (1985). Potential of brown adipose tissue type II thyroxine 5'-deiodinase as a local and systemic source of triiodothyronine in rats. J Clin Invest *76*, 2296-2305.

Silvers, W. K., and Russell, E. S. (1955). An experimental approach to action of genes at the agouti locus in the mouse. J Exp Zool *130*, 199-220.

Sim, L. J., and Joseph, S. A. (1991). Arcuate nucleus projections to brainstem regions which modulate nociception. J Chem Neuroanat *4*, 97-109.

Simerly, R. B. (2002). Wired for reproduction: organization and development of sexually dimorphic circuits in the mammalian forebrain. Annu Rev Neurosci *25*, 507-536.

Sims, E. A., and Danforth, E., Jr. (1987). Expenditure and storage of energy in man. J Clin Invest *79*, 1019-1025.

Sites, C. K., Brochu, M., Tchernof, A., and Poehlman, E. T. (2001). Relationship between hormone replacement therapy use with body fat distribution and insulin sensitivity in obese postmenopausal women. Metabolism *50*, 835-840.

Small, C. J., Kim, M. S., Stanley, S. A., Mitchell, J. R., Murphy, K., Morgan, D. G., Ghatei, M. A., and Bloom, S. R. (2001). Effects of chronic central nervous system administration of agouti-related protein in pair-fed animals. Diabetes *50*, 248-254.

Small, C. J., Liu, Y. L., Stanley, S. A., Connoley, I. P., Kennedy, A., Stock, M. J., and Bloom, S. R. (2003). Chronic CNS administration of Agouti-related protein (Agrp) reduces energy expenditure. Int J Obes Relat Metab Disord *27*, 530-533.

Smith, R. E., and Hock, R. J. (1963). Brown fat: thermogenic effector of arousal in hibernators. Science *140*, 199-200.

Smith, S. R., Lovejoy, J. C., Greenway, F., Ryan, D., deJonge, L., de la Bretonne, J., Volafova, J., and Bray, G. A. (2001). Contributions of total body fat, abdominal subcutaneous adipose tissue compartments, and visceral adipose tissue to the metabolic complications of obesity. Metabolism *50*, 425-435.

Solberg, R., Aas, V., Thoresen, G. H., Kase, E. T., Drevon, C. A., Rustan, A. C., and Reseland, J. E. (2005). Leptin expression in human primary skeletal muscle cells is reduced during differentiation. J Cell Biochem *96*, 89-96.
Son, C., Hosoda, K., Ishihara, K., Bevilacqua, L., Masuzaki, H., Fushiki, T., Harper, M. E., and Nakao, K. (2004). Reduction of diet-induced obesity in transgenic mice overexpressing uncoupling protein 3 in skeletal muscle. Diabetologia *47*, 47-54.
Song, C. K., Jackson, R. M., Harris, R. B., Richard, D., and Bartness, T. J. (2005). Melanocortin-4 receptor mRNA is expressed in sympathetic nervous system outflow neurons to white adipose tissue. Am J Physiol Regul Integr Comp Physiol *289*, R1467-1476.
Standaert, D. G., Watson, S. J., Houghten, R. A., and Saper, C. B. (1986). Opioid peptide immunoreactivity in spinal and trigeminal dorsal horn neurons projecting to the parabrachial nucleus in the rat. J Neurosci *6*, 1220-1226.
Ste Marie, L., Luquet, S., Curtis, W., and Palmiter, R. D. (2005). Norepinephrine- and epinephrine-deficient mice gain weight normally on a high-fat diet. Obes Res *13*, 1518-1522.
Ste Marie, L., Miura, G. I., Marsh, D. J., Yagaloff, K., and Palmiter, R. D. (2000). A metabolic defect promotes obesity in mice lacking melanocortin-4 receptors. Proc Natl Acad Sci U S A *97*, 12339-12344.
Stefanova, N., Bozhilova-Pastirova, A., and Ovtscharoff, W. (1998). Sex and age differences of neurons expressing GABA-immunoreactivity in the rat bed nucleus of the stria terminalis. Int J Dev Neurosci *16*, 443-448.
Stensel, D. J., Lin, F. P., and Nevill, A. M. (2001). Resting metabolic rate in obese and nonobese Chinese Singaporean boys aged 13-15 y. Am J Clin Nutr *74*, 369-373.
Stock, M. J. (1989). Thermogenesis and brown fat: relevance to human obesity. Infusionstherapie *16*, 282-284.
Strack, A. M., Sawyer, W. B., Hughes, J. H., Platt, K. B., and Loewy, A. D. (1989). A general pattern of CNS innervation of the sympathetic outflow demonstrated by transneuronal pseudorabies viral infections. Brain Res *491*, 156-162.
Strobel, A., Issad, T., Camoin, L., Ozata, M., and Strosberg, A. D. (1998). A leptin missense mutation associated with hypogonadism and morbid obesity. Nat Genet *18*, 213-215.
Stunkard, A. J., Berkowitz, R. I., Schoeller, D., Maislin, G., and Stallings, V. A. (2004). Predictors of body size in the first 2 y of life: a high-risk study of human obesity. Int J Obes Relat Metab Disord *28*, 503-513.

Stunkard, A. J., Berkowitz, R. I., Stallings, V. A., and Schoeller, D. A. (1999). Energy intake, not energy output, is a determinant of body size in infants. Am J Clin Nutr *69*, 524-530.
Stunkard, A. J., Foch, T. T., and Hrubec, Z. (1986). A twin study of human obesity. Jama *256*, 51-54.
Stunkard, A. J., Harris, J. R., Pedersen, N. L., and McClearn, G. E. (1990). The body-mass index of twins who have been reared apart. N Engl J Med *322*, 1483-1487.
Surwit, R. S., Wang, S., Petro, A. E., Sanchis, D., Raimbault, S., Ricquier, D., and Collins, S. (1998). Diet-induced changes in uncoupling proteins in obesity-prone and obesity-resistant strains of mice. Proc Natl Acad Sci U S A *95*, 4061-4065.
Suzuki, I., Cone, R. D., Im, S., Nordlund, J., and Abdel-Malek, Z. A. (1996). Binding of melanotropic hormones to the melanocortin receptor MC1R on human melanocytes stimulates proliferation and melanogenesis. Endocrinology *137*, 1627-1633.
Sved, A. F., Cano, G., and Card, J. P. (2001). Neuroanatomical specificity of the circuits controlling sympathetic outflow to different targets. Clin Exp Pharmacol Physiol *28*, 115-119.
Swanson, L. W., and Kuypers, H. G. (1980). A direct projection from the ventromedial nucleus and retrochiasmatic area of the hypothalamus to the medulla and spinal cord of the rat. Neurosci Lett *17*, 307-312.
Swanson, L. W., and Sawchenko, P. E. (1980). Paraventricular nucleus: a site for the integration of neuroendocrine and autonomic mechanisms. Neuroendocrinology *31*, 410-417.
Takatsu, Y., Matsumoto, H., Ohtaki, T., Kumano, S., Kitada, C., Onda, H., Nishimura, O., and Fujino, M. (2001). Distribution of galanin-like peptide in the rat brain. Endocrinology *142*, 1626-1634.
Tartaglia, L. A., Dembski, M., Weng, X., Deng, N., Culpepper, J., Devos, R., Richards, G. J., Campfield, L. A., Clark, F. T., Deeds, J., *et al.* (1995). Identification and expression cloning of a leptin receptor, OB-R. Cell *83*, 1263-1271.
Tasker, J. G., and Dudek, F. E. (1993). Local inhibitory synaptic inputs to neurones of the paraventricular nucleus in slices of rat hypothalamus. J Physiol *469*, 179-192.
Tataranni, P. A., Harper, I. T., Snitker, S., Del Parigi, A., Vozarova, B., Bunt, J., Bogardus, C., and Ravussin, E. (2003). Body weight gain in free-living Pima Indians: effect of energy intake vs expenditure. Int J Obes Relat Metab Disord *27*, 1578-1583.

Thomas, S. A., and Palmiter, R. D. (1997). Thermoregulatory and metabolic phenotypes of mice lacking noradrenaline and adrenaline. Nature *387*, 94-97.
Thor, K. B., and Helke, C. J. (1987). Serotonin- and substance P-containing projections to the nucleus tractus solitarii of the rat. J Comp Neurol *265*, 275-293.
Thornton, J. E., Cheung, C. C., Clifton, D. K., and Steiner, R. A. (1997). Regulation of hypothalamic proopiomelanocortin mRNA by leptin in ob/ob mice. Endocrinology *138*, 5063-5066.
Tiraby, C., Tavernier, G., Lefort, C., Larrouy, D., Bouillaud, F., Ricquier, D., and Langin, D. (2003). Acquirement of brown fat cell features by human white adipocytes. J Biol Chem *278*, 33370-33376.
Trayhurn, P., Thurlby, P. L., and James, W. P. (1977). Thermogenic defect in pre-obese ob/ob mice. Nature *266*, 60-62.
Tulp, O. L., Gregory, M. H., and Danforth, E., Jr. (1982). Characteristics of diet-induced brown adipose tissue growth and thermogenesis in rats. Life Sci *30*, 1525-1530.
Turi, G. F., Liposits, Z., Moenter, S. M., Fekete, C., and Hrabovszky, E. (2003). Origin of neuropeptide Y-containing afferents to gonadotropin-releasing hormone neurons in male mice. Endocrinology *144*, 4967-4974.
Vaisse, C., Clement, K., Guy-Grand, B., and Froguel, P. (1998). A frameshift mutation in human MC4R is associated with a dominant form of obesity. Nat Genet *20*, 113-114.
Valve, R., Heikkinen, S., Rissanen, A., Laakso, M., and Uusitupa, M. (1998). Synergistic effect of polymorphisms in uncoupling protein 1 and beta3-adrenergic receptor genes on basal metabolic rate in obese Finns. Diabetologia *41*, 357-361.
Van Buskirk, R. L., and Erickson, R. P. (1977). Odorant responses in taste neurons of the rat NTS. Brain Res *135*, 287-303.
van Haasteren, G. A., Linkels, E., Klootwijk, W., van Toor, H., Rondeel, J. M., Themmen, A. P., de Jong, F. H., Valentijn, K., Vaudry, H., Bauer, K., and et al. (1995). Starvation-induced changes in the hypothalamic content of prothyrotrophin-releasing hormone (proTRH) mRNA and the hypothalamic release of proTRH-derived peptides: role of the adrenal gland. J Endocrinol *145*, 143-153.
Vidal-Puig, A. J., Grujic, D., Zhang, C. Y., Hagen, T., Boss, O., Ido, Y., Szczepanik, A., Wade, J., Mootha, V., Cortright, R., *et al.* (2000). Energy metabolism in uncoupling protein 3 gene knockout mice. J Biol Chem *275*, 16258-16266.
Visscher, T. L., and Seidell, J. C. (2001). The public health impact of obesity. Annu Rev Public Health *22*, 355-375.

Vulliemoz, N. R., Xiao, E., Xia-Zhang, L., Wardlaw, S. L., and Ferin, M. (2005). Central infusion of agouti-related peptide suppresses pulsatile luteinizing hormone release in the ovariectomized rhesus monkey. Endocrinology *146*, 784-789.
Wadden, T. A., Foster, G. D., Letizia, K. A., and Mullen, J. L. (1990). Long-term effects of dieting on resting metabolic rate in obese outpatients. Jama *264*, 707-711.
Wade, G. N. (1975). Some effects of ovarian hormones on food intake and body weight in female rats. J Comp Physiol Psychol *88*, 183-193.
Wagner, E. J., Ronnekleiv, O. K., Bosch, M. A., and Kelly, M. J. (2001). Estrogen biphasically modifies hypothalamic GABAergic function concomitantly with negative and positive control of luteinizing hormone release. J Neurosci *21*, 2085-2093.
Wahrenberg, H., Engfeldt, P., Arner, P., Wennlund, A., and Ostman, J. (1986). Adrenergic regulation of lipolysis in human adipocytes: findings in hyper- and hypothyroidism. J Clin Endocrinol Metab *63*, 631-638.
Wahrenberg, H., Wennlund, A., and Arner, P. (1994). Adrenergic regulation of lipolysis in fat cells from hyperthyroid and hypothyroid patients. J Clin Endocrinol Metab *78*, 898-903.
Wang, Q., Bing, C., Al-Barazanji, K., Mossakowaska, D. E., Wang, X. M., McBay, D. L., Neville, W. A., Taddayon, M., Pickavance, L., Dryden, S., *et al.* (1997). Interactions between leptin and hypothalamic neuropeptide Y neurons in the control of food intake and energy homeostasis in the rat. Diabetes *46*, 335-341.
Watanabe, M., Houten, S. M., Mataki, C., Christoffolete, M. A., Kim, B. W., Sato, H., Messaddeq, N., Harney, J. W., Ezaki, O., Kodama, T., *et al.* (2006). Bile acids induce energy expenditure by promoting intracellular thyroid hormone activation. Nature *439*, 484-489.
Watson, S. J., Akil, H., Richard, C. W., 3rd, and Barchas, J. D. (1978). Evidence for two separate opiate peptide neuronal systems. Nature *275*, 226-228.
Weinsier, R. L., Hunter, G. R., Zuckerman, P. A., and Darnell, B. E. (2003). Low resting and sleeping energy expenditure and fat use do not contribute to obesity in women. Obes Res *11*, 937-944.
Weyer, C., Tataranni, P. A., Snitker, S., Danforth, E., Jr., and Ravussin, E. (1998). Increase in insulin action and fat oxidation after treatment with CL 316,243, a highly selective beta3-adrenoceptor agonist in humans. Diabetes *47*, 1555-1561.
Williams, D. L., Bowers, R. R., Bartness, T. J., Kaplan, J. M., and Grill, H. J. (2003). Brainstem melanocortin 3/4 receptor stimulation increases

uncoupling protein gene expression in brown fat. Endocrinology *144*, 4692-4697.
Wolff, G. L. (1963). Growth of Inbred Yellow (Aya) and Non-Yellow (Aa) Mice in Parabiosis. Genetics *48*, 1041-1058.
Wortley, K. E., Anderson, K. D., Yasenchak, J., Murphy, A., Valenzuela, D., Diano, S., Yancopoulos, G. D., Wiegand, S. J., and Sleeman, M. W. (2005). Agouti-related protein-deficient mice display an age-related lean phenotype. Cell Metab *2*, 421-427.
Xia, Y., and Wikberg, J. E. (1996). Localization of ACTH receptor mRNA by in situ hybridization in mouse adrenal gland. Cell Tissue Res *286*, 63-68.
Yamazoe, M., Shiosaka, S., Yagura, A., Kawai, Y., Shibasaki, T., Ling, N., and Tohyama, M. (1984). The distribution of alpha-melanocyte stimulating hormone (alpha-MSH) in the central nervous system of the rat: an immunohistochemical study. II. Lower brain stem. Peptides *5*, 721-727.
Yasuda, T., Masaki, T., Kakuma, T., and Yoshimatsu, H. (2004). Hypothalamic melanocortin system regulates sympathetic nerve activity in brown adipose tissue. Exp Biol Med (Maywood) *229*, 235-239.
Yen, T. T., Gill, A. M., Frigeri, L. G., Barsh, G. S., and Wolff, G. L. (1994). Obesity, diabetes, and neoplasia in yellow A(vy)/- mice: ectopic expression of the agouti gene. Faseb J *8*, 479-488.
Yeo, G. S., Farooqi, I. S., Aminian, S., Halsall, D. J., Stanhope, R. G., and O'Rahilly, S. (1998). A frameshift mutation in MC4R associated with dominantly inherited human obesity. Nat Genet *20*, 111-112.
Yoshida, T., Kemnitz, J. W., and Bray, G. A. (1983). Lateral hypothalamic lesions and norepinephrine turnover in rats. J Clin Invest *72*, 919-927.
Yoshimatsu, H., Egawa, M., and Bray, G. A. (1993). Sympathetic nerve activity after discrete hypothalamic injections of L-glutamate. Brain Res *601*, 121-128.
Young, T. K., Dean, H. J., Flett, B., and Wood-Steiman, P. (2000). Childhood obesity in a population at high risk for type 2 diabetes. J Pediatr *136*, 365-369.
Zagon, A. (1993). Innervation of serotonergic medullary raphe neurons from cells of the rostral ventrolateral medulla in rats. Neuroscience *55*, 849-867.
Zhang, C. Y., Baffy, G., Perret, P., Krauss, S., Peroni, O., Grujic, D., Hagen, T., Vidal-Puig, A. J., Boss, O., Kim, Y. B., *et al.* (2001). Uncoupling protein-2 negatively regulates insulin secretion and is a major link between obesity, beta cell dysfunction, and type 2 diabetes. Cell *105*, 745-755.
Zhang, Y., Kilroy, G. E., Henagan, T. M., Prpic-Uhing, V., Richards, W. G., Bannon, A. W., Mynatt, R. L., and Gettys, T. W. (2005). Targeted deletion of melanocortin receptor subtypes 3 and 4, but not CART, alters nutrient

partitioning and compromises behavioral and metabolic responses to leptin. Faseb J *19*, 1482-1491.
Zhang, Y., Matheny, M., Tumer, N., and Scarpace, P. J. (2004). Aged-obese rats exhibit robust responses to a melanocortin agonist and antagonist despite leptin resistance. Neurobiol Aging *25*, 1349-1360.
Zhang, Y., Proenca, R., Maffei, M., Barone, M., Leopold, L., and Friedman, J. M. (1994). Positional cloning of the mouse obese gene and its human homologue. Nature *372*, 425-432.
Zheng, H., Patterson, L. M., Phifer, C. B., and Berthoud, H. R. (2005). Brain stem melanocortinergic modulation of meal size and identification of hypothalamic POMC projections. Am J Physiol Regul Integr Comp Physiol *289*, R247-258.
Zimmet, P., Alberti, K. G., and Shaw, J. (2001). Global and societal implications of the diabetes epidemic. Nature *414*, 782-787.